Chemical Analysis and Biosynthesis of Secondary Alcohols in Plant Cuticular Wax

by

Miao Wen

B.Sc., The Lanzhou University, 1999
M.Sc., The Lanzhou University, 2002
Ph.D., The University of British Columbia, 2008

A THESIS SUBMITTED IN PARTIAL FULFILLMENT OF
THE REQUIREMENTS FOR THE DEGREE OF

Doctor of Philosophy
in

The Faculty of Graduate Studies

(Chemistry)

THE UNIVERSITY OF BRITISH COLUMBIA

(Vancouver)

Feburary, 2009

Abstract

The biosynthesis of secondary alcohols in plant cuticular waxes was investigated in the current study. Two fundamentally different pathways were proposed to introduce the secondary hydroxyl groups. One pathway is by hydroxylation of the elongated substrates. Two hypotheses related to this pathway were proposed: (1.1) the pathway continues beyond secondary alcohols and ketones to bifunctional compounds, and (1.2) the hydroxylases catalyzing all these hydroxylation steps are similar in regiospecificity and substrate preference. These two hypotheses were tested by detailed investigations of plant cuticular waxes from Arabidopsis and pea (*Pisum sativum*) (Chapters 3-4). Nonacosane-14,15-diol, -14,16-diol and -13,15-diol as well as corresponding ketols were identified for the first time in Arabidopsis stem wax. The alkanediols and ketols were dominated by the isomer with functional groups on C-14,15. The absence of alkanediols and ketols in Arabidopsis *mah1* mutants that are deficient in secondary alcohol biosynthesis confirmed the biosynthetic relationship between secondary alcohols and alkanediols/ketols (Chapter 3). In pea (*Pisum sativum*) leaf wax, two novel compound classes were identified. They were primary/secondary alcohols dominated by octacosane-1,14-diol and secondary/secondary alkanediols hentriacontane-9,16-diol, -8,15-diol and -10,17-diol. The secondary/secondary alkanediols were co-localized with the hentriacontan-15-ol and -16-ol, suggesting a biosynthetic relationship between the secondary alcohols and alkanediols (Chapter 4). The diverse structures of compounds identified in the current study suggested that hydroxylases use substrates other than alkanes. The predominance of isomers within homologues indicated a regiospecificity of the hydroxylases involved in wax biosynthesis.

The second pathway is through elongation of carbon chains, which is similar to polyketide biosynthesis. Two hypotheses were proposed for this pathway as well: (2.1) the hydroxyl groups in asymmetric secondary alcohols are introduced during elongation, and (2.2) condensing enzymes play a key role in the introduction of the secondary functional groups during elongation leading to asymmetric secondary alcohols. These two hypotheses were tested by identification of novel compounds in waxes, radioactively labeled assays and characterization of putative condensing enzymes (Chapters 5-7). Homologous series of 5-hydroxyaldehydes (C_{24} and C_{26}-C_{36}) and 1,5-alkanediols (C_{28}-C_{38}) were identified in yew

(*Taxus baccata*) needle wax. The 1,5-relative position of the functional groups in both compound classes suggested that these two compound classes are biosynthetically related and their secondary functional groups are introduced during elongation (Chapter 5). The results of incubation of ^{14}C-labeled malonyl-CoA and acyl-CoAs with different chain lengths in the presence of California poppy (*Eschscholzia californica*) microsomes provided the first evidence to support the elongation hypothesis. The results indicated that a carbonyl group is introduced rather than a hydroxyl group during elongation. To provide molecular tools for further investigations of the hypothetical pathway, three full length cDNAs encoding putative KCSs were cloned and one of them, *PKCSI*, was functionally characterized.

Table of Contents

List of Tables

List of Figures

List of Abbreviations

AFD: (Z,Z)-1-acetoxy-2-hydroxy-4-oxo-heneicosa-12,15-diene
Bp: base pair
BSTFA: bis-*N,O*-(trimethylsilyl)trifluoroacetamide
CoA: coenzyme A
ECR: β-enoyl-CoA reductase
ER: endoplasmic reticulum
EST: expression sequence tag
DGAT: diacylglycerol acyltransferase
DTT: dithiothreitol
FAE: fatty acid elongase
FAME: fatty acid methyl esters
FAR: fatty acyl-CoA reductase
FAS: fatty acid synthase
FID: flame ionization detector
GC: gas chromatography
HCD: β-hydroxyacyl CoA dehydratase
HEPES: 4-(2-hydroxyethyl)-1-piperazineethanesulfonic acid
KCR: β-ketoacyl-CoA reductase
KCS: β-ketoacyl-CoA synthase
KAS: β-ketoacyl-[acyl carrier protein] synthase
MS: mass spectrum/mass spectroscopy
PMSF: phenylmethanesulphonylfluoride
TAG: triacylglycerol
TLC: thin layer chromatography
VLCFA: very-long-chain fatty acid

Acknowledgements

I would like to acknowledge the many people who made this thesis possible.

It is difficult to express my sincere gratitude to my Ph.D. supervisor, Dr. Reinhard Jetter. With his inspiration, and his great efforts to explain things clearly and simply, he helped to make through the PhD study. Throughout my thesis-writing period, he provided encouragement, sound advice and lots of good ideas. I would have been lost without him. In addition, I am grateful to Dr. Martin Tanner for the advice on thesis-writing.

I would like to thank Dr. Ljerka Kunst at the Botany Department, the University of British Columbia for guiding me into the field of molecular biology. In addition, I wish to thank Dr. Tanya Hooker, Dr. Xuemin Wu, Dr. Fengling Li for patiently teaching me theories and techniques of molecular biology. I am grateful to Patricia Lam for providing cell strains and plasmids, as well as Dr. Huanquan Zheng for the pVKH18 and pVKH18-pFAE1 vectors.

I am grateful to all the lab members for providing a stimulating environment in which to learn and grow. I wish to thank many colleague students for inspiring discussions and interesting conversations.

I wish to thank all my friends in Vancouver, especially Ye Wang and Songhua Zhu for helping me get through the difficult times, and for all the emotional support, entertainment, and caring they provided.

To my husband, Jun Lang, for always being there.

To my parents, Yuheng Jiao and Keyi Wen, who bore me, raised me, supported me, taught me, and loved me. To them I dedicate this thesis.

Chapter 1 Introduction: Functions/Properties, Chemical Composition and Biosynthesis of Plant Cuticular Waxes

All primary above ground parts of plants are covered with a cuticle consisting of a polymeric matrix and soluble wax.[1] The backbone of plant cuticles is made of cutin, a three dimensional hydroxy-fatty ester polymer. Cuticular waxes, composed of very-long-chain fatty acid (VLCFA) derivatives, are deposited on the outer surface of a cutin matrix (epicuticular wax) and embedded within the cutin matrix (intracuticular wax). As the outermost layer covering aerial parts of plants, the cuticle prevents non-stomatal water loss and provides protection from biotic and abiotic environment stress. Its importance is underlined by the fact that the cuticle is formed already by primary epidermal cells at very early stages of development. The chemical compositions of the cutin monomers and wax vary among plant species. Such variations are generally thought to be an adaptation to the environment. It is believed that the biosynthesis of cutin and wax is regulated by the environment and, consequently, chemical compositions of cutin and wax vary accordingly.[2] The cuticle functions/properties, chemical compositions and biosynthesis are intertwined with each other, and therefore one cannot be understood without the other two.

In this introduction chapter, the aspects of cuticle biology, chemistry and biochemistry will be reviewed with emphasis on wax composition and biosynthesis. Note that the singular "wax" will be used when cuticular wax is obtained from one source, e.g., by one extraction method from the same plant species/organ. When cuticular waxes are obtained from different sources, e.g., by combination of extraction methods or from various plant species/organs, the plural "waxes" will be used.

1.1 Structures of Plant Cuticles

The cuticle is made up of several layers (Fig. 1.1). The cutin matrix is the backbone of the cuticle. Cutin is covered by epicuticular waxes that directly contact the environment. All plant species have an epicuticular wax film. Some species are covered by epicuticular wax crystals, an extra layer of particles protruding from the epicuticular wax film. The wax

embedded in the cutin matrix is called intracuticular wax. In section 1.1.1, the current knowledge of the chemical composition of cutin monomers and the linkage of these monomers will be reviewed. The spatial resolution of epi- and intracuticular waxes will be reviewed together with the diverse structures of epicuticular wax crystals (section 1.1.2).

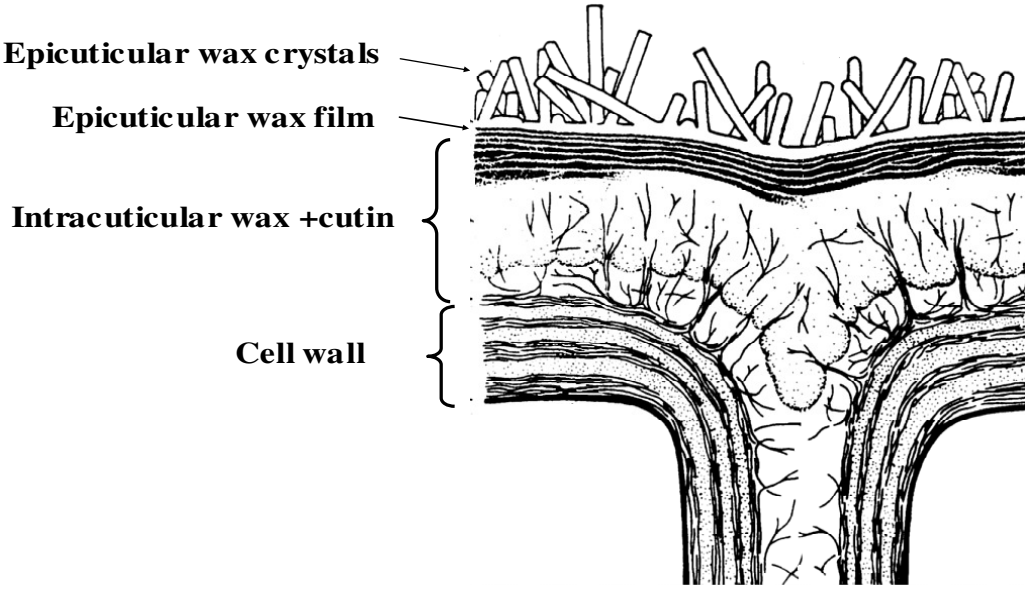

Figure 1.1: Diagram of the transverse view of plant cuticles and epidermal cells. Epicuticular waxes, including crystals and film, are in direct contact with air. Intracuticular waxes and cutin matrix are located outside of epidermal cell walls. The diagram is modified after Jeffree 1986.[3]

1.1.1 Backbones of Plant Cuticles-Cutin Matrix

Cutin coverage varies from 10-500 μg/cm^2 and accounts for 40-80% of the cuticle weight for different species. Cutin is not soluble in any solvents, but can be depolymerised by various methods. Cutin monomers are usually composed of C_{16} and/or C_{18} fatty acid derivatives that have diverse functional groups and substitution patterns (Fig. 1.2). Studies using solid-state nuclear magnetic resonance (NMR), infrared (IR) spectroscopy, atomic force microscopy (AFM) and/or X-ray diffraction of the intact cutin matrix showed that cutin monomers are linked by ester bonds.[4,5] Chemical analyses of oligomers resulting from partial degradation confirmed the spectroscopic results (Fig. 1.3).[6-9] In a recent study, 1- and 2-monoacylglyceryl esters of ω-hydroxyacids were detected in the partially depolymerized cutin of bitter orange. Molar proportions of glycerol would permit the esterification of a significant part of the

aliphatic ω-hydroxyacids, suggesting that glycerol plays an important role in the polyester structure of cutin.[10]

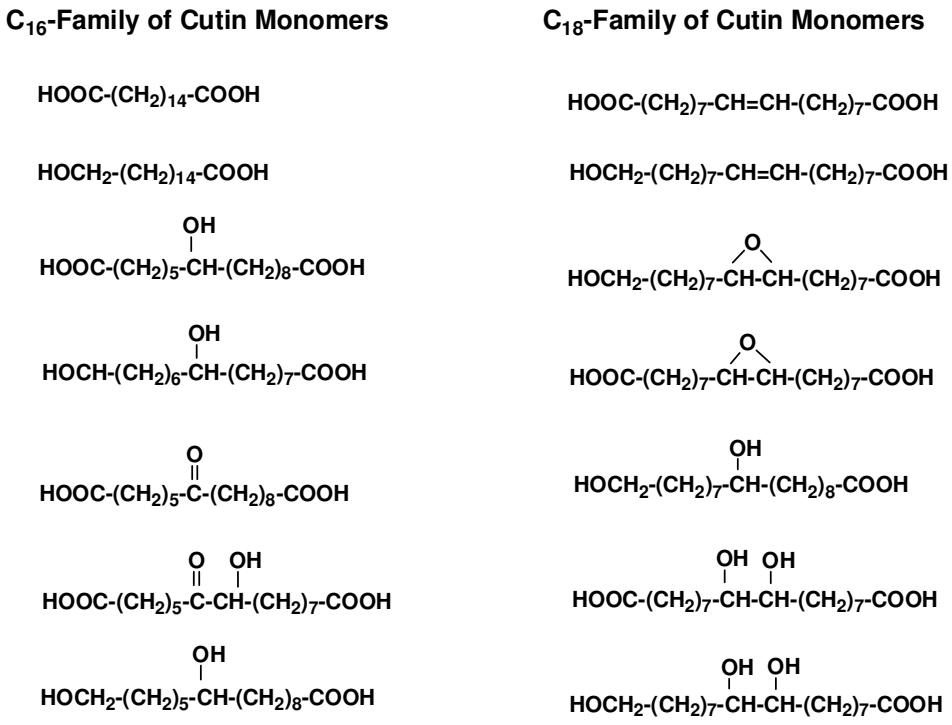

Figure 1.2: Cutin monomers. C_{16} cutin monomers are usually dominated by 10,16- and/or 9,16-dihydroxyhexadecanoic acid. When mixtures of C_{16} and C_{18} compounds occur, 9,10-epoxy-18-hydroxyoctadecanoic acid and 9,10,18-trihydroxyoctadecanoic acid are generally most abundant, and substantial amounts of unsaturated C_{18} derivatives are also present.

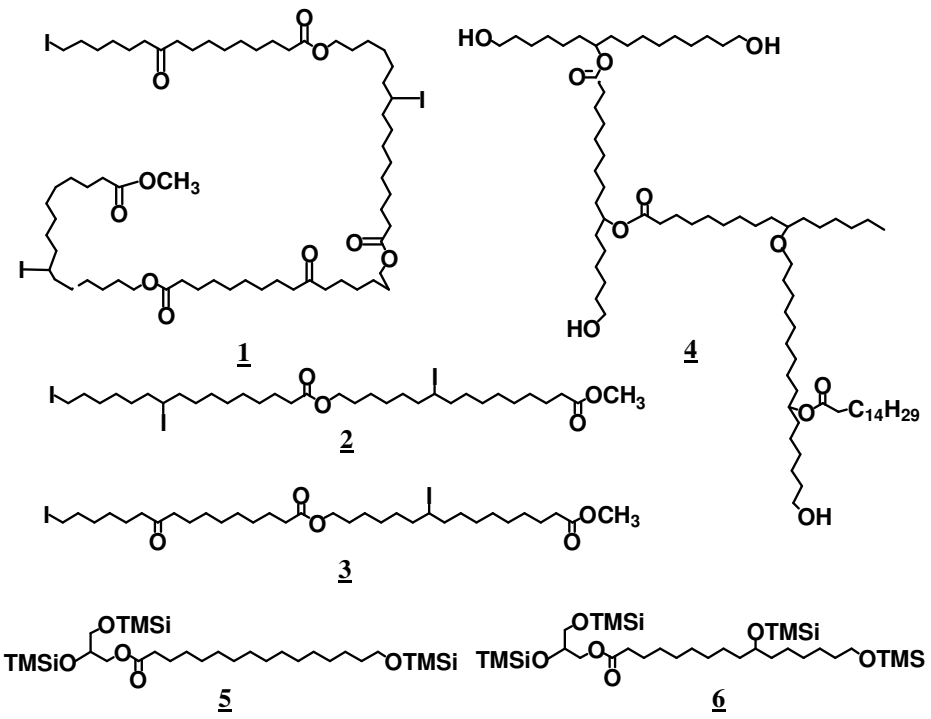

Figure 1.3: Oligomers from partial depolymerization of lime fruit and bitter orange cutin. The oligomers **1**-**3** were produced by iodotrimethylsilane treatment. The primary ester bonds form linear structures. A unique pentamer (**4**) linked exclusively by secondary esters was isolated by porcine pancreatic lipase digestion of lime cutin.[11] The pentamer is composed of 10,16-dihydroxyhexadecanoic acid, hexadecanoic acid, 10-hydroxyhexadecanoic acid, and 1,7,16-hexadecanetriol, which forms both linear and cross linked structures. The oligomers **5**&**6** were released from bitter orange cutin by $NaOCH_3$-catalyzed methanolysis. The TMSi groups were introduced by BSTFA (bis-*N*,*O*-(trimethylsilyl)trifluoroacetamide) derivatization for GC analysis.

1.1.2 Soluble Lipids in Plant Cuticles-Cuticular Waxes

All the components in a cuticle that are extractable by organic solvents are designated as cuticular wax. In most plant species and organs, cuticular waxes are composed of VLCFA derivatives: fatty acids, primary alcohols, esters, alkanes, secondary alcohols and ketones. Triterpenoids are also present in the cuticular waxes of some plant species.[12,13] Early studies showed that the chemical composition of the wax prepared by brief extraction of isolated cuticular membranes was different from that obtained by thorough extraction, suggesting that cuticular waxes are arranged in layers.[14] Selective sampling methods have been developed to remove epicuticular waxes without touching intracuticular waxes.[15,16] Application of these selective sampling techniques finally confirmed that cuticular waxes are arranged in spatially

distinct layers with epicuticular wax on the top of the cutin matrix and intracuticular wax embedded in the cutin matrix.[17,18] Chemical analyses of the samples obtained from different layers show that cyclic and polar compounds tend to be in the intracuticular wax.[19]

Scanning electron microscopy has revealed a fascinating diversity of micro-structures differing in size, shape and arrangement covering plant surfaces. An X-ray powder diffraction study on the four most common micro-structures, platelets, tubules, films and rodlets, showed that the wax molecules are packed with orthorhombic, triclinic or hexagonal symmetry.[20] Molecules of the same chain length form layers and then layers pack together to form three dimensional structures with regular shapes. Therefore, the particles protruding from the epicuticular wax film are considered as crystals. Chemical analyses and re-crystallization experiments indicated that the characteristic crystal structures are correlated with the presence of certain compounds (or compound classes).[17,21-23] For example, high percentages of β-diketones or nonacosan-10-ol coincide with tubular crystals, triterpenoids are correlated with threads, and primary alcohols are correlated with platelets.[21]

1.2 Functions/Properties of Cuticles and Cuticular Waxes

Plant cuticles, as the outermost layer, are in direct contact with the environment. They protect plants from abiotic stress, such as drought, pollutants and UV radiation. They are also the first line of defense when coming into contact with other organisms. The contribution of cuticular waxes to protection against abiotic stress will be reviewed in section 1.2.1, followed by a brief review of the role that waxes play in plant-pathogen and plant-insect interactions in section 1.2.2.

1.2.1 Protection Against Abiotic Stress

1.2.1.1 Prevention of Non-stomatal Water Loss

It has been widely accepted that the primary physiological function of the cuticle is to reduce transpirational water loss. Cuticular waxes play a significant role in this function. After removal of cuticular wax from the isolated cuticular membrane, the water permeability of the membranes increased by one to two orders of magnitude.[24,25] However, attempts to find a correlation between the permeability and the amounts of cuticular waxes or the thickness of

the cutin matrix have failed.[26,27] Significant efforts have also been made to investigate the correlation between permeability and wax spatial arrangement or chemical composition. However, it is still unclear how the epi- or intracuticular waxes contribute to permeability. Evidence obtained by molecular genetic experiments indicated that the transpiration barrier is located in the intracuticular wax.[28]. On the contrary, selective removal of the epicuticular wax from detached *Leucadendron lanigerum* leaves resulted in a significant increase of the transpiration rate, suggesting epicuticular wax as the barrier.[29] Similarly, neither has a correlation between the wax permeability and chemical composition been established.[27]

1.2.1.2 Protection Against Accumulation of Water Droplets and Solid Particles

Epicuticular wax crystals form a water-repellent surface due to their hydrophobicity. Water repellency is characterized by the wettability which is measured by contact angles, "the angle subtended between the leaf surface and the plane of a tangent to the surface of a water droplet originating at the contact point".[30] To form individual water droplets on a surface, contact angles must be bigger than 90^{o}. When water droplets are formed, they easily run off from plant surfaces and, thus, the plant surfaces are kept dry.

Big contact angles result in small contact areas between water droplets and water-repellent surfaces. When a droplet comes into contact with a particle on a water-repellent surface, capillary forces result in adhesion between the droplet and the solid particle. Consequently, the particle is removed by the water droplet when it runs off from the surface. Hence the plant surfaces are protected from accumulation of dust and solid air pollutants. Such a self-cleaning property is known as "lotus-effect".[31]

1.2.1.3 Protection from UV Damage

In addition to protecting plants from particle contamination, epicuticular waxes protect plant tissues from ultraviolet radiation by reflection and/or absorption. UV reflection is correlated to the wax load and the presence of epicuticular wax crystals.[32,33] UV-induced leaf rolling and DNA damage has been observed in the maize (*Zea mays* L.) *glossy1* mutant that is deficient in wax production, demonstrating that cuticular waxes protect plants from UV damage.[34] The presence of UV-absorbing compounds in cuticular wax may also play a role

in protecting plants from UV damage. For example, Cuadra and co-workers detected calycopterin and 3-methoxycalycopterin in *Gnaphalium luteo-album* leaf wax.[35] A recent study found phenolic derivatives in yew (*Taxus baccata*) needle wax.[36]

1.2.2 Interactions with Other Organisms

As the primary contact zone between plant pathogens and their hosts, cuticular waxes must be involved in the physical interaction with pathogens and may function as cues to affect pathogen activities. There is evidence demonstrating that cuticular waxes have an effect on pathogen spore germination.[37-39] In addition to protecting plants from pathogens, cuticular waxes also protect plants from insects. Studies have shown that the plants without epicuticular waxes are more susceptible to herbivorous insects than the same plants with intact epicuticular waxes, an effect that is mostly due to easier attachment of the insects to plant surfaces.[40-42] Cuticular waxes can also act as deterrents protecting plants from insect biting. For example, larvae of fifth-instar tobacco budworm (*Helicoverpa armigera*) were deterred from feeding on glass-fiber disks impregnated with the stilbene (3-hydroxy-4-prenyl-5-methoxystilbene-2-carboxylic acid) extracted from pod surfaces of pigeon pea (*Cajanus cajan*).[43]

1.3 Compositions and Biosynthesis of Cuticular Waxes

Cuticular waxes of most plant species are mixtures containing solely VLCFA derivatives. Cyclic compounds are also found as the major wax components in some plant species. Since cyclic compounds are not my primary research interest, I will focus on VLCFA derivatives in the following sections. In order to understand the biosynthesis of VLCFA derivatives, the elongation of VLCFA precursors will be reviewed (section 1.3.1). Then the chemical compositions of cuticular waxes will be reviewed together with the biosynthetic pathways leading to the wax compounds. The pathways leading to the wax components with primary functional groups are relatively well understood and thus will be described first (section 1.3.2). Some progress has also been made towards a better understanding of the biosynthesis of wax components with secondary functional groups, especially secondary alcohols. However, questions still remain about the biosynthesis of secondary alcohols and wax

components with bifunctional groups. These will be summarized in the second half of this section (sections 1.3.3.3 to 1.3.3.6).

1.3.1 Formation of Very-Long-Chain Fatty Acid Precursors

Saturated VLCFAs are synthesized by fatty acid elongation (FAE) enzyme complexes in the endoplasmic reticulum (ER) of epidermal cells. A two-carbon unit from malonyl coenzyme A (CoA) is added to the pre-existing C_{16} or C_{18} acyl-CoAs. Four enzymatic reactions that are similar to fatty acid biosynthesis are involved in one elongation cycle: (1) condensation of malonyl-CoA with long chain acyl-CoAs, (2) reduction of β-ketoacyl-CoAs to β-hydroxyacyl-CoAs, (3) dehydration of β-hydroxyacyl-CoAs to β-enoyl-CoAs, and (4) reduction of enoyl-CoAs to elongated acyl-CoAs (Fig. 1.4). The first reaction elongates carbon chains while the remaining three reactions modify the β-keto group introduced in the earlier elongation cycle into a methylene unit. VLCFA precursors are then converted to cuticular waxes (section 1.3.2).

The four enzymes in a FAE complex are non-covalently bound. Partial purification of elongases from leek (*Allium porrum*) resulted in an enrichment of several protein bands, indicating that the elongase is not a multifunctional modular synthase.[44,45] The physical interactions of the four core components of the elongase complex in yeast (*Saccharomyces cerevisiae*) have been demonstrated by co-immunoprecipitation.[46-48]

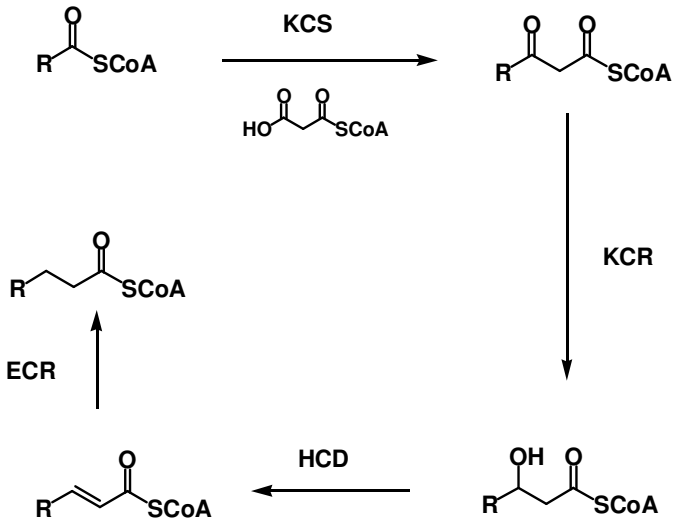

Figure 1.4: Four enzymatic reactions in very-long-chain fatty acid elongation cycles. KCS: β-ketoacyl-CoA synthase; KCR: β-ketoacyl-CoA reductase; HCD: β-hydroxyacyl-CoA dehydratase; ECR: β-enoyl-CoA reductase.

1.3.1.1 β-Ketoacyl-CoA Synthase (KCS)

The first gene encoding a KCS, *FATTY ACID ELONGASE1* (*FAE1*), was isolated after extensive mutant screens for changes in very-long-chain fatty acid composition of Arabidopsis (*Arabidopsis thaliana*) seeds. Based on its homology to three condensing enzymes, chalcone synthase, stilbene synthase and β-ketoacyl-[acyl carrier protein] synthase III, FAE1 was tentatively annotated as a condensing enzyme specific for VLCFA elongation.[49] This was confirmed by over-expression of *FAE1* in tobacco, Arabidopsis and yeast.[50] To date, twenty-one genes have been annotated as putative elongase condensing enzymes in the Arabidopsis genome based on homology to *FAE1*.[51] An unrelated *ELO*-gene family encoding putative condensing enzymes, homologous to ELO1/2/3 in yeast, has also been identified in the Arabidopsis genome.[51]

Five of the KCS candidate genes, *CER6*, *CER60*, *KCS1*, *FDH* and *HIC* have been implicated in wax production and epidermis development. CER6 is one of the key enzymes in the synthesis of VLCFA precursors for the wax production in Arabidopsis shoots. A major reduction of CER6 activity resulted in over 90% reduction of total stem wax and conditional male sterility. RT-PCR showed that *CER6* is highly expressed in developing tissues. *In situ* hybridization localized its expression in the epidermis. All the evidence taken together

demonstrates that CER6 is the condensing enzyme involved in VLCFA biosynthesis.[52] CER60 has high amino acid sequence similarity to CER6, but it does not appear to significantly contribute to the synthesis of stem and pollen surface lipids.[53] This may be due to a very low expression level of CER60 in mature Arabidopsis tissues.[54]

The wax phenotype of a T-DNA-tagged *kcs1* mutant suggests the involvement of KCS1 in wax biosynthesis.[55] The complete loss of KCS1 activity changed the distribution of the wax components, but in no case did it result in the complete loss of any wax component or significant decrease of the total wax load. This indicates that there is either redundancy in the KCS activities or the wax phenotype is a secondary effect resulting from loss of KCS1 function. Therefore, a final conclusion cannot be drawn in terms of the biochemical and biological functions of KCS1.

FDH has been cloned and found to be specifically expressed in the epidermis of mainly petal cells of Arabidopsis.[56,57] The *fdh* mutant has a wild type wax profile, but it shows post-genital fusion of different shoot organs,[58] indicating that epidermal cells require the FDH activity for their normal function. Another KCS-like gene, *HIC*, shows a regulatory function in stomata development.[59] It is expressed only in stomata on leaves. The mutant shows a high stomatal density under a high CO_2 concentration.

In addition to the genes in Arabidopsis, genes or cDNAs encoding KCSs from other plant species, yeast strains and algae have been cloned and characterized (Table 1.1). Most of these *KCS*s were cloned from seed oil producing plants because a possible manipulation of the fatty acid elongation pathway would be significant for agriculture.[60-63]

Table 1.1: Summary of genes or cDNAs that have been cloned and characterized from alga, yeast and plant species other than Arabidopsis

Sources	Names of Genes/cDNAs	Biochemical Functions (in heterologous expression system)	Ref.
Brassica napus	*BnFAE1*	Biosynthesizes erucic acid	[62,64]
Brassica juncea	*BjFAE1*	Increases seed erucic acid content in over-expressor	[63]
Lesquerella fendleri	*LfKCS3*	Elongates hydroxy-fatty acid in seeds	[65]
Lesquerella fendleri	*LfKCS45*	Elongates 26:0 to 28:0 and 30:0fatty acid Root specific elongase	[61]
Simmondsia chinensis		Elongates 18:0 and 18:1 to longer chains in seeds	[60]
Teesdalia nudicaulis		Elongates 18:1 to 20:1 Seed oil production	[66]
Gossypium hirsutum	*GhKCS13/CER6* *GhKCS2,* *GhKCS6,* *GhKCS12,*	Rescues *elo2*Δ*elo3*Δ double mutant and restore fatty acid composition	[67,68]
Tropaeolum majus		Elongates 18:1 and 20:1 substrate to 22:1	[69]
Persea americana	*AvFAE1*	Biosynthesizes AFD[a] precursor	[70]
Physcomitrella patens	*PSE1*	Elongates C_{18} Δ6 polyunsaturated fatty acid (18:4 $\Delta^{6,9,12,15}$)	[71,72]
Isochrysis galbana	*IgASE1*	Elongates C_{18} Δ9 polyunsaturated fatty acid	[73]
Pavlova lutheri	*PlELO1*	Elongates 16:0 to polyunsaturated fatty acid	[74]
Hansenula polymorpha	*HpELO1*	Elongates 22:0 to 26:0 Homologue to *ELO3*	[75]
Hansenula polymorpha	*HpELO2*	Elongates 18:0 to 24:0	[76]

[a] AFD: (Z,Z)-1-acetoxy-2-hydroxy-4-oxo-heneicosa-12,15-diene

Condensing enzymes use not only saturated acyl-CoAs as substrates, but also acyl-CoA chains with functional groups. Increased levels of hydroxy-fatty acids have been observed in yeast cells that were transformed with *LfKCS3* from *Lesquerella fendleri*.[65] Elongated polyunsaturated fatty acids have been detected in yeast cells transformed with *PSE1* and *IgASE1* from a moss (*Physcomitrella patens*) and an alga (*Isochrysis galbana*), respectively, when the medium was supplemented with polyunsaturated acyl substrates.[71-73]

Condensing enzymes show substrate chain length preferences. The fatty acid profile of Arabidopsis mutants lacking a KCS activity indicates the substrate preference of the KCS that is affected by the mutation. In *CER6*-suppressed plants, the C_{24} wax components predominated, indicating that CER6 has a preference for substrates with more than 24

carbons.[52] Both saturated and unsaturated C_{20} and C_{22} fatty acids decreased dramatically in seed oil of the *fae1* mutant. Over-expression of *FAE1* in tobacco, Arabidopsis and yeast resulted in an accumulation of C_{20} and C_{22} fatty acids [50]. Such chain length preferences have also been observed for the condensing enzymes, KASI, KASII and KASIII, in fatty acid synthase (FAS) complexes.[77,78] *In vitro* and *in vivo* biochemical assays have been conducted to study the substrate preference of thirteen KCS candidates in Arabidopsis (Table 1.2).[79-81] It has been shown that it is the condensing enzyme, not the other three enzymes in an elongase complex, that "recognizes" substrates and "determines" the elongation rounds. Sequence swapping of FAE1 revealed that the domain close to the N-terminus controls the substrate chain length.[82] This was confirmed by a more detailed study of chimeric proteins combining peptide fragments from both ELO2 and ELO3 that elongate C_{18}-acyl-CoA to C_{22}-acyl-CoA and C_{18}-acyl-CoA to C_{26}-acyl-CoA in yeast, respectively. By changing the position and portion of the fragments from both proteins, the region of ELO3 extending from the middle of the sixth trans-membrane domain to the C-terminus was found to contain sequence elements that are both necessary and sufficient for ELO3 to produce C_{26} acyl-CoA. Further mutational studies revealed that the VLCFA chain length is determined by the distance between a lysine residue in the sixth trans-membrane domain and the catalytic active site. [48]

Table1.2: Summary of biochemical characterizations of KCS candidate genes from Arabidopsis

Accession Number	**Characterization Methods**	**Biochemical Functions**				**Ref.**
		Substrates		Products		
		Saturated	Unsaturated	Saturated	Unsaturated	
At4g34520 (*FAE1*)	Over expression; *In vitro* assay with His tagged protein	16:0, 18:0, 20:0	16:1, 18:1	20:0, 22:0	20:1, 22:1	[79,81]
At2g01120 (*KCS1*)	*In vitro* assays with His tagged protein	16:0, 18:0, 20:0	16:1, 18:1	N/A	N/A	[81]
At4g34510 (*KCS2*)		16:0, 18:0, 20:0, 22:0		N/A		
At2g26640		16:0, 18:0, 20:0	16:1, 18:1, 20:1	N/A	N/A	
At1g07720	*In vitro* assays with His tagged protein	No activity for C_{16} to C_{20} substrate				
At1g19440						
At4g34250						
At1g71160						
At5g04530						
At5g43760	Expression in *elo1*Δ*elo2*Δ*elo3*Δ triple mutant and *in vitro* assays with microsomes	18:0, 20:0	18:2	22:0	20:2, 22:2	[79]
At2g16280		18:0,20:0, 22:0	24:1	24:0	26:1	
At1g04220		16:0, 18:0, 20:0	16:1, 18:1, 18:2	20:0, 22:0	20:1, 22:1, 20:2, 22:2	
At1g25450 (*CER60*)	Over expression in wild type yeast	N/A	N/A	26:0, 28:0, 30:0	22:1	[80]

1.3.1.2 β-Ketoacyl-CoA Reductase (KCR)

The gene encoding β-ketoacyl-CoA reductase was first identified in higher plants by Xu et al. using the maize *glossy8* mutant.[83] Based on amino acid sequence homology to known proteins, GLOSSY8 (GL8) was predicted to function as a β-ketoacyl-CoA reductase. GL8 immunoreacted with leek anti-acyl-CoA elongase antibodies, indicating that GL8 is a component of an elongase complex. Further biochemical studies showed that GL8 antibodies strongly inhibited β-ketoacyl-CoA reductase activity. Two sequences in the Arabidopsis genome are homologues of yeast *KCR*, both of which show high expression levels in the stem epidermis.[84] One of the candidate genes, *AtKCR1* (At1g67730), is able to rescue the yeast *KCR* mutant *ybr159w*.[47,85] The *atkcr1* mutant has an embryo lethal phenotype. All this information taken together, *AtKCR1* is a very likely candidate for the KCR involved in very-long-chain fatty acid elongation. However, additional molecular and biochemical characterization are needed to establish the biochemical and biological functions of AtKCR1 in the context of cuticular wax formation.

1.3.1.3 β-Hydroxyacyl-CoA Dehydratase (HCD)

A β-hydroxyacyl-CoA dehydratase (HCD) was partially isolated from rat liver microsomes in the 1970's.[86] The HCD activity in leek epidermis elongation complexes was first demonstrated by antibodies raised against the purified β-hydroxyacyl-CoA dehydratase from rat liver.[87] Direct evidence of the function was provided by production of β-enoyl-CoAs when β-hydroxyacyl-CoAs were incubated with leek microsomes.[88,89] The HCD activity has also been isolated from developing rapeseed.[90]

However, the molecular characteristics of β-hydroxyacyl-CoA dehydratase had remained unknown until very recently when the gene encoding HCD was cloned from yeast and Arabidopsis. [48,91] PHS1 was initially identified as a highly conserved ER protein in a large-scale genetic interaction study of the yeast early secretory pathway. Reduced PHS1 levels resulted in accumulation of long chain bases of sphingolipids. The interactions of PHS1 with the other three components of the elongase complex (ELO2/ELO3, YBR159W and TSC13) were demonstrated by co-immunoprecipitation. Incubation of membranes that are genetically depleted of PHS1 with malonyl-CoA and acyl-CoAs produced only β-hydroxyacyl-CoA

intermediates. The function of this enzyme was finally confirmed by the production of enoyl-CoAs when β-hydroxyacyl-CoAs were incubated with epitope-tagged PHS1.[48] *PAS2*, the functional orthologue of *PHS1*, has been identified and characterized in Arabidopsis.[91] The detection of β-hydroxyacyl-CoA intermediates and the general reduction of VLCFA pools in seed storage triacylglycerols (TAGs) demonstrated the biochemical function of PAS2 as a HCD.

1.3.1.4 β-Enoyl-CoA Reductase (ECR)

TSC13 encoding the β-enoyl-CoA reductase in yeast was identified in a screen for suppressors of the calcium sensitivity of *csg2Δ* mutants that are defective in sphingolipid synthesis [85]. Based on sequence homology, a single-copy *ECR* gene *AtTSC13* was identified in the Arabidopsis genome database.[92] *AtTSC13* successfully rescued the temperature sensitive lethal yeast mutant *tsc13-1elo3Δ*, demonstrating that AtTSC13 functions as an ECR. Coimmunoprecipitation showed the physical interactions between the yeast ELO2/ELO3 condensing enzymes and AtTSC13.[92] Complementation tests [93] revealed that the *AtTSC13* is identical to the *CER10* gene defective in a mutant originally identified by Koorneef *et al.*[94] Further chemical analysis of the *cer10* mutant showed a reduced cuticular wax load and decreased content of TAG in seed and sphingolipids in shoots, indicating that the Arabidopsis ECR is required for the synthesis of all the VLCFA containing-lipids.[93] Because of the universal role of ECR in VLCFA biosynthesis, it is surprising that the ECR-deficient *cer10* mutant still accumulates considerable amounts of cuticular wax as well as VLCFAs in sphingolipids and seed TAGs. This suggests that another ECR exists in Arabidopsis, or alternatively, unknown enzymes functionally similar to the ECR may complement the *cer10* deficiency to maintain VLCFA synthesis.[93]

1.3.2 Wax Components with Primary Functional Groups

1.3.2.1 Chemical Composition

Alkanes, primary alcohols, aldehydes, fatty acids and alkyl esters are the most common wax components and widely distributed among plant species. Primary alcohols, aldehydes and fatty acids are characterized by unbranched saturated carbon chains varying from 20 to 34 carbons. These three compound classes are dominated by homologues with even-numbered

chain lengths. Alkanes have the same chain length range, but are dominated by homologues with odd-numbered chain lengths. Alkyl esters are composed of fatty acids and wax primary alcohols, and therefore the chain lengths range from 38 up to 70 carbons. Esters are usually composed of isomers due to the chain length variations of both acyl and alkyl moieties. There are homologues that the chain lengths of either acyl or alkyl moieties remain constant however the ester chain lengths are in a certain range. The chain lengths of the esters in rye (*Secale cereale* L.) leaves range from 40 to 48 carbons with hexacosyl as the sole alkyl moiety.[95] In contrast, the alkyl moieties of esters in Arabidopsis vary but the acyl moieties are mainly palmitoyl and stearoyl.[96]

1.3.2.2 Pathway Leading to Primary Alcohols

Very-long-chain fatty acids, aldehydes and primary alcohols have similar chain length distribution patterns within the mixture of a given species. These wax components all have primary functional groups with different oxidation state, therefore it has been proposed that acyl-CoAs are the common precursors and primary alcohols are produced through an acyl reduction pathway (Fig. 1.5). Biochemical evidence combined with molecular genetic evidence from various species demonstrated that alcohols are indeed formed by reduction of acyl precursors.

A fatty acyl-CoA reductase (FAR) was first cloned from jojoba embryos.[97] Functional expression of this FAR in *E. coli* produced primary alcohols that were absent in control cells. Over-expression of native and re-synthesized jojoba FAR in high erucic acid rapeseed (*B. napus* cv Reston) plants resulted in elevated amounts of primary alcohols. A homology search using jojoba FAR sequences resulted in a gene family containing eight *FAR*-like genes in the Arabidopsis genome database, and one of them has been found to be identical to *CER4*. Arabidopsis *cer4* mutants show a reduced level of primary alcohols and an increased level of aldehydes, suggesting that CER4 is a fatty acyl-CoA reductase.[98] Heterologous expression in yeast produced C_{24} and C_{26} primary alcohols, confirming the enzyme function as a FAR. Gene expression analysis revealed that *CER4* is expressed in the epidermal cells of aerial tissues and roots.[99]

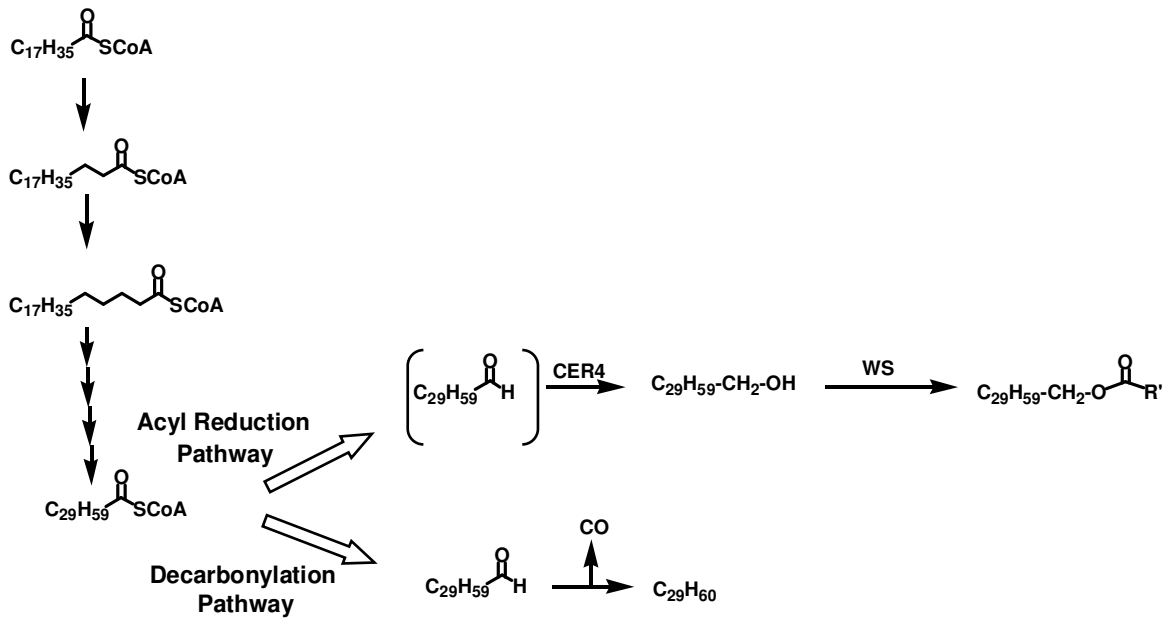

Figure 1.5: Biosynthetic pathways leading to wax components with primary functional groups. CER4 and WS are the enzymes involved in primary alcohol and wax ester production in Arabidopsis, respectively.

Aldehyde-generating reductase activities have been isolated from *Brassica oleracea* and a green alga (*Botryococcus braunii*).[100,101] The aldehyde-generating reductase showed different co-factor requirements from the alcohol-generating reductase isolated from *B. oleracea* (NADH for generating aldehydes, NADPH for generating alcohols). However, to date, genes encoding aldehyde-generating reductases have not been cloned.

The primary alcohols are further used to synthesize wax esters. Partially purified wax synthase (WS) from jojoba catalyzes the formation of esters by transferring acyl chains to primary alcohols.[102] Over-expression of the jojoba *WS* in Arabidopsis under the control of a seed specific promoter resulted in an increase of esters in embryos, which confirmed the biochemical functions *in vivo*.[102] *WS*s have also been cloned and studied in mammalian and bacterial cells.[103,104] There are twelve Arabidopsis genes that have homology to the jojoba *WS*. Very recently a bifunctional synthase that has acyl-CoA:fatty alcohol acyltransferase (wax ester synthase, WS) as well as acyl-CoA:diacylglycerol acyltransferase (DGAT) activity was found to be involved in Arabidopsis stem wax biosynthesis.[105]

1.3.2.3 Pathway Leading to Alkanes

Questions regarding the precursors for alkane biosynthesis were raised as alkanes have predominantly odd-numbered chain lengths, while VLCFA precursors have even-numbered chains. Compelling evidence demonstrated that alkanes do use VLCFA precursors as substrates. Early labeling experiments comparing the radioactivity of potential substrates and product alkanes suggested that alkanes result from elongation rather than condensation.[106] This hypothesis was further supported by incorporation of labeled long chain fatty acids into elongated alkanes. [1-^{14}C]Palmitic and stearic acid were incorporated into C_{27}, C_{29} and C_{31} alkanes when incubated with faba bean (*Vicia faba*) petals. The incorporation could be stopped by addition of an elongation inhibitor.[107] The conclusion that alkanes originate from elongation products was further supported by genetic studies of Arabidopsis in which the mutant *cer6* was found to show drastic reductions of all the wax components including alkanes.

To convert VLCFA precursors into alkanes with odd-numbered chain lengths, one carbon atom must be lost or added. A large body of evidence supports the scenario of loss of carbon. Wax analyses of various species showed that the chain length pattern of the compound classes with odd-numbered carbons shifted by one carbon down from the co-occurring compound classes with even-numbered carbons. Stem waxes of Arabidopsis *cer1* and *cer22* were found to have decreased levels of C_{29} alkane partially compensated by an increase of C_{30} aldehyde. The one carbon loss hypothesis was further confirmed by the results of feeding experiments. C_{30} and C_{32} fatty acids were converted into C_{29} alkane (nonacosane) and C_{31} alkane (hentriacontane), respectively, by faba bean flower petals in the presence of elongation inhibitors [107]. The conversion of C_{30} fatty acid into C_{29} alkane has also been observed for growing *B. oleracea* leaf discs.[108] The overall loss-of-one-carbon process is established, but the genes encoding the enzymes have not been cloned so far.

1.3.3 Wax Components with Secondary Functional Groups

In addition to the wax constituents with primary functional groups, components with secondary functional groups are also detected in many plant cuticular waxes. Compounds with one or two (in rare cases three) functional groups have been described, with various

combinations of hydroxyl and carbonyl groups giving rise to secondary alcohols, ketones, alkanediols, ketols and diketones. The wax components with secondary functional groups are not as widespread as the ones with primary functional groups, and therefore the formation of the secondary functional groups is not as well understood as the biosynthesis of components with primary functional groups.

According to the position of the secondary functional groups, these wax components can be grouped into two broad categories. One of them is characterized by one or more functional groups located on the central carbon of the hydrocarbon chain, or very close to it. Consequently, the two alkyl side chains attached to the functionalized carbon(s) are of the same (or very similar) length. Accordingly, these wax constituents will be designated as "symmetric" secondary compounds in the following sections. The other group of compounds has secondary functional groups located towards one end of the chain. Since their alkyl side chains are necessarily of different length, they will be summarized as "asymmetric" compounds in the following discussion.

Some progress has been made towards the understanding of the biosynthetic pathways leading to symmetric secondary alcohols/ketones in Arabidopsis and *B. oleracea* as well as β-diketones in barley. Therefore, in the following sections, symmetric secondary alcohols/ketones (section 1.3.3.1) and β-diketones (section 1.3.3.3) will be reviewed followed by other related wax components and their hypothetical biosynthetic pathways (sections 1.3.3.2, and 1.3.3.4 to 1.3.3.6).

1.3.3.1 Symmetric Secondary Alcohols and Ketones

As mentioned above, symmetric secondary alcohols/ketones are characterized by the same alkyl side chains attached to the functionalized carbons, e.g., nonacosan-15-ol and nonacosan-15-one. The symmetric secondary alcohols/ketones are usually found together with isomers with functional groups on the carbon next (close) to the central carbon, e.g., nonacosan-14-ol and nonacosan-13-ol. These compounds will be considered as symmetric secondary alcohols/ketones as well. It has been reported repeatedly that nonacosan-15-ol and nonacosan-14-ol are the dominant compounds in *Brassica napus* and *B. oleracea* leaf waxes,

accompanied by small amounts of other isomers and homologues.[109,110] Pea (*Pisum sativum*) leaf wax contains 4.7% secondary alcohols dominated by isomeric C_{31} compounds hentriacontan-16-ol and hentriacontan-15-ol, together with C_{29} alcohol isomers.[39] As closely related to *B. napus* and *B. oleracea*, it is expected that Arabidopsis cuticular wax contains similar wax components to *B. napus* and *B. oleracea* wax. Arabidopsis has been found to contain large amounts of symmetric secondary alcohols, nonacosan-15-ol and nonacosan-14-ol, in its stem wax (30% of the total stem wax). However, in contrast to the *Brassica* species, isomers and homologues of secondary alcohols other than nonacosan-14-ol and -15-ol have not been described in Arabidopsis.

Secondary alcohols (and ketones) are often found in plants/organs where alkanes are the dominant compound class, e.g., in Arabidopsis stem wax and *Brassica* leaf wax. Such a correlation suggested a precursor-product relationship between alkanes and secondary alcohols (and ketones). Early biochemical experiments showed that the carbonyl group of ketones in *B. oleracea* leaf wax originated from a -CH_2- group and not from the -CO- group in the acyl precursors, implying that the acyl chain undergoes elongation before the mid-chain oxygen functionalities are introduced. More direct evidence for the oxidation reactions was provided by incorporation of labeled alkanes into secondary alcohols and ketones.[111] Very recently, a reverse genetics approach led to the discovery of a cytochrome P450 enzyme involved in secondary alcohol and ketone production in Arabidopsis.[112] The mutant *mah1* has reduced levels of secondary alcohols and ketones, indicating that the corresponding P450 enzyme functions as a mid-chain alkane hydroxylase that can first hydroxylate alkanes on the central -CH_2- group and then rebind the resulting secondary alcohols for a second hydroxylation to produce geminal diols which will rearrange into ketones.

The Arabidopsis *mah1* mutant shows a reduction of both nonacosan-14-ol and -15-ol, indicating that MAH1 hydroxylates on both C-14 and C-15, thus targeting a narrow region of CH_2 groups in the substrate. However, because it hydroxylates on (at least) two carbon positions, "limited regiospecificity" will be used to describe MAH1. Incubation of *B. oleracea* leaf discs with radioactively labeled alkanes produced almost equal amounts of nonacosan-14-ol and -15-ol, in agreement with the secondary alcohol composition of the *B.*

oleracea leaf wax.[113] This result demonstrated that the enzyme hydroxylating nonacosane to nonaocsan-14-ol and -15-ol in *B. oleracea* has a similar regiospecificity as MAH1. Because Arabidopsis and *B. oleracea* are closely related species, the similar products are likely produced by the same enzyme family. The similar secondary alcohol composition in Arabidopsis and *B. oleracea* makes it reasonable to believe that the secondary alcohols in *B. oleracea* are biosynthesized by a MAH1-like enzyme. Therefore, the results of the biochemical experiment with *B. oleracea* and the *mah1* mutant wax profile suggested that the limited regiospecificity may be a general property of all the MAH1-like hydroxylases. This hypothesis is yet to be tested in other plant species.

1.3.3.2 Symmetric Secondary/secondary Ketols

In the wax mixture of some species, there are ketols that have similar structural characteristics to symmetric secondary alcohols and ketones. These ketols have one of their functional groups on the central carbon and another functional group on one of the carbons next or close to it, e.g., 15-hydroxynonacosan-14-one and 15-hydroxynonacosan-13-one in the leaf wax of *B. napus* and *B. oleracea*.[114] These compounds will be classified as symmetric secondary/secondary ketols. The symmetric secondary/secondary ketols are accompanied by secondary/secondary ketols with both functional groups on the carbons next to the central carbon, e.g., 16-hydroxynonacosan-14-one in *B. napus* and *B. oleracea.*[110,114] They will also be considered as symmetric secondary/secondary ketols.

The symmetric secondary/secondary ketols were only detected in plants that have large amounts of symmetric secondary alcohols.[110,114] The range of the functional group positions in the symmetric ketols is consistent with that in the co-occurring secondary alcohols, suggesting that the symmetric secondary/secondary ketols are biosynthetically related to symmetric secondary alcohols and ketones. It seems very likely that the two functional groups are introduced in consecutive steps. Once the secondary alcohols are formed, they serve as substrates for further hydroxylations (Fig. 1.6). The substrate-product relationship is yet to be determined, which can be tested by searching for symmetric alkanediol intermediates and ketols in plant species in which symmetric secondary alcohols are present, e.g., Arabidopsis and pea.

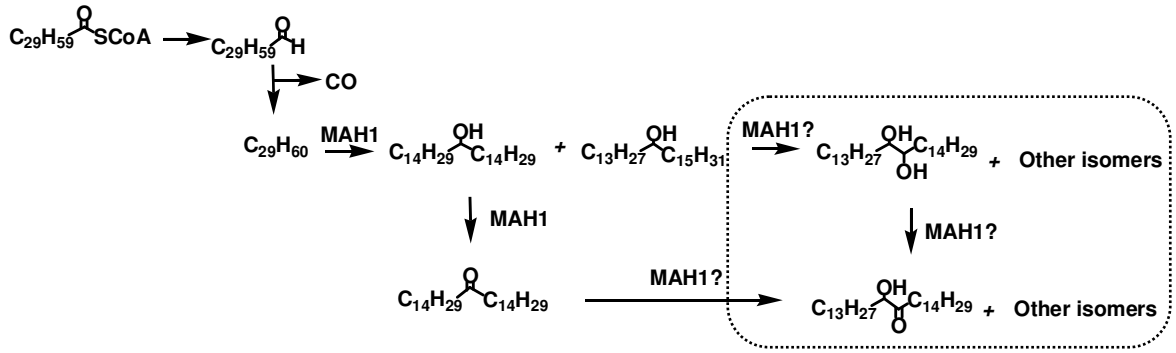

Figure 1.6: Hypothetical pathways leading to ketols in Arabidopsis stem wax. Ketols could be biosynthesized by hydroxylating ketones or alkanediols. These hydroxylation steps could be catalyzed by MAH1. Alkanediols and ketols have not been detected in Arabidopsis stem wax and, therefore, they are depicted in the box.

1.3.3.3 β-Diketones and Their Derivatives

β-Diketones have been detected as the predominant compound class in the leaf waxes of many plant species, e.g., species of Gramineaeand *Eucalyptus*.[115,116] This compound class is dominated by odd-numbered chain lengths ranging from 27 to 33 carbons with two carbonyl groups in 1,3-position to each other. The most frequently detected isomer is hentriacontane-14,16-dione in the waxes of barley (*Hordeum vulgare*) and wheat (*Triticum aestivum*).[117-119] Depending on plant species and organs, diketones with different chain lengths and positions of functional groups have also been detected as major wax constituents, e.g., hentriacontane-8,10-dione in the leaf wax of common box (*Buxus sempervirens*).[120] Hydroxy-β-diketones have been detected along with corresponding diketones in many species, such as 8- and 9-

hydroxyhentriacontane-14,16-dione in the leaf wax of wheat (*T. aestivum*), as well as 5-, 6- and 7-hydroxyhentriacontane-14,16-dione in the wax of oat (*Avena sativa*).[121-123]

Based on biochemical evidence, it has been proposed that the two carbonyl groups in β-diketones are introduced during elongation (Fig. 1.7). The labeling patterns of hentriacontane-14,16-dione in the cuticular wax of the barley mutant *cer-u* fed with [1-^{14}C]acetate and [2-^{14}C]acetate suggested that C-1 and C-2 are the last two carbons introduced into the molecule, i.e., the diketone carbon chain is elongated synthesized by elongation towards the C-1 end of the molecule.[124] Inhibition studies showed that β-diketone and hydrocarbon biosynthesis was catalyzed by different enzyme systems. The β-diketone biosynthesis system was far more sensitive to arsenite, which inhibits elongation of palmitate to stearate, than the hydrocarbon biosynthesis system. The existence of two different elongation systems was confirmed by a study using labeled fatty acids with chain lengths C_{12} to C_{18} (homologues with even-numbered chain lengths only). The incorporation efficiency of all four fatty acids into hydrocarbons was the same. In contrast, lauric, myristic and palmitic acids showed similar incorporation efficiency to produce β-diketones and only trace amounts of stearic acid were incorporated into β-diketones.[125,126] All the biochemical evidence supports a biosynthetic pathway leading to β-diketones through elongation rather than hydroxylation. The pathway for hentriacontane-14,16-dione biosynthesis is illustrated in figure 1.7. Palmitoyl-CoA serves as the primer and is elongated to C_{18} β-ketoacyl chain. Before the β-keto group is reduced as in the normal elongation cycle (section 1.3.1), the C_{18} β-ketoacyl chain is elongated to a C_{20} 3,5-diketoacyl intermediate. Then the C_{20} 3,5-diketoacyl chain undergoes six rounds of normal elongation. After elimination of one carbon, hentriacontane-14,16-dione is produced. Because of the repeated C_2-addition reactions, the functional groups introduced can only be on every other carbon giving rise to a 1,3,5-substitution pattern. In contrast, hydroxylation by MAH1 or MAH1-like enzymes introduces hydroxyl groups on adjacent carbons (section 1.3.3.1).

It has been suggested that β-diketones are biosynthesized on a polyketide pathway that is similar to fatty acid biosynthesis by omitting either one enzyme or a combination of function(s) of KCR, HCD and ECR (section 1.3.1).[124,125] The geometry of the functional groups of β-diketones is in the nature of polyketides, and the currently available evidence

also supports the overall pathway. However, the enzymes responsible for introducing carbonyl groups remain unknown. Hence, the exact nature of the biosynthetic pathway is yet to be discovered.

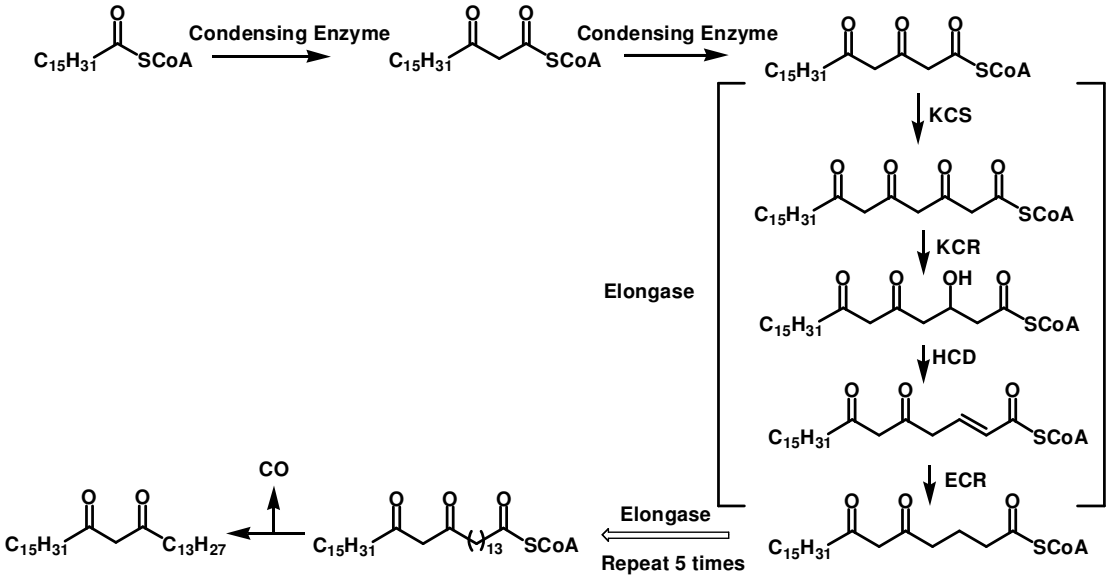

Figure 1.7: β-Diketone biosynthetic pathway. The pathway is illustrated using hentriacontane-14,16-dione as an example (see text).

1.3.3.4 Primary/secondary Bifunctional Components

Compounds with a primary and a secondary (primary/secondary) hydroxyl groups are characterized by even-numbered chain lengths and by one functional group on one end of the carbon chain and another functional group on odd-numbered carbons, resulting in 1,3-, 1,5-, 1,7- and 1,9-bifunctional compounds. In this compound class, the homologous series of 1,2-, 1,4- and 1,6-substitution patterns are often missing or only trace amounts are detected. There are three groups of compounds with primary/secondary bifunctional groups. The first group is characterized by fixed chain lengths and shifting positions of the secondary functional groups, e.g., dotriacontane-1,9-diol, -1,11-diol and -1,13-diol in the leaf cuticular wax of *Myricaria germanica*, as well as 1-hydroxyhentriacontan-7-one, 9-one, 11-one and 13-one in the frond cuticular wax of royal fern (*Osmunda regalis*).[127,128] The second group is characterized by varying chain lengths and fixed position of the secondary functional groups, e.g., 1,3-alkanediols and 3-hydroxyaldehydes with chain lengths ranging from C_{22} to C_{28} in the leaf cuticular wax of castor bean (*Ricinus communis*), as well as δ-lactones with chain

lengths ranging from C_{22} to C_{32} in the leaf cuticular wax of *Cerinthe minor*.[129,130] The third group is characterized by varying chain lengths and shifting positions of secondary functional groups, e.g., hexacosane-1,7-diol, octacosane-1,9-diol and triacontane-1,11-diol in the wax of poppy (Papaveraceae) leaves.[131]

There is nothing known about the biosynthetic pathways leading to wax components with primary/secondary functional groups. There are two major questions about the biosynthetic pathways of the bifunctional wax components: (1) which functional group is introduced first? (2) How are these two functional groups introduced?

It is noteworthy that the chain length distribution patterns of the components with primary/secondary functional groups are similar to those of the components with primary functional groups in the same wax mixture, suggesting that the primary functional groups are introduced in a similar way as those in fatty acids/primary alcohols/aldehydes. It is very characteristic that all the secondary functional groups in the components with primary/secondary functional groups are only on odd-numbered carbons, which is different from the secondary hydroxyl groups in symmetric secondary alcohols. Moreover, the 1,3-, 1,5- and 1,7-geometry of these primary/secondary bifunctional components is in perfect analogy to the geometry of products resulting from polyketide pathways. Therefore, I hypothesize that the secondary functional groups in the components with primary/secondary bifunctional groups with 1,3-, 1,5- and 1,7-substitution patterns are introduced during elongation, in a similar way as polyketides and β-diketones are biosynthesized. Consequently, the secondary functional groups are expected to be introduced before the primary functional groups. The proposed pathway for the introduction of the hydroxyl groups in hexacosane-1,7-diol, octacosane-1,9-diol and triacontane-1,11-diol in Iceland poppy (*Papaver nudicaule*) is illustrated in figure 1.8. The secondary hydroxyl group could be introduced• during an elongation step by omitting the ECR and HCD activities and the resulting β-hydroxyacyl-CoA intermediate would be further elongated and modified into the final products.

• **Footnote1:** In this thesis, the step that functional groups introduced during elongation refers to the step that β-carbons of β-ketoacyl-CoA or β-hydroxyacyl-CoA are not being modified into methylene units due to the lack of certain enzyme activities in an elongase complex.

Alternatively, the functional group introduced during elongation could be a carbonyl group. Instead of β-hydroxyacyl-CoA, β-ketoacyl-CoA intermediates would then be elongated. To produce alkanediols, the carbonyl group could be reduced at a later step on the biosynthetic pathway.

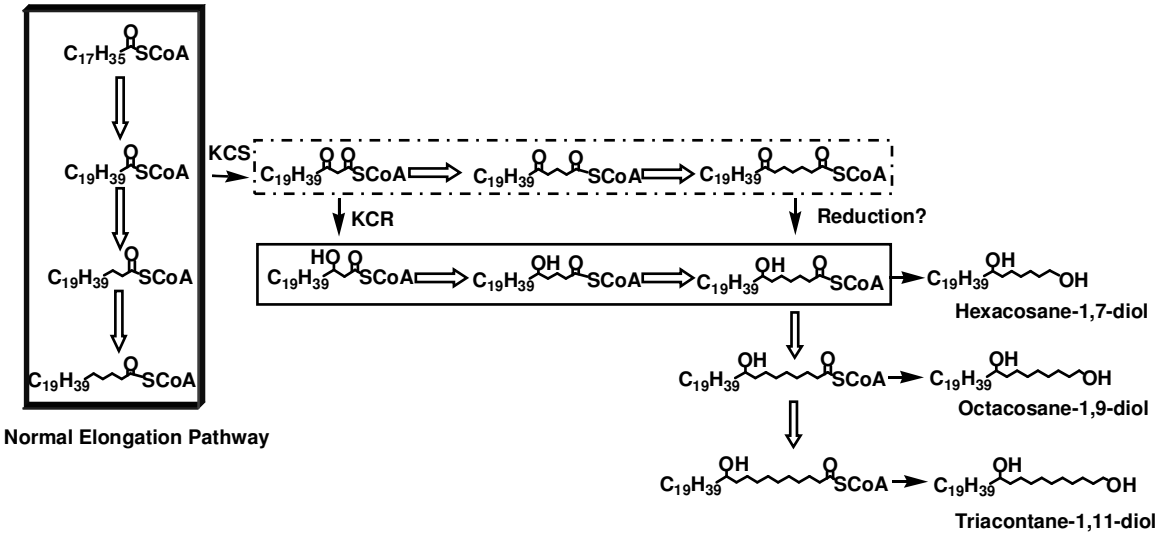

Figure 1.8: Hypothetical biosynthetic pathways leading to primary/secondary alkanediols. The hypothetical pathways are depicted using homologous series of hexacosane-1,7-diol, octacosane-1,9-diol and triacontane-1,11-diol in Iceland poppy as an example. The hydroxyl group could be introduced by omitting ECR and HCD functions during the cycle of elongating C_{20} acyl-CoA to C_{22} acyl-CoA, resulting in C_{22} β-hydroxyacyl-CoA (shown in the box with black line). Alternatively, a carbonyl group could be introduced by omitting KCR, ECR and HCD functions, resulting in C_{22} β-ketoacyl-CoA (shown in the box with dashed line), and then the carbonyl group could be reduced later along the pathway. Reduction of this carbonyl group could occur at a later stage than where it is indicated. Normal carbon chain elongation is shown in the box with shade. Hollow arrows indicate enzyme complex activities, and black arrows indicate a single enzyme activity.

1.3.3.5 Asymmetric Secondary Alcohols and Ketones

In contrast to symmetric secondary alcohols/ketones (see section 1.3.3.1), asymmetric secondary alcohols/ketones are characterized by different side chains attached to a functionalized carbon. The most widely distributed compound in this group is nonacosan-10-ol, detected in most gymnosperm waxes investigated to date, various poppy species, and blue lotus (*Nelumbo nucifera*).[132-136] Other asymmetric secondary alcohols/ketones have also been detected. According to their structural characteristics, these asymmetric secondary alcohols/ketones will be classified into three groups. The first group is characterized by a

fixed chain length and shifting positions of the secondary functional groups, e.g., heptacosan-8-ol, -10-ol and -12-ol in the capsule wax of Iceland poppy.[132] The second group is characterized by varying chain lengths and a fixed position of the secondary functional groups, e.g., 10-ketones with chain lengths of C_{27}-C_{33} in royal fern fronds.[137] The third group is characterized by varying chain lengths and shifting positions of the secondary functional groups, e.g., heptacosan-10-ol, nonacosan-12-ol and hentriacontan-14-ol in fern frond wax.[137]

It has been proposed that all the secondary alcohols/ketones are biosynthesized by hydroxylation. To date, the secondary alcohols that are known to be biosynthesized by MAH1 and MAH1-like enzymes are composed of isomers with hydroxyl groups on the adjacent carbon positions, e.g., nonacosan-14-ol and nonacosan-15-ol in Arabidopsis stem wax and *B. oleracea* leaf wax. However, asymmetric secondary alcohols usually do not contain isomers. When isomers are present, the functional groups are located on alternating carbons. Therefore, if the functional groups in asymmetric secondary alcohols/ketones are introduced by hydroxylation, the regiospecificity of the hydroxylase must be different from MAH1 (or MAH1-like enzymes). Alternatively, the secondary hydroxyl groups can be introduced during carbon chain elongation, analogous to the proposed primary/secondary alkanediol biosynthetic pathway. The functional group could be introduced as a hydroxyl group or a carbonyl group during elongation (Fig. 1.9). To produce secondary alcohols, the hydroxythiol ester (ketothiol ester) would be reduced, and then the end carbon would be eliminated in analogy to alkane biosynthesis.

An alternative way to introduce the functional group is during the C_{10} acyl-ACP to C_{12} acyl-ACP elongation step, i.e., the introduction could happen early on during fatty acid elongation. However, this possibility seems unlikely because the possible intermediates, e.g., 7-hydroxyhexadecanoic acid and 9-hydroxyoctadecanoic acid, have not been detected in plants.

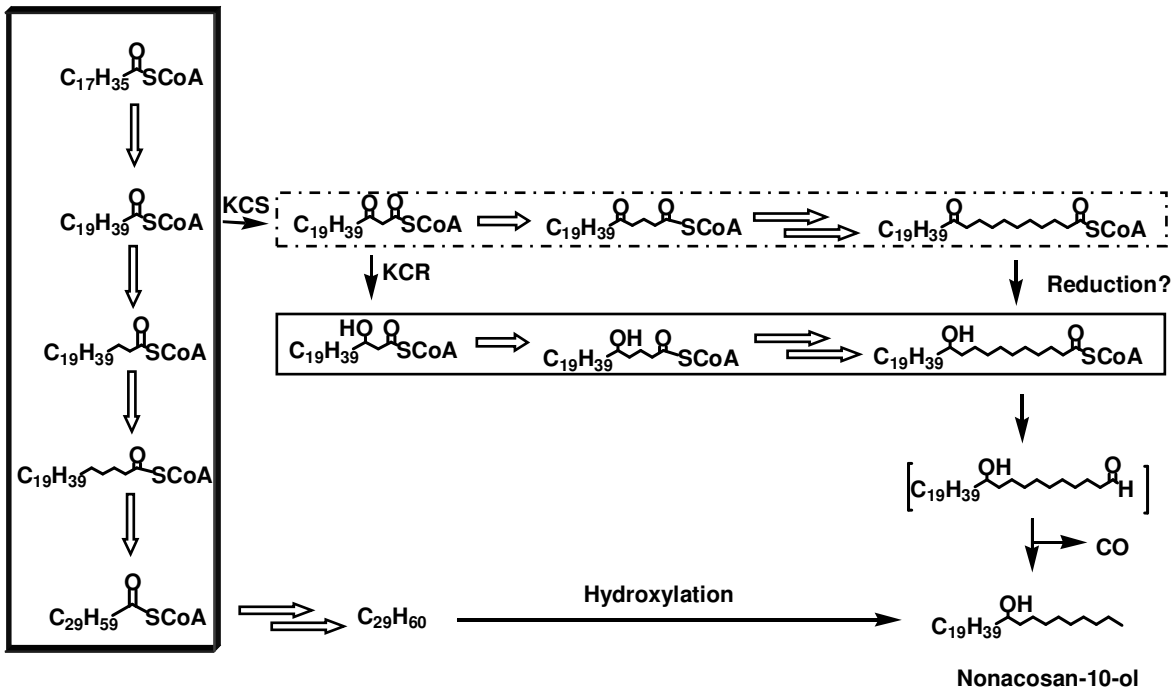

Figure 1.9: Hypothetical pathways leading to asymmetric secondary alcohols. The pathways are depicted using nonacosan-10-ol as an example. The hydroxyl group can be introduced either by hydroxylation of alkanes or by elongation in analogy to primary/secondary alkanediol biosynthesis as illustrated in figure 1.8. The hydroxyl group could be introduced by omitting ECR and HCD functions during the step of elongating C_{20} acyl-CoA to C_{22} acyl-CoA, resulting in C_{22} β-hydroxyacyl-CoA (shown in the box with black line). Alternatively, a carbonyl group could be introduced by omitting KCR, ECR and HCD functions, resulting in C_{22} β-ketoacyl-CoA (shown in the box with dashed line), and then the carbonyl group could be reduced later along the pathway. Reduction of this carbonyl group could occur at a later stage than where it is indicated. Normal carbon chain elongation is shown in the box with shade. Hollow arrows indicate enzyme complex activities, and black arrows indicate a single enzyme activity.

1.3.3.6 Asymmetric Secondary/secondary Alkanediols

Alkanediols and ketols that have one functional group on C-10 or C-12 and another functional group on one of the carbons between C-3 and C-16 have been detected together with asymmetric secondary alcohols, i.e., within a homologue one hydroxyl group shifts the position on adjacent carbons while the other one is fixed on one carbon position. For example, nonacosane-4,10-diol and nonacosane-5,10-diol are frequently detected in the waxes of gymnosperms as important components together with small amounts of nonacosane-3,10-diol, -6,10-diol, -7,10-diol, -10,13-diol and -10,16-diol.[138,139] Hentriacontanediols with one

hydroxyl group on C-12 and the other one ranging from C-2 to C-8 have been found in *Myricaria germanica* leaf wax.[127]

It is reasonable to hypothesize that these asymmetric secondary/secondary alkanediols are biosynthetically related to asymmetric secondary alcohols because the position of one hydroxyl group is the same as that in the corresponding secondary alcohol. The isomerism observed for the other secondary functional groups is in analogy to that of symmetric secondary alcohols, suggesting that these secondary functional groups are introduced by hydroxylation. Because the hydroxyl groups in symmetric secondary alcohols are introduced by hydroxylation of alkanes, it is likely that asymmetric secondary alcohols serve as substrates for hydroxylation to produce asymmetric alkanediols. However, direct experimental evidence is needed to support this hypothesis.

1.4 Objectives

In summary, a variety of constituents with secondary functional groups has been described for plant cuticular waxes. Currently, only little is known about the biosynthesis of these compound classes. There is evidence showing how the secondary groups are introduced for a few of these compound classes. Biochemical and molecular genetic evidence showed that the hydroxyl groups in the symmetric secondary alcohols are introduced by hydroxylation of alkanes. The corresponding ketones are very likely produced by hydroxylation of secondary alcohols on the functionalized carbons. Different from the introduction of the carbonyl groups in symmetric ketones, the carbonyl groups in β-diketones are introduced by elongating acyl-CoA chains. Thus, the current knowledge on the biosynthesis of wax components with secondary functional groups points to two types of pathways greatly differing in substrates and product isomer compositions. The introduction of secondary functional groups by hydroxylation produces isomers with functional groups on the adjacent carbon positions. In contrast, the introduction by elongation produces products without isomers or produces isomers with functional groups located on alternating carbons. Therefore, the isomer patterns can be used to predict how a secondary functional group is introduced, i.e. on which pathway a compound is formed.

The overall goal of the current work was to further establish both types of pathways. The fundamental hypothesis is that all secondary functional groups in the diverse compounds are formed on one of these pathways (Fig. 1.10). This leads to four specific hypotheses, two of them are related to the hydroxylation pathway: (1) the secondary alcohols and ketones can be further hydroxylated to symmetric bifunctional compounds, and (2) the hydroxylases catalyzing all these hydroxylation steps are similar in regiospecificity and substrate preference. The other two hypotheses are related to the elongation pathway: (3) the asymmetric secondary alcohols are formed on this pathway, and (4) a condensing enzyme is responsible for the introduction of hydroxyl groups in asymmetric secondary alcohols during carbon chain elongation. According to these hypotheses, the objectives of this work were

(1) To test the precursor-product relationship between symmetric secondary alcohols and symmetric alkanediols/ketols. This hypothesis is so far only based on the symmetric secondary alcohols and ketols detected in *Brassica napus* and *B. oleracea* leaf waxes. Therefore, complete analyses of more plant species are needed. To this end, detailed analyses of Arabidopsis (wild type, *mah1* mutant and MAH1 over-expressors) (Chapter 3) wax and pea leaf wax (Chapter 4) were conducted.

(2) To test the regiospecificity and substrate preference of MAH1 (and MAH1-like) hydroxylases. To this end, identification and quantification of unknown components in the wax mixtures from plant species likely having MAH1 (and MAH1-like) hydroxylases were conducted. Arabidopsis stem wax (Chapter 3) and pea leaf wax (Chapter 4) were targeted because they are known to contain symmetric secondary alcohols.

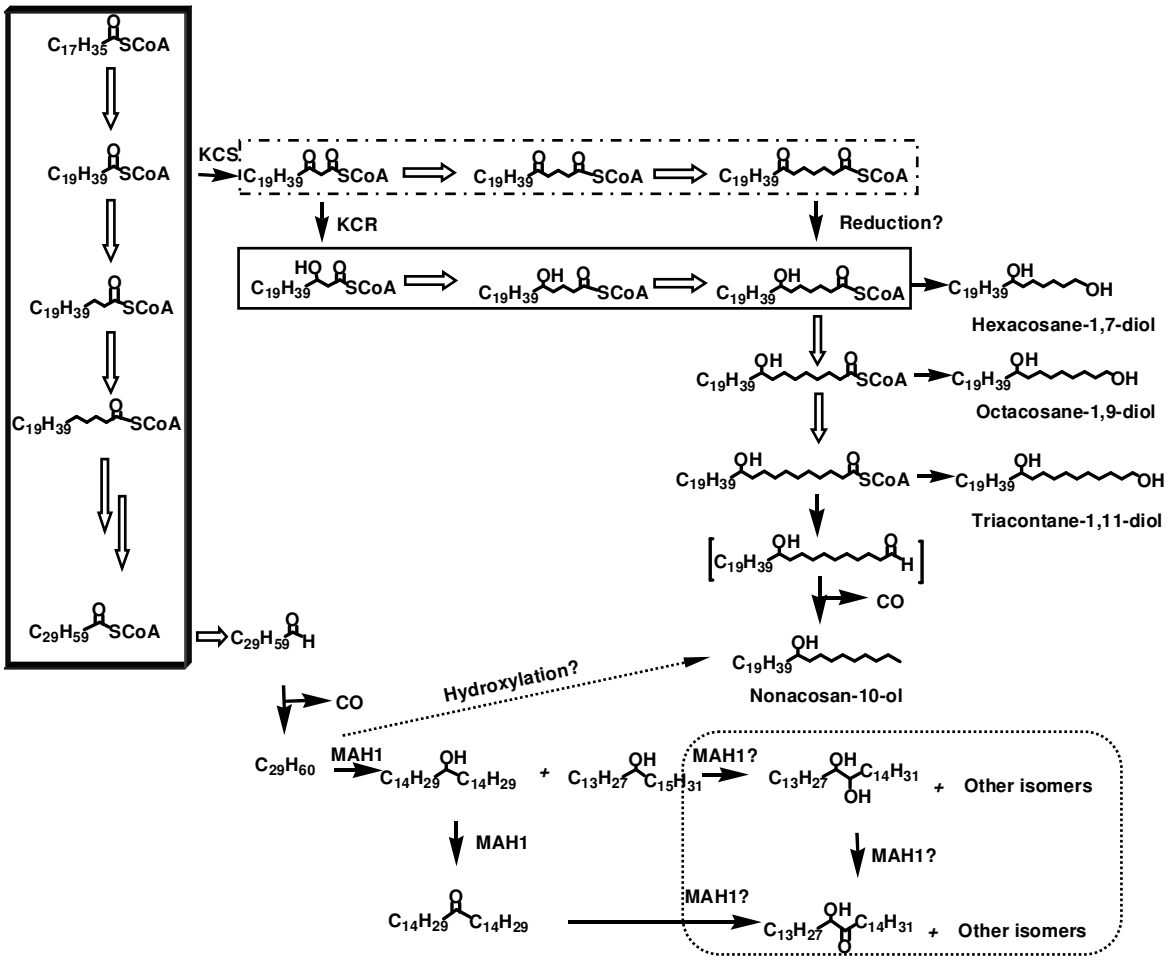

Figure 1.10: Hypothetical biosynthetic pathways leading to wax components with secondary functional groups. There are two fundamentally different pathways to introduce secondary hydroxyl groups: hydroxylation and elongation. The current evidence favors hydroxylation for symmetric secondary alcohols and elongation for asymmetric secondary alcohols as well as primary/secondary alkanediols. For the hydroxylation pathway, the hydroxylation could go beyond secondary alcohols to alkanediols and ketols (shown in the round corner box with dashed line). For the elongation pathway, secondary functional groups can be introduced as a carbonyl group (shown in box with dashed line) or directly as a hydroxyl group (shown in the box with black line). Normal carbon chain elongation is shown in the box with shade. Hollow arrows indicate enzyme complex activities, and black arrows indicate a single enzyme activity.

(3) To test whether asymmetric secondary alcohols are formed by elongation or by hydroxylation. The absence of isomerism and/or the distribution pattern of hydroxyl groups of asymmetric secondary alcohols in some plant species currently favors the elongation hypothesis. Here, two approaches were adopted: (a) analyzing waxes of more species containing asymmetric secondary alcohols in detail and identifying

novel components with asymmetric secondary functional groups (Chapter 5), (b) conducting ^{14}C-labeled experiments using a system that biosynthesizes asymmetric secondary alcohols (Chapter 6).

(4) To provide molecular tools for future studies of the elongation hypothetical pathway. If the hydroxyl groups are introduced during elongation, then the next question is what controls the chain extension round in which the functional group is introduced, i.e., is not further modified into -CH_2-). Since the pathway is similar to polyketide biosynthetic pathways, the complex introducing the functional group could be a polyketide synthase. However, the known plant polyketide synthases catalyze iterative condensation followed by cyclization reactions, e.g., chalcone synthase and stilbene synthase.[140,141] Polyketide synthases that catalyze a single condensation followed by acyl reduction have not been identified in plant. Therefore, attention was focused on other enzyme activities. To produce nonacosan-10-ol, the functional group would be introduced when C_{20} acyl-CoA is elongated. Apparently, the elongase complex responsible for introducing the functional group can "recognize" substrate by chain lengths. Based on the current knowledge of the enzymes involved in elongation (section 1.3.1), only condensing enzymes have substrate chain length preference. Therefore, to provide molecular tools for future studies, cDNAs encoding putative KCS enzymes were cloned from a plant species producing nonacosan-10-ol and functionally characterized (Chapter 7).

Preliminary analysis of wax from yew (*Taxus baccata*) needles showed the presence of large amounts of asymmetric secondary alcohols and unidentified components that may contain novel compounds, therefore, this species was selected for further chemical analysis (Chapters 5). The ^{14}C-labeled biochemical assays and cloning work were conducted using California poppy leaves because this species offered technical advantages for molecular cloning over yew trees (Chapters 6 and 7).

If the above objectives can be reached, this will advance our understanding of the biosynthesis of wax components containing secondary functionalities by further

distinguishing the two fundamentally different pathways, and by characterizing the enzymes catalyzing key reactions on the pathways.

Chapter 2 Material and Experimental Methods

2.1 Plant Materials

Yew (*Taxus baccata*) Needles. Twigs were harvested in spring from yew trees growing continuously on the campus of the University of British Columbia. Mature needles were cut from the twigs using razor blades. Five independent batches of 30 - 40 needles were used for total wax analysis.

Pea (*Pisum sativum*) Leaves. Seeds of *P. sativum* cv Avanta were obtained from IPK Gatersleben Genebank, Germany. Plants were grown in soil:sand (1:1) mixed with 50% vermiculite in plastic pots (diameter 9 cm). The plants were kept in growth chambers under the following conditions: day/night 14 h/10 h, temperature 22°C/18°C, light intensity 300-400 µmol photons/m^2·s, relative humidity 70%. For analysis, fully expanded 13 d-old leaves were harvested randomly (BBCH macro stage 1, Code 15).

Arabidopsis （*Arabidopsis thaliana*）. Seeds of Arabidopsis (ecotype Columbia-0) were spread on 0.8% AT agar plates (recipe see section 2.3.1) and kept in the dark at 4°C for 3 d. Plates were then placed under continuous light (approximately 150 µmol photons/m^2·s photosynthetically active radiation) for 7-10 d at 21°C for germination. Young seedlings were transplanted into soil (1:1 ratio of Sunshine Mix 5 (SunGro Horticulture) and Seeding Mix (West Creek Farms)) and grown under the same light and temperature conditions as above. For the transformed Arabidopsis, seeds were selected on 0.8% AT agar plates containing 25 µg/l hygromycin B. The growth conditions were the same as those for wild type Arabidopsis described above. Stems were collected for wax analyses when they were 10 cm high.

California poppy (*Eschscholzia californica*). Newly emerged leaves were harvested from plants of California poppy growing from March to October on the campus of the University of British Columbia.

2.2 Chemical Analyses

2.2.1 Sample Preparation

Wax Extraction from Yew Needles. Total needle wax was extracted by dipping entire needles into chloroform twice for 30 s at room temperature. A defined amount of *n*-tetracosane was added to the extracts as an internal standard. Needle widths and lengths were measured with a sliding caliper, and the surface area was calculated assuming rectangular needle shape and flat surfaces.

Wax Extraction from Pea Leaves. Total leaf wax extracts were obtained by dipping entire leaves twice for 30 s into 100 ml chloroform that had been heated to approximately 40°C. The resulting leaf extracts were used for identification of compounds and for quantification of isomers and homologues within compound classes.

Wax Extracts for Structure Elucidation. Wax mixtures were separated by TLC (sandwich technique,[142] silica gel, mobile phase chloroform) and localized by staining with primuline and UV-light. Bands were removed from the plates, eluted with chloroform, filtered, concentrated in a stream of nitrogen and stored at 4°C.

2.2.2 Syntheses of Reference Compounds

Octacosane-1,14-diol. Tetradecane-1,14-diol (0.748 g, 2 mmol, Fluka) was oxidized into tetradecanedial by pyridinium chlorochromate (0.518 g, 2.4 mmol) at room temperature for 1 h in anhydrous dichloromethane, and then the solvent was removed under reduced pressure. The remaining solid was extracted with diethyl ether. Column chromatography (hexane/ethyl acetate 9:1) gave 0.4 g tetradecanedial. The purified tetradecanedial (50 mg, 0.14 mmol) then reacted with tetradecylmagnesium chloride (0.14 ml, 0.14 mmol, 1.0 M solution in tetrahydrofuran, Sigma-Aldrich) at 50^{o}C for 20 min. The reaction was quenched by addition of water. The product mixture was extracted with chloroform. Organic phases were combined, dried with anhydrous sodium sulfate, filtered and concentrated by removing all the solvent. The following reactions were on µg level (< 1 mg), so the reagents were not quantified. The above product mixture was reduced by lithium aluminum hydride, and then acetylated as described in section 2.2.4 by acetic anhydride.

5-Hydroxyoctacosanal. 1-Tetracosanol (0.708 g, 2 mmol, Sigma-Aldrich) was oxidized into tetracosanal by pyridinium chlorochromate (0.518 g, 2.4 mmol) at room temperature for 1 h in anhydrous dichloromethane, and then dichloromethane was evaporated under reduced pressure. The resulting solid was washed by diethyl ether to extract tetracosanal. The extract was purified through a silica column (hexane/ethyl acetate 4:1), giving 0.505 g tetracosanal. The purified tetracosanal (176 mg, 0.5 mmol) reacted with 3-butenylmagnesium bromide (1.2 ml, 0.6 mmol, 0.5 M solution in dichloromethane, Sigma Aldrich) while refluxing for 1 h. The reaction was quenched by addition of water, extracted with chloroform, and dried with sodium sulfate, filtered, and concentrated by evaporating solvent under reduced pressure. The crude product was then purified by column chromatography on silica gel (100% hexane to wash away unreacted tetracosanal, then chloroform to elute 5-hydroxy-1-octacosene). 5-Hydroxyoctacosanal was then synthesized using cross metathesis followed by oxidation as described by Njardarson et al.[143] Briefly, 4,4,5,5-tetramethyl-2-vinyl-1,3,2-dioxaborolane (57.6 mg, 0.375 mmol, Sigma Aldrich) and Grubbs catalyst (10.22 mg, 0.0125 mmol, Sigma Aldrich) were added to 5-hydroxy-1-octacosene (60 mg, 0.125 mmol) solution in dichloromethane. The reaction was kept refluxing for 8 h. After the reaction cooled down, the reaction mixture was concentrated by evaporating solvents under reduced pressure and then separated on preparative TLC (Merck) with chloroform as developing solvents. The band containing 5-hydroxyvinylboronate ester (R_f 0.27) was removed from TLC and eluted with chloroform. Purified 5-hydroxyvinylboronate ester (16 mg, 0.03 mmol) was oxidized by trimethylamine *N*-oxide (12 mg, 0.15 mmol, Sigma Aldrich) in refluxing dichloromethane for 4 h. The resulting mixture was dried by removing solvents, derivatized by bis-(*N*,*O*-trimethylsilyl)-trifluoroacetamide (BSTFA) as described in section 2.2.4 and analyzed by GC (condition see section 2.2.3).

2.2.3 Derivatization Reactions

Prior to GC analysis, chloroform was evaporated from the samples under a gentle stream of nitrogen while heating to 50°C. Then the wax mixtures were treated with BSTFA in pyridine (30 min at 70°C) to transform all hydroxyl-containing compounds into the corresponding trimethylsilyl (TMSi) derivatives.

For structure elucidation of unknown compounds, TLC separated compound classes (section 2.2.1) were subjected to the following derivatization(s): (1) hydroxyl groups were acetylated by adding pyridine and acetic anhydride, heating the mixture to 70°C for 5 min, keeping it at root temperature overnight and then removing the solvent in a stream of nitrogen. The products were isolated by addition of water and extraction with chloroform; (2) the unknown constituents were subjected to reduction by excess of lithium aluminum hydride in refluxing tetrahydrofuran overnight, hydrolysis with 10% sulfuric acid, and extraction of the solution with chloroform.

2.2.4 GC Analyses

Program for GC-MS. The qualitative composition of lipid mixtures was studied with capillary GC (5890N, Agilent, Avondale, PA; column 30 m HP-1, 0.32 mm i.d., df = 0.1 µm, Agilent) with helium carrier gas inlet pressure programmed for constant flow of 1.4 ml/min and mass spectrometric detector (EI, 70 eV, 5973N, Agilent). GC was carried out with temperature-programmed on-column injection at 50°C, oven 2 min at 50°C, raised by 40°C/min to 200°C, held for 2 min at 200°C, raised by 3°C/min to 320°C and held for 30 min at 320°C.

Program for GC-FID. The wax mixtures were quantified by capillary GC (5890N, Agilent, Avondale, PA; column 30 m HP-1, 0.32 mm i.d., df = 0.1 µm, Agilent) with hydrogen carrier gas inlet pressure programmed for constant flow of 2.0 ml/min and flame ionization detector at 300°C with nitrogen as makeup gas at 20 psi. GC was carried out with temperature-programmed on-column injection at 50°C, oven 2 min at 50°C, raised by 40°C/min to 200°C, held for 2 min at 200°C, raised by 3°C/min to 320°C and held for 30 min at 320°C.

Qualitative and Quantitative Analyses. Individual wax components were identified by comparison of their mass spectra with those of authentic standards and literature data. The coverage (µg/cm²) of the compound classes and total wax was quantified by GC-FID after adding a defined amount of *n*-tetracosane into total wax extracts as an internal standard by automatically integrating peak areas. Relative compositions (weight%) of isomers within

individual homologues were quantified based on relative abundance of characteristic fragments of mass spectra.

2.3 *In vitro* Protein Assay, Cloning and Characterization

2.3.1 Solutions and Media Preparation

Methanolic HCl. 1 M methanolic HCl was obtained by diluting 3 M methanolic HCl (Sigma-Aldrich) with methanol (100 %).

Salmon Sperm Carrier DNA. Salmon sperm DNA powder was dissolved in distilled water at a concentration of 2 mg/ml, and then aliquoted into 100 µl per Eppendorf tube. The tubes were incubated in boiling water for 5 min for immediate use or stored at -20^{o}C for later use.

LB Medium. The following components were added to the final concentrations indicated: 0.5% yeast extracts, 0.5% NaCl, 1% pepetone, 1% agar (for plates) and distilled water. The mixture was autoclaved at 120^{o}C for 20 min. The selection medium was made by adding filtration-sterilized antibiotics to autoclaved LB. Final concentration of antibiotics in LB medium: Kanamycin (50 mg/l), Ampicillin (100 mg/l).

YPAD Medium. The following components were added to the final concentrations indicated: 1% yeast extract, 2% glucose, 2% bacto pepetone, 0.1% 1-adenine hemisulphate salt, 1.5% agar (for plates) and distilled water. The mixture was autoclave at 120^{o}C for 20 min.

SD and SG Dropout Medium. To make the SD dropout medium for the selection of pYES2-*PKCSI* transformed yeast cells, the following components were added to the final concentrations indicated: 0.67% yeast nitrogen base without amino acids, 2% glucose, 0.01% each of adenine, arginine, cysteine, leucine, lysine, threonine, tryptophan, 0.005% each of aspartic acid, histidine, isoleucine, methionine, phenylalanine, proline, serine, tyrosine and valine, 1.5% agar (for plates) and distilled water. SG dropout medium was prepared in the same way as SD dropout medium was made, except for using galactose in the SG dropout medium instead of glucose.

AT Medium. The following components were added to the final concentrations indicated: 5 mM KNO_3, 2.5 mM KH_2PO_4, 2 mM $MgSO_4$, 2 mM $Ca(NO_3)_2$, 50 μM NaFe(EDTA), 70 μM H_3BO_3, 14 μM $MnCl_2$, 10 μM NaCl, 1 μM $ZnSO_4$, 0.2 μM $NaMoO_4$, 0.05 μM $CuSO_4$, 0.01 μM $CoCl_2$ and 7% Agar (for plates). The pH was adjusted to 5.6 with potassium hydroxide. The above mixture was autoclaved at 121°C for 20 min.

2.3.2 *In vitro* Protein Assay

Acyl-CoA Synthesis. Acyl-CoAs with different chain lengths were synthesized according to the methods by Taylor et al.[144] with modifications. C_{20} acyl-CoA will be used as an example to describe the method. C_{20} fatty acid was dissolved in chloroform and dried under a stream of nitrogen. The following components were mixed with C_{20} fatty acid (0.316 mg, 1 μmol, 1 mM) to the final concentrations indicated in the brackets: 100 μl of 1% Triton X-100 (0.1%), 1.4 mg of CoA lithium salt (5 mM), 50 μl of 200 mM ATP (10 mM), 10 μl of 100 mM DTT (1 mM), 20 μl of 500 mM $MgCl_2$ (10 mM), 500 μl of 160 mM pH 7.2 HEPES-KOH (80 mM) and 320 μl water to a final volume of 1 ml. The mixture was sonicated in ice water for 10 min. 0.25 Units of acyl-CoA synthase from *Pseudomonas* sp. (Sigma) was then added. The reaction mixture was incubated with shaking at 35°C for 2 h, and then used directly or frozen in liquid nitrogen and stored at -80°C.

The synthetic acyl-CoAs were characterized by comparison with authentic standard of C_{18} acyl-CoA (Sigma) on TLC (n-butanol/acetic acid/water: 5/2/3 as developing solvent). Acyl-CoAs were identified by nitroprusside color test.[145]

Plant Microsome Preparation. California poppy (*E. californica*) leaf microsomes were prepared according to the method by Evenson et al. with modifications.[45] Freshly collected poppy leaves (~10 g) were pulverized in liquid nitrogen. The resulting powder was extracted in 80 ml extraction buffer (80 mM HEPES-KOH, pH 7.2, 2 mM EDTA, 320 mM sucrose, 2 mM DTT, and 0.3 mM PMSF). The following steps were carried out at 4°C. The lysate was centrifuged at 5,000 *g* for 10 min. The resulting supernatant was filtered through four layers of cheesecloth, and the filtrate was further centrifuged at 10,000 *g* for 40 min. The supernatant was collected and centrifuged at 106,000 *g* for 1 h (Beckman, 50Ti rotor), and

the resulting microsome pellet was re-suspended in a total of 1 ml 80 mM HEPES-KOH buffer (pH 7.2) with 1 mM DTT and 15% glycerol. The dissolved microsomes were either used immediately or frozen in liquid nitrogen and stored at -80°C. The protein concentration was determined with a commercial protein assay reagent (Bio-Rad) and bovine serum albumin (BSA) as the standard.

Elongation Assays. Solubilized microsomes (200 ng protein) were incubated at 30°C for 90 min (300 µl assays) in 80 mM HEPES-KOH (pH 7.2), 0.5 mM NADPH, 1 mM DTT, 0.005% Triton X-100, 1 mM ATP, 5 mM $MgCl_2$, 0.018 mM [2-^{14}C]malonyl-CoA (American Radiolabeled Chemicals, 50-60 mCi/mmol, 0.1 mCi/ml) and 50 µl synthetic acyl CoA (~50 µM). The reaction was stopped by addition of 300 µl 5 M sodium hydroxide. After heating for 20 min at 80°C, the mixture was neutralized by addition of 300 µl of 6 M hydrochloric acid. Lipids were extracted three times with 300 µl chloroform. The extracts were pooled together, concentrated in a stream of nitrogen and separated on TLC. To visualize the products with radioactivity, a piece of medical X-ray film (GE) was placed directly against the TLC plate, exposed for 4 weeks and developed in a film developer.

2.3.3 Cloning

Cloning of *KCS* cDNAs from California Poppy Leaves. Actively growing poppy (*E. californica*) leaves were collected and frozen in liquid nitrogen immediately. Total RNA was isolated from poppy leaves with RNeasy Plant Mini Kit (Qiagen). 5 µg of total RNA was used for first strand cDNA synthesis with an oligo dT18 primer (Fermentas) and reverse transcriptase (RevertAid H Minus M-MulV RT, Fermentas) in a 20 µl reaction at 42°C for 60 min. The reaction was stopped by heating to 70°C for 10 min. The template RNA was digested by 5 µl RNase at 37°C for 30 min. The resulting cDNA mixture served directly as template for the following PCR. For the homology-based cloning (Chapter 7), the core sequence was obtained by PCR with degenerate primers, Mcon3F and Mcon3R (Table 2.1). The resulting PCR products were separated by gel electrophoresis (1% agarose) and extracted with the QIAquick Gel Extraction Kit (Qiagen). The purified DNA fragments were each cloned into the sequencing vector pSTBlue by blunt end ligation. The clones with DNA insertion were confirmed by colony PCR and inoculated for plasmid preparation. Plasmid

DNAs were purified with QIAprep Spin Miniprep Kit (Qiagen) and sequenced. All the other PCR products mentioned below were cloned and sequenced with the same procedure.

The full length sequences were obtained by Rapid Amplification of cDNA Ends (RACE). For 3'-end amplification of the open reading frame, cDNA was synthesized by incubation of 5 µg of total RNA with AP-primer and reverse transcriptase for 2 h at 37°C. The product served as template in the PCR with the adapter primer AUAP and a gene specific primer (Table 2.1). 5'-Ends were amplified by the Invitrogen 5'-RACE system (Version 2.0) with modifications. The first strand cDNA was synthesized with an oligo dT18 primer and SuperScript II reverse transcriptase (Invitrogen). The resulting cDNA was purified with a SNAP column (Invitrogen). An oligo(dC) tail was added to the purified cDNA with the terminal deoxynucleotidyl-transferase (TdT, Invitrogen). Tailed cDNA was amplified directly by PCR with the Abridged Anchor primer and a gene specific primer (Table 2.1, Eca9 did not require 5'-RACE). To obtain the full length sequences, PCR was performed with gene specific primers with Phusion high fidelity DNA polymerase (Finnzymes, Finland).

Table 2.1: Summary of primers used in cloning

Name of Primers	Sequences	Notes
Mcon3F	5' AAYCTNGGHGGVATGGG 3'*	PKCSI core sequence
Mcon3R	5' ATGTAKGCBATRTCRTACCA 3'*	PKCSI core sequence
AP	5'GGCCACGCGTCGACTAGTACTTTTTTTTTTTTT TTT 3'	3' RACE
AUAP	5' GGCCACGCGTCGACTAGTAC 3'	3' RACE
Abridged Anchor	5'GGCCACGCGTCGACTAGTACTGGIIGGGIIGGGIIG 3'	5'RACE
Pcon5RACE1-1	5' AGACTAGCATTGAACGGTCGTTACC 3'	PKCS1 5' RACE
Pcon3RACE	5' GAAGCTAGGACTTTCTGAATGG 3'	PKCSI 3' RACE
PKCSF4-1BamH1	5' ACGGATCCGGAGATATCTAATGGATGATC 3'	Yeast expression Arabidopsis expression
PKCSR8-2EcoR1	5' GGGAATTCACCTCTAGTACTTAACTGAAG 3'	Yeast expression
PKCSNhe1F	5' ACGCTAGCGGAGATATCTAATGGATGATC 3'	Arabidopsis expression
Eca2-5RACE1	5' AAGGAACTCTACAAGTAACAGG 3'	Eca2 5' RACE
Eca2-3RACE1	5' GTTAG TTCAAGAAGTGAAGC 3'	Eca2 3' RACE
Eca9-3RACE1	5' GAATTATGGAGGAAATTATGG 3'	Eca9 3' RACE
Eca2F	5' AGATCAACCAAAAACACCAAG 3'	Eca2 Full length
Eca2R	5' TGAGAAGAAGATCCATCCATCC 3'	Eca2 Full length
Eca9F	5' CTTTCAATCTAGCTAGAAACC 3'	Eca9 Full length
Eca9R	5' TAGACCAGTCACAGGATATTG 3'	Eca9 Full length

* Y: C+T, N: G+T+C+A, H: A+T+C, V: G+C+A, R: G+A, B: C+T, K: A+T

Construction of Plasmids. For sequencing, PCR products amplified with Phusion High-Fidelity DNA Polymerase (New England Biolabs) were ligated to the *ECo*RV site of pSTBlue. To produce the pYES2-*PKCSI* construct, the open reading frame of PKCSI was amplified using the primers PKCSF4-1BamH1 and PKCSR8-2EcoR1 (Table 2.1) and introduced into pSTBlue by blunt end ligation. The plasmid pSTBlue-*PKCSI* was then digested with *Eco*R1 and *Bam*H1. The resulting *PKCSI* fragment was gel purified and ligated to the corresponding sites of pYES2. The other two plasmids, pVKH18-*PKCSI* (for over-expression in Arabidopsis under the control of the CaMV35S promoter) and pVKH18-FAE1p-*PKCSI* (for over-expression in Arabidopsis seeds under the control of the FAE1p promoter) were constructed with the same procedure. The primers used for amplifying the corresponding *PKCSI* fragments are listed in table 2.

***Escherichia coli* Competent Cells**. *E. coli* cells (strain Top10) were inoculated in LB medium and grown on a shaker at 37^{o}C overnight. 50 µl overnight cultures were inoculated into 5 ml of fresh LB medium and grown on a shaker at 37^{o}C until OD_{600} is around 0.5-0.6. The tube was kept on ice for 5-10 min. The cells were divided into 1.5 ml centrifuge tubes (1-1.5 ml each) and collected by centrifuging at 10,000 rpm for 1 min. The pellets were gently re-suspended in 1 ml ice cold calcium chloride (0.1 M) and kept on ice for at least 20 min. The cells were collected again by centrifuging at 10,000 rmp for 1 min. The pellets were gently re-suspended in 100 µl ice calcium chloride. The suspension was kept on ice for 4 h for further use. For long term storage, glycerol was added to 15% of the suspensions and the cells were kept at -80^{o}C.

***Agrobacterium tumefaciens* Competent Cells.** *A. tumefaciens* cell stock (strain GV3101) was inoculated in 5 ml LB medium and grown overnight at 28^{o}C. The overnight cultures (2 ml) were added to 50 ml LB medium and incubated at 28^{o}C until the culture reached an OD_{600} of 0.5-1.0. The culture was chilled on ice and centrifuged at 10,000 rpm for 5 min. The supernatant was discarded. The pellet was then re-suspended in 1 ml of ice cold calcium chloride solution (20 mM) and immediately dispensed to 100 µl aliquots. The aliquots were used directly for transformation or frozen in liquid nitrogen and stored at -80^{o}C for later use.

***E. coli* Transformation.** A ligation mixture (2-4 µl) was added into 50 µl competent cells and kept on ice for 20 min. While waiting, the tube was gently flicked to mix ligation products with cells. After 20 min, the cells were heat shocked for 60 s in a water bath at 42°C, transferred immediately onto ice and chilled for 2 min. LB medium (600 µl) was added to the cells transformed with ligation products. The cells were then incubated for 45 min at 37°C with shaking. The transformed cells were plated onto LB plates with antibiotics. For white/blue selection, IPTG and X-Gal were spread evenly on plates before plating transformants. The plates were incubated at 37°C for 16-18 h.

Yeast (*Saccharomyces cerevisiae*) Transformation. Plasmid pYES2-*PKCSI* was transformed into *Saccharomyces cerevisiae* (strain InvSc1) by the modified lithium acetate method.[146] The over-night yeast cultures (2 ml) was collected by centrifuging at 10,000 rpm for 2 min. The pellet was washed twice with 1 ml sterilized water. The following components were then added to the yeast cells: 240 µl of 50% v/v PEG3500, 36 µl of 1.0 mM LiAc, 50 µl of 2 mg/ml salmon sperm carrier DNA, 0.1-1 µg of plasmid DNA and water to make the final volume of 360 µl. The above transformation mixture was vortexed for 2 min and then incubated at 42°C for 1 h. The cells were collected by centrifuging at 10,000 rpm for 1 min and washed with 1 ml sterilized water by gentle pippeting. The washed cells were collect by centrifugation and re-suspended in 100 µl sterilized water. All 100 µl cell suspensions were then evenly spread on SD dropout plates and incubated at 30°C for 2-3 d.

***A. tumefaciens* Transformation.** Plasmids (0.1-1 µg) were added to 100 µl competent cells and kept on ice for 45 min. The tube containing cells was put into liquid nitrogen or 100% ethanol pre-chilled at -80°C. When the cells became white, the tube was taken out and thawed at room temperature. LB medium (500 µl) was added to the tube and incubated at 28°C for 2-3 h. The transformed cells were spread on plates and incubated for 2-3 d at 28°C.

2.3.4 Biochemical Characterization of Full Length cDNAs

Yeast Expression. Colonies were picked from SD plates, inoculated in 5 ml SD dropout medium and incubated at 30°C for 30 h. The cells were collected by centrifuging 2 ml of the

culture at 10,000 rpm for 2 min. The pellet was washed three times with sterilized water, re-suspended in 100 µl sterilized water and evenly spread on a SG dropout plate for expression. The plate was incubated at 30^{o}C for 4 d before GC analysis of fatty acyl chain compositions.

Arabidopsis Transformation. The first batch of bolting inflorescence stems of Arabidopsis was clipped to encourage proliferation of many secondary stems. One week before the plants were ready, *Agrobacterium* carrying *PKCSI* on a binary vector was prepared. A single *Agrobacterium* colony carrying the *PKCSI* was inoculated in 5 ml of LB medium with kanamycin. On the second day, the overnight culture was transferred to 200 – 500 ml LB with kanamycin. The medium was incubated overnight at 28^{o}C . On the third day, the cells were collected, re-suspended by addition of 5% freshly made sucrose solution to OD_{600} ~0.8. Before dipping, Silwet L-77 was added to the cell mixture to a concentration of 0.02%. When the *Agrobacterium* solution was ready, Arabidopsis plants were held upside down and dipped into the *Agrobacterium* solution for 5-10 s with gentle agitation. The dipped plants were covered by a piece of black plastic for 16-24 h to maintain high humidity and to keep them away from light. The plants were grown under normal condition afterwards.

Chemical Analysis of Compositions of Fatty Acyl Chains in Transformed Yeast and Arabidopsis. For yeast cell analysis, the cells on SG dropout plates were scraped off by a pipette tip and placed into a glass vial. For Arabidopsis seed analysis, ~ 50 seeds were placed in a glass vial. Methanolic HCl (2 ml, 1 M) was added to the vial and heated to 80^{o}C for 2 h. After the vial had cooled down, 2 ml of 15% sodium chloride solution was added. The resulting mixture was extracted three times with 2 ml hexane for each extraction. The organic phases were combined, dried with anhydrous sodium sulphate and filtered. The solvent was evaporated under reduced pressure. The dried sample was derivatized before GC analyses.

Chapter 3 Composition and Biosynthesis of Secondary Alcohols, Ketones, Alkanediols and Ketols in the Cuticular Waxes of Arabidopsis

3.1 Introduction

Symmetric secondary alcohols and corresponding ketones had been detected as the major constituents of cuticular waxes in several studies.[39,147,148] In *Brassica oleracea* leaf wax, small amounts of α- and β-ketols had been detected together with the major wax constituents nonacosan-14-ol, nonacosan-15-ol and nonacosan-15-one.[114,148] Because the functional groups of the ketols in *B. oleracea* leaf wax are located at similar positions as those of the co-occurring secondary alcohols and ketones, it was postulated that symmetric secondary alcohols serve as substrates for ketol biosynthesis.[114] However, direct evidence for the biosynthetic relationship between secondary alcohols/ketones and ketols is lacking to date. Therefore, one of the goals of this chapter was to test the biosynthetic relationship between secondary alcohols/ketones and wax components containing two functional groups (objective 1 of the thesis).

It had been reported repeatedly that Arabidopsis stem wax contains large amounts of symmetric secondary alcohols and ketones. Because Arabidopsis is closely related to *B. oleracea*, and because both species have relatively similar wax compositions, it seemed likely that ketols could be present in Arabidopsis stem wax. Thus, it should be possible to use Arabidopsis mutants to test a precursor-product relationship between secondary alcohols and ketols. The mutant *mah1* has recently been described to lack secondary alcohol biosynthetic activity,[112] providing a suitable system to test the biosynthetic relationship between both compound classes. If ketols are indeed derived from secondary alcohols, then they should not be detected in the wax of the *mah1* mutant. In contrast, if the precursor-product relationship does not exist, the ketol content would not be affected in the mutant wax.

Arabidopsis can also serve as a system for studying the enzyme(s) involved in the biosynthesis of wax ketols. If a biosynthetic relationship exists between secondary alcohols

and ketols, hydroxylations seem likely to be involved in the formation of ketols, in which process one or more hydroxylases required. Therefore, in addition to testing the biosynthetic relationship between secondary alcohols and ketols, I also wanted to know the regiospecificity and substrate preference of this unknown hydroxylase and to compare them with the regiospecificity and substrate preference of MAH1 (objective 2 of the thesis). The regiospecificity and substrate preference of MAH1 and of the unknown hydroxylase can be inferred from the isomer patterns of secondary alcohols/ketones and ketols, respectively.

The current work was conducted in two steps. First, wax was extracted from wild type Arabidopsis stems, fractionated on TLC and analyzed by GC-MS in order to identify unknown compounds that were suspected to contain secondary functional groups. In the second step, waxes were extracted from wild type Arabidopsis stems, *mah1* mutant stems and MAH1 over-expressing leaves. For each wax mixture, the constituents containing secondary functional groups were quantified separately. Based on the isomer and homologue compositions, the biosynthetic relationships between these constituents and the hydroxylases involved in their biosynthesis will be discussed.

3.2 Results

To identify all the homologues and isomers of secondary alcohols and ketones, and to identify alkanediols and ketols, Arabidopsis stem wax was extracted with chloroform and TLC separated into five fractions of interest. Two fractions were suspected to contain secondary alcohols (R_f 0.56) and ketones (R_f 0.80) as they co-migrated with respective standards. The other three fractions were found to contain unidentified compounds. The first one, designated as compound class **A** (R_f 0.65), migrated between secondary and primary alcohols. The second one, designated as compound class **B** (R_f 0.32), co-migrated with primary alcohols. The third one, designated as compound class **C** (R_f 0.19), migrated between primary alcohols and fatty acids. The fractions containing secondary alcohols and ketones were analyzed first to identify unknown isomers (3.2.1), and then the other three fractions were investigated (3.2.2).

3.2.1 Identification of Secondary Alcohol and Ketone Isomers

The mass spectra of nonacosan-14-ol, -15-ol and nonacosan-15-one, the major wax constituents in Arabidopsis stems, have been deposited in public databases. Therefore, these compounds can be easily identified by characteristic mass spectral fragments. The goal of this work was to identify minor secondary alcohols and ketones. The mass spectral fragmentation patterns of these minor components were expected to be very similar to those of the major secondary alcohols and ketones, but to differ by 14 mass units for some fragments.

3.2.1.1 Secondary Alcohols

The TLC fraction co-migrating with secondary alcohols was separated by GC after derivatization with bis-(*N,O*-trimethylsilyl)-trifluoroacetamide (BSTFA). The GC trace showed five peaks. The mass spectra of all compounds in the five peaks showed characteristic OTMSi fragments *m/z* 73 $[TMSi]^+$ (TMSi: trimethylsilyl), *m/z* 75 $[(CH_3)_2Si{=}OH]^+$ and *m/z* 103 $[CH_2OTMSi]^+$, indicating the presence of hydroxyl groups. The common fragmentation pattern suggests that the five GC peaks are a homologous series. The most dominant GC peak in this fraction was found to contain nonacosan-14-ol and nonacosan-15-ol. Both compounds were identified by pairs of the characteristic secondary alcohol ions ($[C_nH_{2n}OTMSi]^+$ and $[C_mH_{2m}OTMSi]^+$) originating from α-cleavage of the C-C bonds adjacent to the secondary functional groups (Fig. 3.1).[149] These fragments are generated due to the easy loss of one electron from the lone pair electrons on oxygen. In addition, another pair of *α*-fragments *m/z* 271 ($[C_{13}H_{26}OTMSi]^+$) and *m/z* 327 ($[C_{17}H_{34}OTMSi]^+$) were detected in the mass spectrum of the same GC peak. Thus, nonacosan-13-ol was identified. The compounds in the other four GC peaks had molecular ions $[C_nH_{2n+1}OTMSi]^+$ and corresponding daughter ions $[M\text{-}CH_3]^+$ (resulting from loss of a CH_3 of a TMSi group) that differed by 14 mass units, indicating that these compounds belonged to a homologous series of secondary alcohols. Based on the molecular ions obtained from each GC-peak, the remaining four homologues were identified as C_{27}, C_{28}, C_{30} and C_{31} secondary alcohols. Pairs of α-ions were used to identify heptacosan-12-ol, -13-ol and -14-ol, octacosan-13-ol and -14-ol, triacontan-14-ol and -15-ol, as well as hentriacontan-14-ol, -15-ol and -16-ol. Overall, thirteen secondary alcohols were identified in this fraction.

In Arabidopsis, the C_{27}, C_{29} and C_{31} chain lengths of secondary alcohols had been reported before.[98,150,151] Nonacosan-14-ol and -15-ol had been identified as the major wax components while isomer compositions of the other two homologues had not been specified. The C_{28} and C_{30} homologues were detected for the first time in Arabidopsis stem wax. All the thirteen secondary alcohols detected here had been identified in *Brassica napus* and *B. oleracea* leaf waxes.[148]

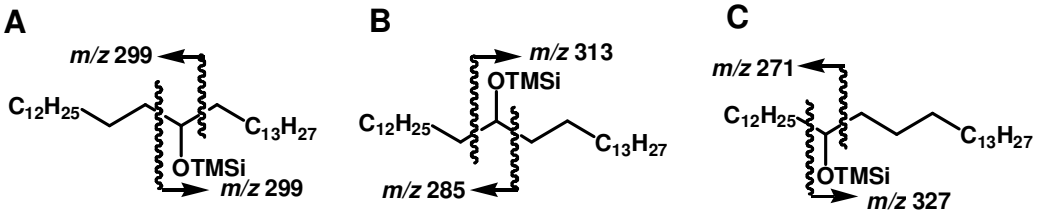

Figure 3.1: Structures and mass spectral fragments of the TMSi derivatives of secondary alcohols in the stem wax of Arabidopsis. (A) Nonacosan-15-ol, (B) nonacosan-14-ol and (C) nonacosan-13-ol.

3.2.1.2 Ketones

The TLC fraction co-migrating with ketones was separated by GC, resulting in three GC peaks. Nonacosan-15-one was identified in the major GC peak by the characteristic ketone fragments *m/z* 225 $[CH_3(CH_2)_{13}CO]^+$ and *m/z* 241. Pairs of ketone α-ions *m/z* 211 $[CH_3(CH_2)_{12}CO]^+$ and 239 $[CH_3(CH_2)_{14}CO]^+$ as well as *m/z* 197 $[CH_3(CH_2)_{11}CO]^+$ and 253 $[CH_3(CH_2)_{15}CO]^+$ suggested the presence of nonaocosan-14-one and nonacosan-13-one. To confirm the isomer composition, the ketone fraction was reduced to secondary alcohols by lithium aluminium hydride. After reduction, only C_{29} secondary alcohols were detected by GC-MS. In addition to the α-fragments originating from nonacosan-15-ol TMSi ether, pairs of fragments *m/z* 271 and 327 as well as *m/z* 285 and 313 were detected, demonstrating the presence of nonacosan-13-ol and -14-ol. Thus, before lithium aluminium hydride reduction, the fraction must have contained nonacosan-13-one and -14-one. The compounds in the two minor GC peaks also showed ketone fragmentation patterns. Based on the molecular ions, the compounds in these two peaks were identified as ketones with chain lengths C_{28} and C_{30}. Because the abundance of the C_{28} and C_{30} homologues was very low, the isomer composition of these two homologues could not be determined. In summary, nonacosan-13-one, -14-one and -15-one were identified together with two other minor ketone homologues with chain lengths C_{28} and C_{30}. Nonacosan-15-one was the only compound that had been reported in

Arabidopsis wax before. In *B. napus* and *B. oleracea* leaf waxes, nonacosan-13-one, -14-one and -15-one had been detected together with C_{28}, C_{30} and other homologous ketones. The isomer compositions of the C_{28} and C_{30} ketones had not been resolved.[148]

3.2.2 Identification of Alkanediols and Ketols

3.2.2.1 Secondary/secondary α-Ketols

Compound class **A** migrated between secondary and primary alcohols on TLC, and therefore likely contained compounds with a secondary hydroxyl group and one (or more) carbonyl group(s). GC analysis of compound class **A** after BSTFA derivatization resulted in one peak. The mass spectrum of the compound in this peak showed fragments *m/z* 73, 75 and 103 characteristic for OTMSi groups, but lacked a diol signal *m/z* 147 $[(CH_2)_2SiOSi(CH_3)_3]^+$, indicating the presence of only one hydroxyl group (Fig. 3.2A).[152] It was identified as a secondary hydroxyl group by the characteristic α-fragments *m/z* 299 ($[CH_3(CH_2)_{13}CHOTMSi]^+$) and *m/z* 285 ($[CH_3(CH_2)_{12}CHOTMSi]^+$) (Fig. 3.2C). When two α-ions (X: $[CH_3(CH_2)_nCHOTMSi]^+$ and Y: $[CH_3(CH_2)_mCHOTMSi]^+$) originate from one molecule, the molecular ion can be inferred by piecing the two fragments together (M = X + Y - CHOTMSi). Hence, if *m/z* 299 and 285 resulted from the same compound, the molecular ion would have to be at *m/z* 482 and its daughter ion ($[M\text{-}CH_3]^+$) at *m/z* 467, both of which were missing in the mass spectrum obtained from the GC peak. Instead, the combination of the signals at *m/z* 510 and 495 indicated that they were a molecular ion and a daughter ion ($[M\text{-}CH_3]^+$), respectively. The discrepancy between the predicted and detected molecular ions was clear evidence showing that *m/z* 299 and 285 originated from two isomers. This was supported by the detection of two other fragments *m/z* 225 ($[C_{15}H_{29}O]^+$) and *m/z* 211 ($[C_{14}H_{27}O]^+$) that could be interpreted as α-bond fragments of the carbonyl groups in two isomers. The α-ions from CH_2OTMSi groups and from carbonyl groups together could be used to infer ketol structures that matched the molecular ion. Thus, the ketol isomers contained in the GC peak were identified as 15-hydroxynonacosan-14-one and 14-hydroxynonacosan-15-one.

Alternative structures in fraction **A**, containing additional hydroxyl groups, could also give the fragments described so far for this fraction. However, the presence of additional hydroxyl

groups seems unlikely, as ions containing two hydroxyl groups could not be detected in the mass spectrum of the TMSi derivative, and because the TLC behaviour of the compounds indicated the presence of two rather than three functional groups.

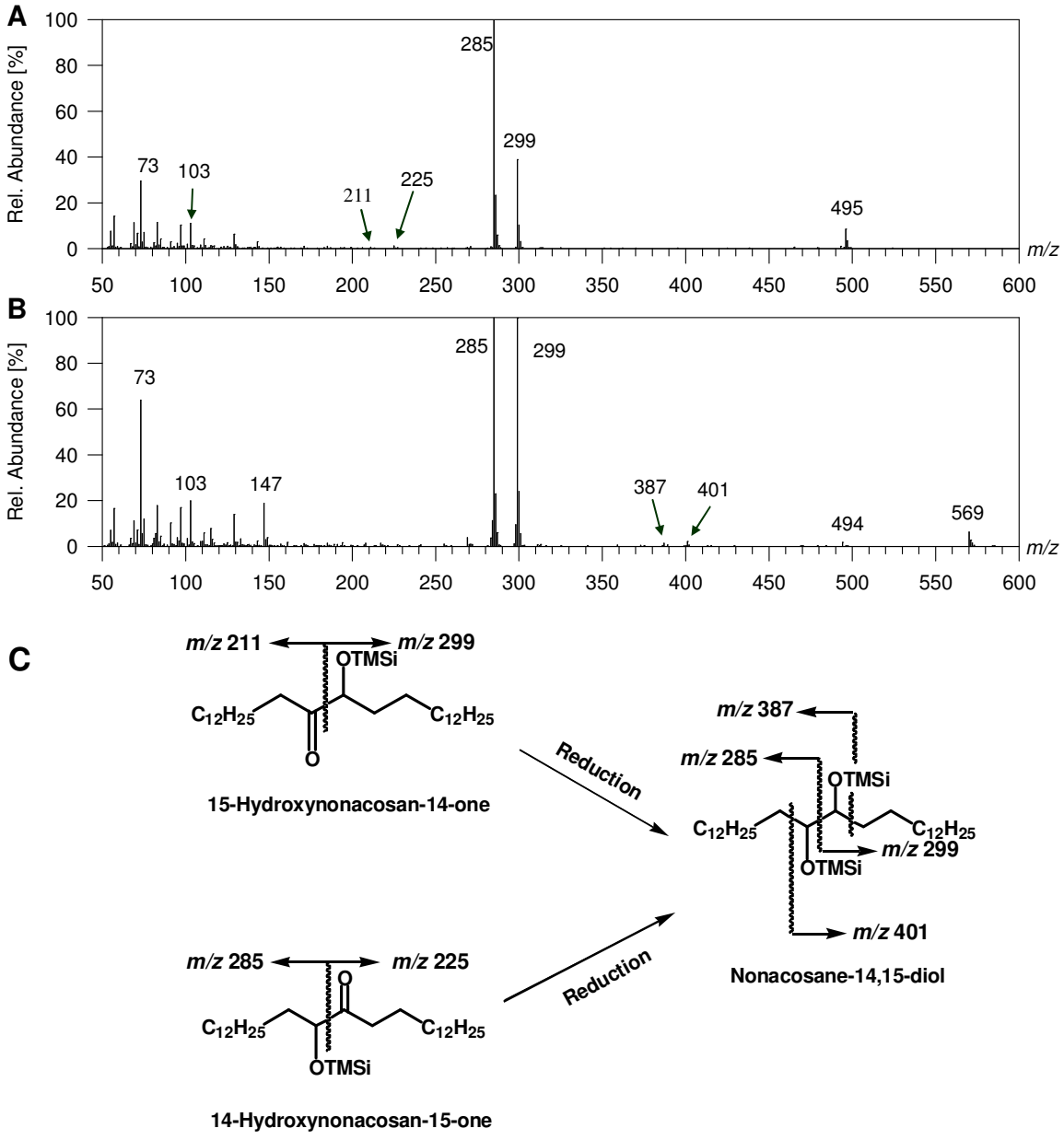

Figure 3.2: Mass spectra and fragmentation diagram of secondary/secondary α-ketols in the stem wax of Arabidopsis. (A) Mass spectrum of the bis TMSi ether of the secondary/secondary α-ketol isomer mixture, (B) mass spectrum of the bis TMSi ether of nonacosane-14,15-diol, and (C) mass spectral fragmentation diagram of the TMSi derivatives of the α-ketols and nonacosane-14,15-diol.

To also exclude the possibility of the presence of additional carbonyl groups, fraction **A** was reduced by lithium aluminium hydride and then derivatized by BSTFA. The mass spectrum of the resulting compound showed not only the characteristic alcohol fragments *m/z* 73, 75 and 103, but also a diol fragment *m/z* 147, suggesting the presence of two hydroxyl groups. The alkanediol nature and positions of the functional groups were confirmed by a pair of α-fragments *m/z* 285 ($[C_{14}H_{28}OTMSi]^+$) and *m/z* 299 ($[C_{15}H_{30}OTMSi]^+$) containing one OTMSi group, and another pair of α-fragments *m/z* 387 ($[C_{15}H_{29}(OTMSi)_2]^+$) and *m/z* 401 ($[C_{16}H_{31}(OTMSi)_2]^+$) containing two OTMSi groups (Fig. 3.2A and C). For the alkanediols, the molecular ion can be inferred by piecing together an α-ion containing one OTMSi group and an α-ion containing two OTMSi groups. For example, the molecular ion here would be *m/z* 584 ($[C_{29}H_{58}(OTMSi)_2]^+$), inferred from the combination of *m/z* 299 ($[C_{15}H_{30}OTMSi]^+$) and *m/z* 387 ($[C_{15}H_{29}(OTMSi)_2]^+$). The predicted molecular ion was confirmed by another pair of α-ions (*m/z* 285 and 401) and was further supported by the daughter ions *m/z* 569 ($[M-CH_3]^+$) and *m/z* 494 ($[M-TMSiOH]^+$) (Fig. 3.2B). Ions $[C_nH_{2n-2}(OTMSi)_3]^+$ could not be detected in the mass spectrum of the TMSi derivative after lithium aluminium hydride reduction, excluding the presence of a third functional group. All this evidence taken together, the reduced compound was identified as nonacosane-14,15-diol, thus confirming the presence of two functional groups on carbons 14 and 15 in all the compounds in fraction **A**. Therefore, the unknown compounds in fraction **A** were identified as 15-hydroxynonacosan-14-one and 14-hydroxynonacosan-15-one.

Finally, the structure assignments of 15-hydroxynonacosan-14-one and 14-hydroxynonacosan-15-one were confirmed by comparing their mass spectral data to the literature.[114] These two α-ketols had not been described for Arabidopsis stem wax, but had been identified in *B. napus* and *B. oleracea* leaf waxes.[114]

3.2.2.2 Secondary/secondary β-Ketols

GC analysis of fraction **B** after BSTFA derivatization resulted in one peak. The mass spectrum of TMSi derivatives of compounds in this GC peak showed characteristic fragments for OTMSi groups at *m/z* 73, 75 and 103, but lacked a diol signal with *m/z* 147, indicating the presence of only one hydroxyl group (Fig. 3.3A). The presence of hydroxyl

groups was confirmed by a series of secondary alcohol α-ions differing by 14 mass units. Thus, it appeared that the components in fraction **B** contained at least one secondary hydroxyl group. Fraction **B** co-migrated with a primary alcohol standard, yet the mass spectral characteristics of the fraction were different from those of primary alcohols. Therefore, the compounds in this fraction must have contained a secondary hydroxyl group together with one (or more) other functional group(s). A series of ketone α-fragments ($[CH_3(CH_2)_nCO]^+$) suggested the additional presence of a carbonyl group (Fig. 3.3C). The fragment *m/z* 130 had previously been reported as a characteristic ion for β-ketol functional geometry.[137] Thus, the fragment *m/z* 130 confirmed the presence of at least one carbonyl group and, more importantly, pointed to the 1,3-geometry between a hydroxyl and a carbonyl group. The molecular ion *m/z* 510 and the daughter ion *m/z* 495 ($[M\text{-}CH_3]^+$) indicated a C_{29} carbon chain length of the ketols. One ketone α-ion and one of the secondary alcohol α-ions were expected to belong together, representing the two complementary pieces of a ketol molecule. Pairs of α-ions from both types belonging to the same compound could be recognized based on their identical relative abundance. Thus, the most abundant compound, 16-hydroxynonacosan-14-one, could be assigned by piecing the fragments *m/z* 285 and 211 together. This structure was confirmed by another secondary alcohol ion *m/z* 387. In the same way as 16-hydroxynonacosan-14-one was identified, 15-hydroxynonacosan-13-one and 13-hydroxynonacosan-15-one were then identified and accounted for all the α-ions detected. Alternative structures that contain additional hydroxyl groups can also give the fragments described so far. However, these structures were excluded because α-ions containing two or more OTMSi groups were not present in the mass spectra of this fraction.

To confirm the tentative structures, fraction **B** was reduced by lithium aluminium hydride and derivatized by BSTFA. The mass spectral data showed a characteristic diol ion *m/z* 147, suggesting the presence of two hydroxyl groups. The secondary/secondary diol structure was confirmed by a series of α-ions *m/z* 271 ($[CH_3(CH_2)_{11}CHOTMSi]^+$), *m/z* 285 ($[CH_3(CH_2)_{12}CHOTMSi]^+$) and *m/z* 299 ($[CH_3(CH_2)_{13}CHOTMSi]^+$) containing one OTMSi group, and another series of α-ions *m/z* 415 ($[C_{17}H_{33}(OTMSi)_2]^+$), *m/z* 401 ($[C_{16}H_{31}(OTMSi)_2]^+$) and *m/z* 387 ($[C_{15}H_{29}(OTMSi)_2]^+$) containing two OTMSi groups (Fig. 3.3B and C). Ions containing three OTMSi groups were not detected in the mass spectrum,

excluding the presence of a third functional group. The α-ions containing two OTMSi groups showed a low relative abundance due to the loss of TMSiOH (*m/z* 90), giving corresponding daughter ions *m/z* 325, *m/z* 311 and *m/z* 297. A 14 mass unit difference between ions within each series of fragments indicated the presence of isomers. Thus, pairs of α-ions allowed the identification of nonacosane-14,16-diol and nonacosane-13,15-diol. This was supported by the detection of the molecular ion *m/z* 584 ($[C_{29}H_{58}(OTMSi)_2]^+$) and its daughter fragments *m/z* 569 ($[M\text{-}CH_3]^+$) and 484 ($[M\text{-}TMSiOH]^+$). The identification of nonacosane-14,16-diol and -13,15-diol confirmed the presence of two isomers with functional groups on C-14,16 and C-13,15 in fraction **B**. Therefore, the unknown compounds in this fraction were identified as 16-hydroxynonacosan-14-one, 15-hydroxynonacosan-13-one and 13-hydroxynonacosan-15-one.

Finally, by comparing the mass spectral data to the literature, 16-hydroxynonacosan-14-one, 15-hydroxynonacosan-13-one and 13-hydroxynonacosan-15-one were identified.[114] All three β-ketols were identified for the first time in Arabidopsis stem wax, but had been described in *B. napus* and *B. oleracea* leaf waxes before.[114]

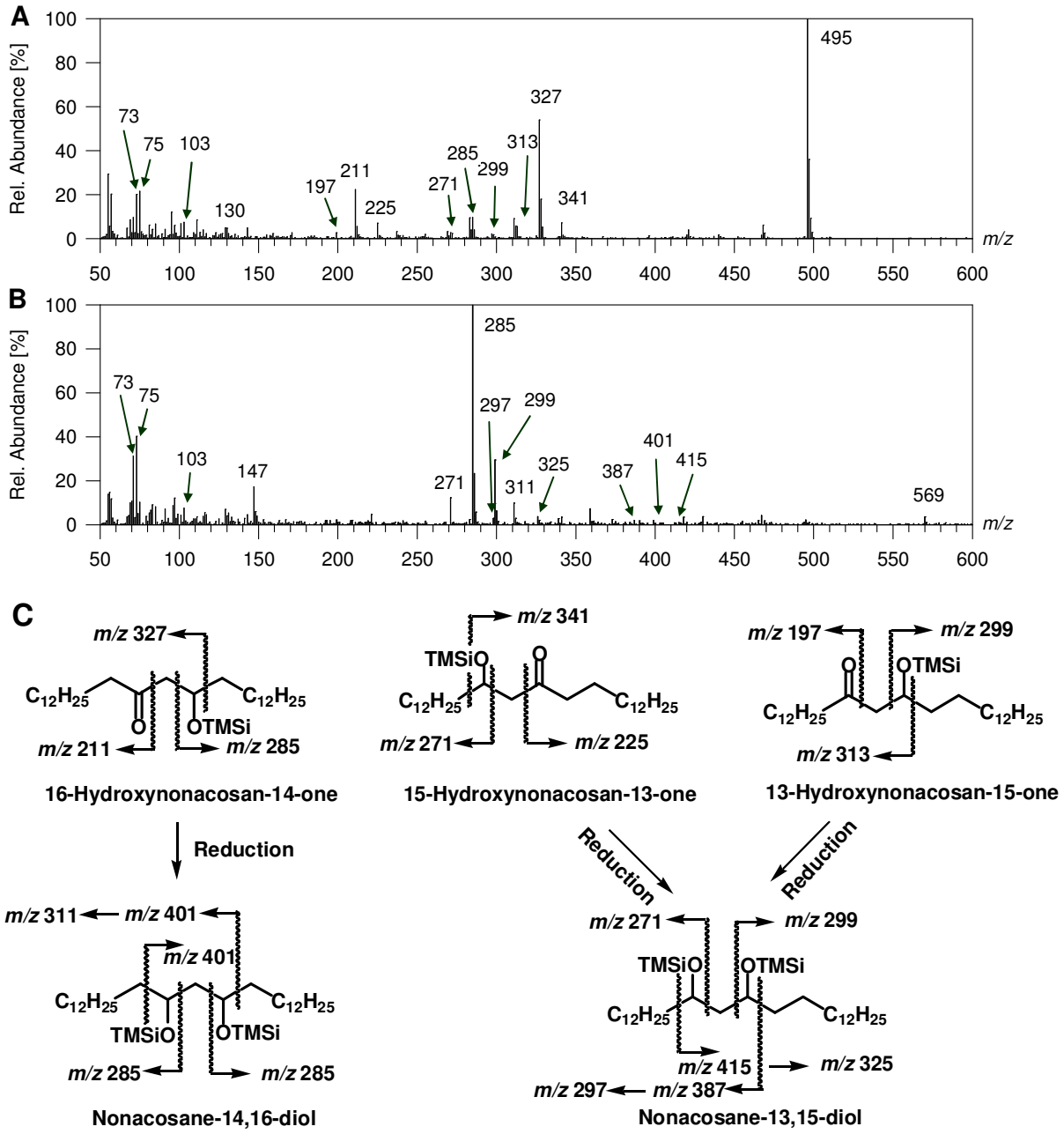

Figure 3.3: Mass spectra and fragmentation diagram of the secondary/secondary β-ketols in the stem wax of Arabidopsis. (A) Mass spectrum of the bis TMSi ethers of the β-ketol isomer mixture, (B) mass spectrum of the bis TMSi ethers of the secondary/secondary β-alkanediol isomer mixture, and (C) mass spectral fragment diagram of the TMSi derivatives of the β-ketols and β-alkanediols.

.

3.2.2.3 Secondary/secondary Alkanediols

It appeared that the compounds in fraction **C** contained two (or more) secondary functional groups because they migrated between primary alcohols and fatty acids on TLC. GC analysis of fraction **C** after BSTFA derivatization resulted in one peak. The mass spectral data of the TMSi derivatives showed the same fragments as those of the mixture of nonacosane-14,16-diol and nonacosane-13,15-diol TMSi derivatives (Fig. 3.4 and Fig. 3.3B), indicating that fraction **C** contained nonacosanediols. If the α-fragments *m/z* 271 and 299 originated from nonacosane-13,15-diol TMSi ether alone, they would be expected to have the same relative abundance. However, the relative abundance of the fragment *m/z* 299 was much higher than that of *m/z* 271. The difference in relative abundance between these two ions in the mass spectrum of this fraction was much more dramatic than that in figure 3.3B, suggesting that, in addition to nonacosane-13,15-diol, this fraction must have contained nonacosanediol at least one other isomer producing fragment *m/z* 299 to account for its high relative abundance. Because only three α-ions were detected in the mass spectrum, the α-ion *m/z* 299 could only originate from an isomer that also gave the signals at *m/z* 271 or 285. Thus, nonacosane-14,15-diol was the only possible structure that could account for the high relative abundance of *m/z* 299. To confirm that there were no carbonyl groups, fraction **C** was subjected to lithium aluminum hydride reduction. The mass spectral data of the resulting mixture was the same as those before lithium aluminum hydride treatment (data not shown). The presence of additional hydroxyl groups seems unlikely because ions $[C_nH_{2n-2}(OTMSi)_3]^+$ were not detected. Thus, fraction **C** was found to contain nonacosane-14,16-diol, nonacosane-13,15-diol and nonacosane-14,15-diol. These alkanediols were identified for the first time in plant waxes, but had been synthesized before.[114]

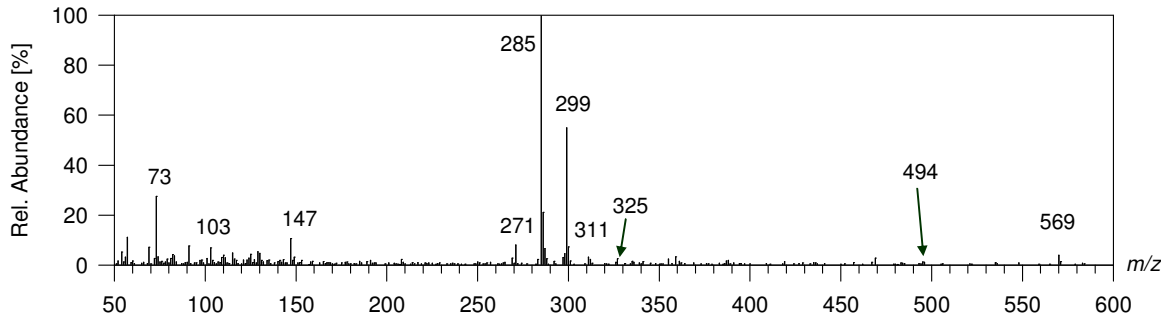

Figure 3.4: Mass spectrum of the bis TMSi ethers of the secondary/secondary alkanediol isomer mixture in the stem wax of Arabidopsis.

3.2.3 Quantification of Secondary Alcohols, Ketones, Alkanediols and Ketols

Secondary alcohols and ketones in the waxes of wild type Arabidopsis stems, *mah1-1* mutant stems and MAH1 over-expressing leaves were quantified by GC-FID (coverage, μg/cm^2). Because of the low abundance and co-elution with other wax components in the total wax mixtures, the coverages of alkanediols and ketols were estimated by the ratio between the relative abundance of their α-ions and the relative abundance of corresponding α-ions of secondary alcohols in the mass spectra. The isomers within each homologue could not be separated by GC because differences in the geometry of functional groups between the multiple isomers were too small. Consequently, the relative amounts (%) of isomers were quantified by the relative abundance of characteristic α-ions in the mass spectra.[153]

3.2.3.1 Stem Wax of Arabidopsis Wild Type

Arabidopsis wild type stem wax contained 9.5% (2.4 μg/cm^2) of secondary alcohols. The C_{29} homologue accounted for 98% of the fraction, while only trace amounts of the other homologues between C_{27} and C_{31} could be detected. Each of the homologues with even-numbered chain lengths was dominated by one isomer. For example, the C_{28} and C_{30} secondary alcohols were dominated by octacosan-14-ol (91%) and triacontan-15-ol (93%), respectively (Table 3.1). In contrast, the isomers were more evenly distributed within the homologues with odd-numbered chain lengths. The C_{29} homologue was composed of nonacosan-14-ol and -15-ol in a ratio of 1:2. The C_{27} homologue contained heptacosan-12-ol,

-13-ol and -14-ol in a ratio of approximately 1:4:5. The C_{31} homologue contained equal amounts of hentriacontan-15-ol and -16-ol.

Ketones were the second dominant compound class, accounting for 24% (6.0 μg/cm^2) of the total stem wax. The C_{29} homologue accounted for over 99% of this compound class. Only trace amounts of C_{28} and C_{30} homologues were detected. The C_{29} homologue contained 94% of nonacosan-15-one and 6% of nonacosan-14-one. Due to the extremely low amounts of the C_{28} and C_{30} homologues, their isomer compositions could not be quantified (Table 3.1).

The Ketols were minor components in Arabidopsis wild type stem wax. The coverage of the α-ketols was 0.16 μg/cm^2 (0.1% of the total stem wax mixture). Due to their low abundance, the coverage of the β-ketols could not be quantified by GC-FID. The β-Ketols were thus estimated as 4% of the α-ketols by the abundance of their α-ions[2]. Within the α-ketols, 14-hydroxynonacosan-15-one and 15-hydroxynonacosan-14-one accounted for 73% and 27%, respectively (Table 3.1). Within the β-ketols, 16-hydroxynonacosan-14-one amounted to 80% while 15-hydroxynonacosan-13-one and 13-hydroxynonacosan-15-one amounted to 9% and 11%, respectively (Table 3.1).

Since the alkanediols co-eluted with triacontanal in GC analysis of total wax mixtures, the coverage of the alkanediols could not be quantified by GC-FID. However, the alkanediol amounts could be assessed using a procedure similar to that used for quantification of the β-ketols, and were found to be present at approximately 33% of the α-ketol level (0.05 μg/cm^2)[3]. Nonacosane-14,15-diol was the most abundant isomer (61%) of all the alkanediols. The other two isomers, nonacosane-14,16-diol and noancosane-13,15-diol, contributed 31% and 8%, respectively (Table 3.1).

---

[2] **Footnote 2**: Calculation of the ratio between β-ketols and α-ketols: The sum of the abundance of fragments *m/z* 271, 285 299 in the β-ketol GC-MS peak was divided by sum of the abundance of fragments *m/z* 285 and 299 in the α-ketol peak. The calculation is based on the assumption that mass spectral detector has the same sensitivity to similar fragments.

[3] **Footnote 3**: The total abundance of alkanediol ions is $I_{271}+ (I_{299}-I_{271}) + (I_{285}-I_{299})/2$. In the formula, I_{271} is the abundance of the ion originating from nonacosane-13,15-diol, $(I_{299}-I_{271})$ is the abundance of the ion originating from nonacosane-14,15-diol and $(I_{285}-I_{299})/2$ is the abundance of the ion originating from nonacosane-14,16-diol.

Table 3.1: Relative homologue and isomer compositions (%) of secondary alcohols, ketones, secondary/secondary alkanediols, ketols and alkanes in the total wax mixture of wild type Arabidopsis stems.[a]

Homologue chain length	Homologue composition	Isomer composition within homologues					Homologue composition
		C-12	C-13	C-14	C-15	C-16	
Secondary Alcohols							**Alkanes**
C_{27}	tr[b]	8.5 ± 0.9	39.3 ± 0.3	52.1 ± 0.4			0.8 ± 0.2
C_{28}	tr		9.7 ± 0.5	90.7 ± 0.2			tr
C_{29}	98.4		1.2 ± 0.02	36.4 ± 0.7	62.4 ± 0.9		95.2 ± 0.5
C_{30}[c]	tr			7.3	92.7		0.8 ± 0.1
C_{31}[c]	tr			4.2	49.1	46.7	3.1 ± 0.7
Ketones							
C_{28}	tr						
C_{29}	100		0.2 ± 0.01	5.7 ± 1.2	94.1 ± 0.3		
C_{30}	tr						
		C-14,15	**C-14,16**	**C-13,15**			
Alkanediols[e]							
C_{29}	100	60.9 ± 1.3	30.9 ± 1.4	8.1 ± 1.2			
		C-14[d],15	**C-14,15[d]**				
α-Ketols[e]							
C_{29}	100	27.4±1.4	72.6±1.7				
			C-14 [d],16	**C-13[d],15**	**C-13,15[d]**		
β-Ketols[f]							
C_{29}	100		80.2 ± 2.4	8.9 ±1.4	10.9 ±1.7		

[a] The values are given as mean (of five independent samples) ± standard error (SE) unless otherwise specified. Homologues were quantified within compound classes, and isomers were quantified within each chain length.

[b] tr: <0.5%.

[c] The isomer composition was calculated based on only two GC-runs of the TLC-separated samples, thus SE is not shown.

[d] Positions of the carbonyl groups.

[e] The isomer compositions were calculated by relative abundance of α-ions.

[f] The isomer composition was calculated by averaging three sets of α-ions from one GC-MS run of the TLC-separated sample.

3.2.3.2 Stem Wax of *mah1* Mutants

Three *mah1* mutant alleles, *mah1-1*, *mah1-2* and *mah1-3*, with T-DNA insertions in different regions of the gene had previously been described. RT-PCR showed that *MAH1* expression is not detectable in *mah1-1* while it is detectable but strongly reduced in the other two alleles.[112] In the same study, stem cuticular waxes of homozygous *mah1* mutants were analyzed and compared with the wax of the Arabidopsis wild type. It was found that the drop in wax levels was well correlated with the reduced *MAH1* expression levels. The secondary alcohols in *mah1-1* stem wax were decreased to 1% of the wild type level, while the secondary alcohols and ketones in *mah1-2* and *mah1-3* stem waxes were partially reduced (Table 3.2). Thus, the knockout mutant *mah1-1* provided a convenient tool to study the biosynthetic relationship between secondary alcohols and ketols. In the following, the stem wax of *mah1-1* was further analyzed to quantify the residual compounds containing secondary functional groups.

Table 3.2: Composition of Arabidopsis wild type and *mah1* mutant stem waxes. Total wax amounts and coverages of individual compound classes ($\mu g/cm^2$) are given as mean values (of nine independent sample) $\pm$ SE.[112]

	Wild Type	***mah1-1***	***mah1-2***	***mah1-3***
Alkanes	9.6 $\pm$ 0.4	11.2 $\pm$ 0.7	11.8 $\pm$ 0.3	13.7 $\pm$ 0.5
Secondary Alcohols	2.4 $\pm$ 0.1	0.1 $\pm$ 0.0	1.7 $\pm$ 0.1	2.5 $\pm$ 0.1
Ketones	6.0 $\pm$ 0.2	tr[a]	1.5 $\pm$ 0.1	3.2 $\pm$ 0.2
Aldehydes	1.1 $\pm$ 0.2	0.4 $\pm$ 0.1	1.2 $\pm$ 0.2	0.9 $\pm$ 0.2
Fatty Acids	0.4 $\pm$ 0.1	0.1 $\pm$ 0.0	0.4 $\pm$ 0.1	0.4 $\pm$ 0.1
Primary Alcohols	2.4 $\pm$ 0.3	1.3 $\pm$ 0.1	1.6 $\pm$ 0.3	2.4 $\pm$ 0.2
Esters	1.0 $\pm$ 0.1	0.9 $\pm$ 0.1	0.9 $\pm$ 0.1	1.5 $\pm$ 0.2
Triterpenoids	0.6 $\pm$ 0.1	0.5 $\pm$ 0.1	0.6 $\pm$ 0.1	0.8 $\pm$ 0.0
Unidentified	1.8 $\pm$ 0.2	1.2 $\pm$ 0.2	1.4 $\pm$ 0.2	1.6 $\pm$ 0.2
Total Wax	25.1 $\pm$ 0.6	15.7 $\pm$ 1.0	21.2 $\pm$ 0.6	27.1 $\pm$ 0.1

[a] tr: trace, < 0.05 $\mu g/cm^2$

Only very small amounts of secondary alcohols were detected in the *mah1-1* stem wax (0.1 $\mu g/cm^2$). The isomer composition of the mutant secondary alcohols was very similar to that of the wild type stem wax. All the secondary alcohols detected in wild type stem wax were found in the mutant, except for triacontan-14-ol (Table 3.3). Octacosan-14-ol (92%) and triacontan-15-ol (99%) strongly dominated the C_{28} and C_{30} homologues, respectively.

Heptacosan-12-ol, -13-ol and -14-ol were found in a ratio of approximately 2:3:6. The C_{29} homologue contained mainly nonacosan-14-ol and -15-ol in a ratio of 1:2. The two major isomers within the C_{31} homologue, hentriacontan-15-ol and -16-ol, had similar abundance (48% each). In addition to secondary alcohols, trace amounts of C_{29} ketones were detected in *mah1-1* stem wax. The C_{29} ketones were found to be composed of 97% nonacosan-15-one and 3% nonacosan-14-one (Table 3.3). Alkanediols and ketols were not detected in *mah1-1* stem wax.

Table 3.3: Relative homologue and isomer compositions (%) of secondary alcohols, ketones and alkanes in the total stem wax of Arabidopsis mutant *mah1-1*. Homologues were quantified within compound classes, and isomers were quantified within each chain length.

Homologue chain length	Homologue composition[a]	Isomer composition within homologues[a]					Homologue composition [b]
		C-12	C-13	C-14	C-15	C-16	
Secondary Alcohols							**Alkanes**
C_{27}	tr[c]	16	27	57			0.9 ± 0.1
C_{28}	tr		8	92			0.5 ± 0.1
C_{29}	99		1	37	61		96.5 ± 0.1
C_{30}	tr			1	99		0.6 ± 0.2
C_{31}	tr			4	47	49	1.5 ± 0.2
Ketones							
C_{29}	100			3	97		

[a] The homologue and isomer compositions were calculated based on one GC-MS run of the TLC-separated sample and, thus, no standard errors are given.
[b] Values are given as mean (of five independent samples) ± standard error (SE).
[c] tr: trace, <0.5%

3.2.3.3 Leaf Wax of MAH1 Over-expressing *mah1* Mutants

The leaf wax of Arabidopsis wild type contains a large percentage of alkanes but is absent of secondary alcohols. Therefore, leaves provide a convenient system to study the biochemical properties of MAH1. Plants ectopically over-expressing *MAH1* under the control of the CaMV35S-promoter had previously been generated in the *mah1-1* background.[112] In the present study, the leaf waxes from individual lines of these transgenic plants were analyzed. Two lines (a and b) were found to contain relatively high levels of secondary alcohols and ketones that could be quantified by GC-FID and GC-MS. (Table 3.4). C_{29} and C_{31} secondary alcohols were detected in the leaf waxes of both transgenic lines. The secondary alcohols

were composed of nonacosan-12-ol, -13-ol, -14-ol and -15-ol, as well as hentriacontan-13-ol, -14-ol, -15-ol and -16-ol. Within the C_{29} homologue, nonacosan-15-ol and nonacosan-14-ol were found in a 2:1 ratio, while the other two isomers were present at much lower levels (1.6% each). Hentriacontan-15-ol and -16-ol had similar amounts (47% each) within the C_{31} homologue. In contrast to the strong dominance of the C_{29} homologue (98%) in wild type stem wax, the C_{29} homologue accounted for only 54% of all the secondary alcohols in the leaf wax of the transgenic Arabidopsis. The secondary alcohols amounted to 4.2% and 3.2% of the total leaf waxes in each of the transgenic lines, respectively. In addition to secondary alcohols, ketones were also detected and found to contain 4% nonacosan-14-one and 96% nonacosan-15-one. Ketones amounted to 3.7% and 3.1% of the total leaf waxes of the two individual lines. No alkanediols and ketols were detected in the wax of the transgenic leaves.

Table 3.4: Relative homologue and isomer compositions (%) of secondary alcohols, ketones and alkanes in the total leaf waxes of the MAH1 over-expressing lines (a and b). Homologues were quantified within compound classes, and isomers were quantified within each chain length.

Homologue chain length	**Homologue composition**		**Isomer composition within homologues**										**Homologue composition**	
			C-12		**C-13**		**C-14**		**C-15**		**C-16**			
	a	b	a	b	a	b	a	b	a	b	a	b	A	b
Secondary Alcohols													**Alkanes**	
C_{29}	55.1	53.5	1.6	1.8	1.6	1.4	33.3	31.7	63.5	65.1			33.6	32.0
C_{31}	44.9	46.5			2.8	3.1	2.7	3.3	49.3	51.7	45.2	42.8	66.4	68.0
Ketones														
C_{29}	100	100					5.7	6.2	94.3	93.8				

3.3 Discussion

The current study examined compounds containing secondary functional groups in Arabidopsis (1) to test the biosynthetic relationship between secondary alcohols and ketols, and (2) to determine the regiospecificity and substrate preference of the enzyme involved in ketol biosynthesis and, thus, to test the possible involvement of MAH1 in ketol biosynthesis. In the following, the specificity of MAH1 for the conversion of alkanes to secondary alcohols (section 3.3.1) and from secondary alcohols to ketones (section 3.3.2) will be discussed based on the isomer and homologue quantification data and the MAH1-

overexpressor data. Then, the substrate-product relationships between the various compound classes with secondary functional groups can be addressed (section 3.3.3). Finally, by taking all the previous arguments together, the involvement of MAH1 in alkanediol and ketol biosynthesis can be discussed.

3.3.1 Conversion of Alkanes to Secondary Alcohols by MAH1: Substrate Chain Length and Product Isomer Preferences

In vitro assays with radioactively labeled alkanes had shown that alkanes are the substrates for secondary alcohol biosynthesis in *B. oleracea*.[113] As discussed in section 1.3.3.1, the similar secondary alcohol isomer composition of *Brassica oleracea* leaf wax and Arabidopsis stem wax suggested that both species have hydroxylases not only with similar product specificities, but also with similar substrate requirements. Accordingly, it is believed that alkanes serve as substrates for secondary alcohol formation in Arabidopsis. Since the alkanes in Arabidopsis stem wax are dominated by the C_{29} homologue, they have a chain length distribution very similar to that of the co-occurring secondary alcohols. Consequently, the preferential accumulation of the C_{29} secondary alcohols in the stem wax might be a result of substrate availability rather than substrate specificity of the hydroxylase involved. Thus, the substrate specificity of this enzyme cannot be assessed based on the previously available wild type wax analyses alone.

It had been demonstrated that MAH1 is the enzyme responsible for hydroxylating alkanes into secondary alcohols in Arabidopsis stem wax.[112] In the current study, transgenic Arabidopsis leaves over-expressing MAH1 were found to contain nonacosane and hentriacontane in a ratio of 1:2 while the homologue ratio of the corresponding secondary alcohol products was 6:5. This result clearly shows that the product composition can differ from that of the substrate, indicating that MAH1 has a preference for the C_{29} alkane. However, the product ratio found for the over-expressor leaves also differed from that in wild type stems, showing that the different substrate pools available in both systems also affected product formation. Thus, both substrate preference of MAH1 and substrate availability together determine the homologue distribution of secondary alcohols in Arabidopsis wax.

The secondary alcohols and ketones in Arabidopsis wild type stem wax had been reported to contain multiple isomers, suggesting that MAH1 hydroxylates on more than one carbon position. However, the exact hydroxylation pattern of MAH1 remained unknown prior to this study. To determine the range of carbon atoms hydroxylated, the previously unknown secondary alcohol and ketone isomers were identified in the current study. In each of the six secondary alcohol homologues (C_{27} to C_{32}) and the C_{29} ketone homologue, two to three isomers were detected, demonstrating that MAH1 hydroxylates on a narrow range of carbons. Based on the relative isomer abundances, I propose that two factors are governing the hydroxylation specificity of MAH1: (1) the hydroxylase shows high preference for the central carbon in odd-numbered homologues, e.g. forming nonacosan-15-ol (61%), and for the carbon next to the center of even-numbered chains, e.g. forming octacosan-14-ol (91%) and triacontan-15-ol (93%); (2) hydroxylation occurs preferentially on C-15, e.g. leading to nonacosan-15-ol and hentriacontan-15-ol. The narrow range of isomers described here characterizes MAH1 as a hydroxylase with limited regiospecificity.

3.3.2 Conversion of Secondary Alcohols to Ketones by MAH1: Substrate Chain Length and Product Isomer Preferences

Indirect evidence had previously indicated that MAH1 can use secondary alcohols as substrates for a second hydroxylation on the carbon carrying the hydroxyl group, leading to a geminal diol structure that will rearrange into a carbonyl function.[112] The strong dominance of nonacosan-15-one indicated that MAH1 has the same regioselectivity in the second hydroxylation as that in the first hydroxylation. The substrate chain length preference for the second hydroxylation step of MAH1 is also consistent with that for the first hydroxylation step. In the leaf wax of MAH1 over-expressors, the C_{29} and C_{31} secondary alcohols were detected at a similar abundance while only C_{29} ketones were found, demonstrating that MAH1 prefers to hydroxylate C_{29} secondary alcohols.

3.3.3 Substrate-product Relationships between Secondary Alcohols, Ketones, Alkanediols and Ketols

Ketols had been described for the leaf waxes of *B. napus* and *B. oleracea*.[114] Because the

positions of functional groups in these ketols are very similar to those of the co-occurring secondary alcohols and ketones, it had been proposed that secondary alcohols and ketones serve as the substrates for ketol biosynthesis in the Brassicas. In the current study, ketols were identified for the first time in wild type Arabidopsis stem wax. Interestingly, it was found that the functional groups of these ketols were located on carbon positions similar to those of the hydroxyl groups in the accompanying secondary alcohols. This correlation provided further indirect evidence to support the precursor-product relationship between secondary alcohols and the bifunctional constituents, here in a second plant genus beside the Brassicas. As a third line of evidence, the absence of the bifunctional components from the stem wax of the Arabidopsis *mah1* mutant also confirmed the substrate-precursor relationship between secondary alcohols and ketols. All taken together, it can now be concluded that ketols are formed as derivatives of secondary alcohols (Fig. 3.5).

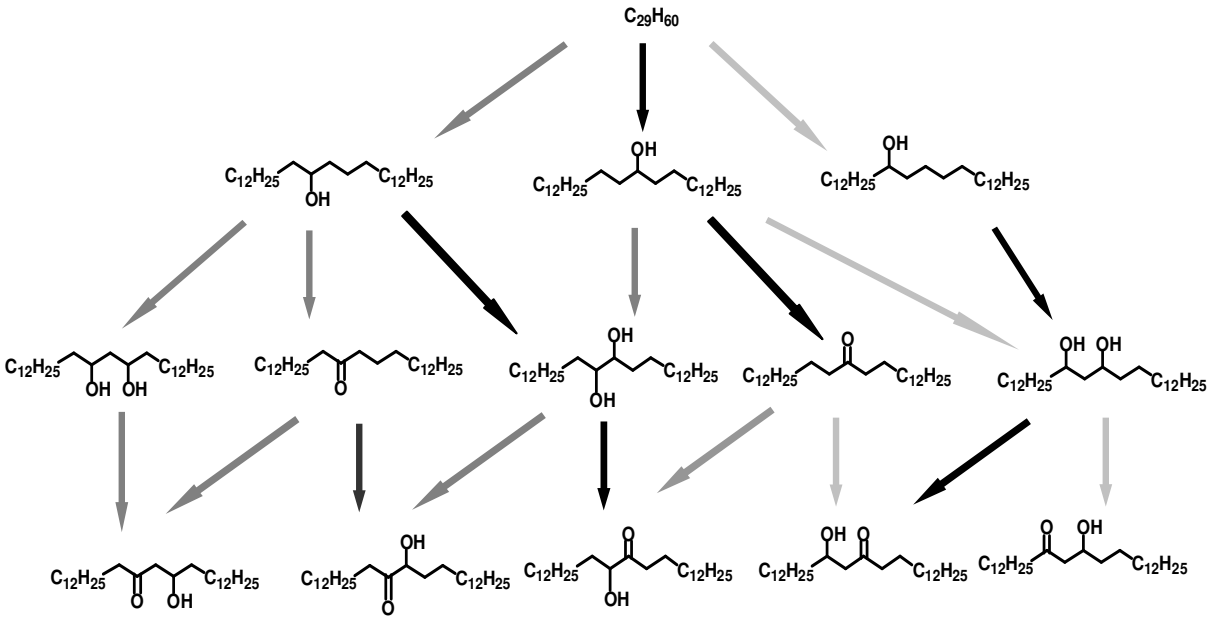

Figure 3.5: Proposed biosynthetic relationships between alkanes, secondary alcohols, ketones and ketols in the stem wax of Arabidopsis. All the steps may be catalyzed by MAH1. The shades of grey in the arrows indicate the regioselectivity of MAH1. Black: carbon position-15 grey: carbon position-14; light grey: carbon position-13)

The findings on Arabidopsis ketols discussed above were closely paralleled by qualitative and quantitative results on alkanediols in the same wax mixtures. The Arabidopsis wild type diols were found to have homologue and isomer compositions similar to those of the

secondary alcohols and ketols. The *mah1* mutant stem wax lacked diols and ketols, coincident with reduced levels of secondary alcohols. All these results taken together, it is very likely that alkanediols are formed by hydroxylation of secondary alcohol substrates, and that the diols in turn serve as substrates for ketol formation. Thus, I conclude that alkanediols are intermediates on the pathway from secondary alcohols to ketols (Fig. 3.5).

Ketones could also serve as intermediates between secondary alcohols and ketols. For example, nonacosan-15-one could be hydroxylated on C-13 or C-14 to give 13-hydroxynonacosan-15-one and 14-hydroxynonacosan-15-one, respectively (Fig. 3.5). The qualitative wax analyses carried out in the present study showed that the isomer and homologue distributions of the ketols matched those of the ketones to a certain degree. This finding confirms the hypothesis that ketones are intermediates of ketol formation, on pathways parallel to those via alkanediols. However, it should be noted that the quantitative results revealed discrepancies between isomer patterns of ketones and ketols, indicating that the pathways leading via ketones to ketols account for only a small portion of the ketols formed.

3.3.4 Conversion of Secondary Alcohols and Ketones to Alkanediols and Ketols: Substrate Chain Length and Product Isomer Preferences

The conversions involved on both pathways leading from secondary alcohols to ketols, via ketones or alkanediols, are very similar as they can all be explained by simple hydroxylation reactions. They involve either hydroxylation of methylene carbons to secondary hydroxyl groups or of –CHOH- groups to geminal diols that will rearrange to carbonyl groups. Thus, it is expected that all the transformations occurring on these pathways are catalyzed by hydroxylases. Conversely, it can be excluded that either of the hydroxyl/carbonyl functional groups is introduced during elongation, and formation of the symmetric alkanediols/ketols in the Brassicaceae species does not involve polyketide-like biosynthetic steps. In the following, the substrate and regiospecificity of the hydroxylases will be discussed based on the isomer compositions found for the various compound classes.

All the alkanediols and ketols detected in Arabidopsis stems have their functional groups on

carbon positions between C-13 to C-15, which is in the same range as the hydroxyl positions in the accompanying secondary alcohols. Furthermore, the most abundant isomers of alkanediols or ketols are the ones with one functional group on C-15. Thus, it seemed that the hydroxylase(s) involved in alkanediol and ketol biosynthesis has (have) a similar limited regiospecificity as MAH1. In the stem wax of Arabidopsis wild type, only alkanediols and ketols with chain length C_{29} were detected. This result could be due to substrate chain length preference of the hydroxylase(s) or to substrate availability, because the hypothetical substrates for alkanediols and ketols, secondary alcohols and ketones, are dominated by C_{29} homologues.

In summary, MAH1 and the hydroxylase(s) involved in alkanediol/ketol biosynthesis have similar regiospecificity and may also have same substrate chain length preference. This raises an interesting question regarding the relationship between MAH1 and the hydroxylase(s) involved in alkanediol/ketol biosynthesis. All the results of this chapter can be taken together to give a tentative first answer to this question. The steps leading from alkanes to secondary alcohols, from secondary alcohols to either ketones or alkanediols, and from ketones and diols to ketols can all be described as similar hydroxylations. Thus, all the compounds described here are formed by single, double or triple hydroxylation. All these hydroxylation steps occur with similar chain length preference and regiospecificity, and may therefore be carried out by MAH1. However, the different reaction steps differ in the numbers of hydroxyl groups that are present in the substrates handled in each step. Thus, if MAH1 is indeed the only enzyme involved, then it must be relatively flexible with respect to the functional groups present on or near the carbon it hydroxylates. This hypothesis is plausible since MAH1 also exhibits only limited regiospecificity, implying promiscuity not only for the exact substrate configuration but also for product geometry.

Chapter 4 Secondary Alcohols and Alkanediols in the Leaf Cuticular Wax of Pea (*Pisum sativum*)

4.1 Introduction

Arabidopsis and *Brassica oleracea* (and various other *Brassica* species) belong to the Brassicaceae family and are, thus, closely related. They have very similar wax compositions characterized by C_{29} alkanes, secondary alcohols and ketones as major wax constituents. The major secondary alcohols are nonacosan-14-ol and -15-ol. Furthermore, according to the results presented in Chapter 3, C_{29} ketols are present in Arabidopsis stem wax and have the same isomer pattern as that of the ketols in *B. oleracea* leaf wax. Therefore, it seems likely that Arabidopsis and *B. oleracea* possess similar enzymes that can synthesize secondary alcohols and other wax components with secondary functional groups.

MAH1 is a P450-dependent hydroxylase known to be involved in symmetric secondary alcohol biosynthesis in Arabidopsis stems.[112] Reduced amounts of the secondary alcohols in the *mah1* mutant were partially compensated by an increase of alkanes, demonstrating a substrate-product relationship between both compound classes.[112]. Similarly, *in vitro* assays by incubating radioactively labeled alkanes with *B. oleracea* leaf discs showed that alkanes are the substrates for the MAH1-like hydroxylase in this system.[113] In Chapter 3, MAH1 was predicted to also use secondary alcohols for alkanediol biosynthesis. Again very similar to the Arabidopsis enzyme, the MAH1-like hydroxylase in *B. oleracea* had also been proposed to use ketones for ketol biosynthesis.[114] Thus, besides alkanes, MAH1 and MAH1-like enzymes are thought to use symmetric secondary alcohols and ketones as substrates. As discussed in Chapter 3, MAH1 shows limited regiospecificity for hydroxylating on or near the central carbon of the hydrocarbon chain. Similarly, equal amounts of nonacosan-14-ol and -15-ol detected in the *B. oleracea* leaf disc assay indicated that the MAH1-like hydroxylase thought to be involved in secondary alcohol biosynthesis also has limited regiospecificity for the central carbon.

All the available information taken together, it seems likely that the Brassicaceae contain similar MAH1-like hydroxylases involved in formation of symmetric secondary alcohols and their derivatives. This implies that biosynthesis of these compounds occurs by modification of pre-formed acyl precursors rather than by introduction of the secondary functional groups during elongation in a polyketide-like fashion. However, it is not clear whether similar enzymes exist outside the family of Brassicaceae, and whether the findings for Arabidopsis can be generalized to other plant lineages. This raises the questions (1) whether other plant species have MAH1-like enzymes, (2) which substrates these MAH1-like enzymes use, and (3) what the regiospecificity of these MAH1-like enzymes is. This chapter will focus on these questions by identifying wax components containing secondary functional groups in a non-Brassicaceae plant species that could have MAH1-like hydroxylases.

Recently, the chemical composition of waxes on the leaf surfaces of four pea (*Pisum sativum*) cultivars has been investigated in detail.[39] The adaxial wax consisted mainly of primary alcohols (71%), with strong predominance of hexacosanol and octacosanol, while the abaxial wax was characterized by very high amounts of alkanes (73%) with a predominance of hentriacontane. Symmetric secondary alcohols were found to accumulate together with alkanes on the abaxial leaf surface. Hentriacontan-16-ol and hentriacontan-15-ol were reported to dominate this compound class in a 2:1 ratio, with trace amounts of hentriacontan-14-ol and of nonacosan-13-ol, -14-ol and -15-ol being present. The presence of isomeric secondary alcohols makes pea a promising candidate that could contain a MAH1-like hydroxylase. In addition, a number of compounds in the pea wax mixture remained unidentified and were suspected to contain secondary functional groups. Thus, pea leaf wax was targeted for novel structure identifications.

4.2 Results

4.2.1 Structure Elucidation of Secondary Alcohols and Alkanediols

The mixture of cuticular wax was prepared by surface extraction of pea leaves with chloroform. TLC separation yielded a number of fractions with all the previously reported wax constituents and two bands containing unidentified compounds. One of them, designated as compound class **A** (R_f 0.79), co-migrated with a secondary alcohol standard. Another band

(R_f 0.16), migrating between a primary alcohol and a fatty acid standard, appeared to contain two compound classes **B1** and **B2** according to their GC-retention behaviour and mass spectral characteristics.

4.2.1.1 Secondary Alcohols

Compound class **A** co-migrated with a secondary alcohol standard, suggesting that the components in this compound class have one secondary hydroxyl group. Within fraction **A**, five peaks were separated by GC after TMSi-derivatization with bis-(*N,O*-trimethylsilyl)-trifluoroacetamide (BSTFA). All five mass spectra showed fragments characteristic for alcohol TMSi ethers at *m/z* 73, 75 and 103, but lacked a diol fragment *m/z* 147, indicating the presence of only one hydroxyl group (Table 4.1). The five peaks were further characterized by molecular ions $[CH_3(CH_2)_nCH_2OTMSi]^+$ differing by 14 mass units, and by corresponding fragments $[M\text{-}CH_3]^+$ indicating the loss of a methyl group from the TMSi derivatives. All the present evidence taken together, fraction **A** was identified as a homologous series of secondary alcohols with chain lengths C_{29} to C_{33}.

Within the C_{31} homologue peak, the isomer hentriacontan-16-ol could be unambiguously identified due to the presence of an α-fragment at *m/z* 299 ($[CH_3(CH_2)_{14}CHOTMSi]^+$), a molecular ion at *m/z* 524 and the corresponding fragment $[M\text{-}CH_3]^+$ at *m/z* 509. This finding confirmed previous reports describing hentriacontan-16-ol as the most abundant secondary alcohol in the wax of pea leaves.[39,149] The mass spectrum from the same GC peak contained a series of other α-fragments ($[CH_3(CH_2)_nCHOTMSi]^+$), suggesting the presence of various other C_{31} alcohol isomers. Pairs of these fragments, resulting from the cleavage of the α-bonds on both sides of the functionality, were used to identify hentriacontan-12-ol, -13-ol, -14-ol and -15-ol. The other four secondary alcohol homologues in fraction **A** were also found to contain multiple isomers. They were identified, according to the α-fragments of their TMSi derivatives, as nonacosan-13-ol, -14-ol and -15-ol, triacontan-13-ol, -14-ol and -15-ol, dotriacontan-14-ol, -15-ol and -16-ol, as well as tritriacontan-13-ol, -14-ol, -15-ol, -16-ol and 17-ol. Among these secondary alcohols, dotriacontan-14-ol, -15-ol and -16-ol, as well as tritriacontan-15-ol, -16-ol and 17-ol had not been described before.

4.2.1.2 Secondary/secondary Alkanediols

Fraction **B** migrated between primary alcohols and fatty acids on TLC (R_f 0.16), and was therefore expected to contain compounds with two (or more) functional groups of intermediate polarity.[128] In the GC trace of fraction **B**, one peak **B1** had special retention behaviour and could hence not be assigned to any homologous series. The mass spectrum of its TMSi ether (Fig. 4.1A) showed alcohol fragments *m/z* 75 and 103 together with a fragment *m/z* 147, indicating the presence of two (or more) OTMSi groups.[152] Assuming an alkanediol structure, characteristic mass differences between four ions belonging to two types of ions $[C_nH_{2n}OTMSi]^+$ and $[C_mH_{2m-1}(OTMSi)_2]^+$ allowed the assignment of the molecular ion *m/z* 612, and corresponding fragments *m/z* 597 ($[M\text{-}CH_3]^+$), *m/z* 522 ($[M\text{-}TMSiOH]^+$) and *m/z* 432 ($[M\text{-}(TMSiOH)_2]^+$). The alkanediol structure of the compound was further verified by daughter ions Δ*m/z* -90 ($[\text{-}TMSiOH]^+$) accompanying the four α-fragments. **B1** was therefore tentatively identified as a C_{31} alkanediol, giving rise to a bis TMSi ether derivative $C_{31}H_{62}(OTMSi)_2$.

The α-ions *m/z* 215 and 313 matched the compositions of $[C_9H_{18}OTMSi]^+$ and $[C_{16}H_{32}OTMSi]^+$, respectively, thus indicating the presence of hydroxyl groups on carbons C-9 and C-16 of the hentriacontanediol backbone. This isomer assignment was confirmed by the other two α-fragments *m/z* 401 ($[C_{16}H_{31}(OTMSi)_2]^+$) and 499 ($[C_{23}H_{45}(OTMSi)_2]^+$). All the data taken together, this compound was identified as hentriacontane-9,16-diol.

Alternative structures for **B1**, containing either additional hydroxyl or carbonyl groups, could also give the fragments described so far for this fraction. However, these other structures can be excluded for two reasons: (1) the presence of an additional hydroxyl group seems unlikely, as ions $[C_nH_{2n-2}(OTMSi)_3]^+$ could not be detected in the mass spectrum of the TMSi derivative; (2) the presence of a carbonyl group can also be excluded, because lithium aluminum hydride treatment left fraction **B1** unchanged (identical mass spectrum of the resulting TMSi derivative, data not shown).

The presence of two series of other α-ions indicated that fraction **B1** also contained a number of C_{31} alkanediol isomers besides hentriacontane-9,16-diol. Based on the fragments at *m/z*

201, 327, 387 and 513 and at *m/z* 229, 299, 415 and 485, hentriacontane-10,17-diol and hentriacontane-8,15-diol could be identified, respectively. To corroborate the assignment of all the different α-fragments to the various C_{31} alcohol isomers, all the relevant single ion traces were calculated for multiple GC-MS runs of **B1**. Each resulting extracted chromatogram showed a single peak, with those of ions that had been assigned to the same isomer coinciding. Overall, three partially separated peaks were detected, indicating that hentriacontane-10,17-diol eluted shortly before, and hentriacontane-8,15-diol shortly after the predominant isomer of hentriacontane-9,16-diol. This result matches previous reports, for example demonstrating similar partial GC separation of isomers for C_{33} secondary alcohols in *Myricaria germanica*.[153]

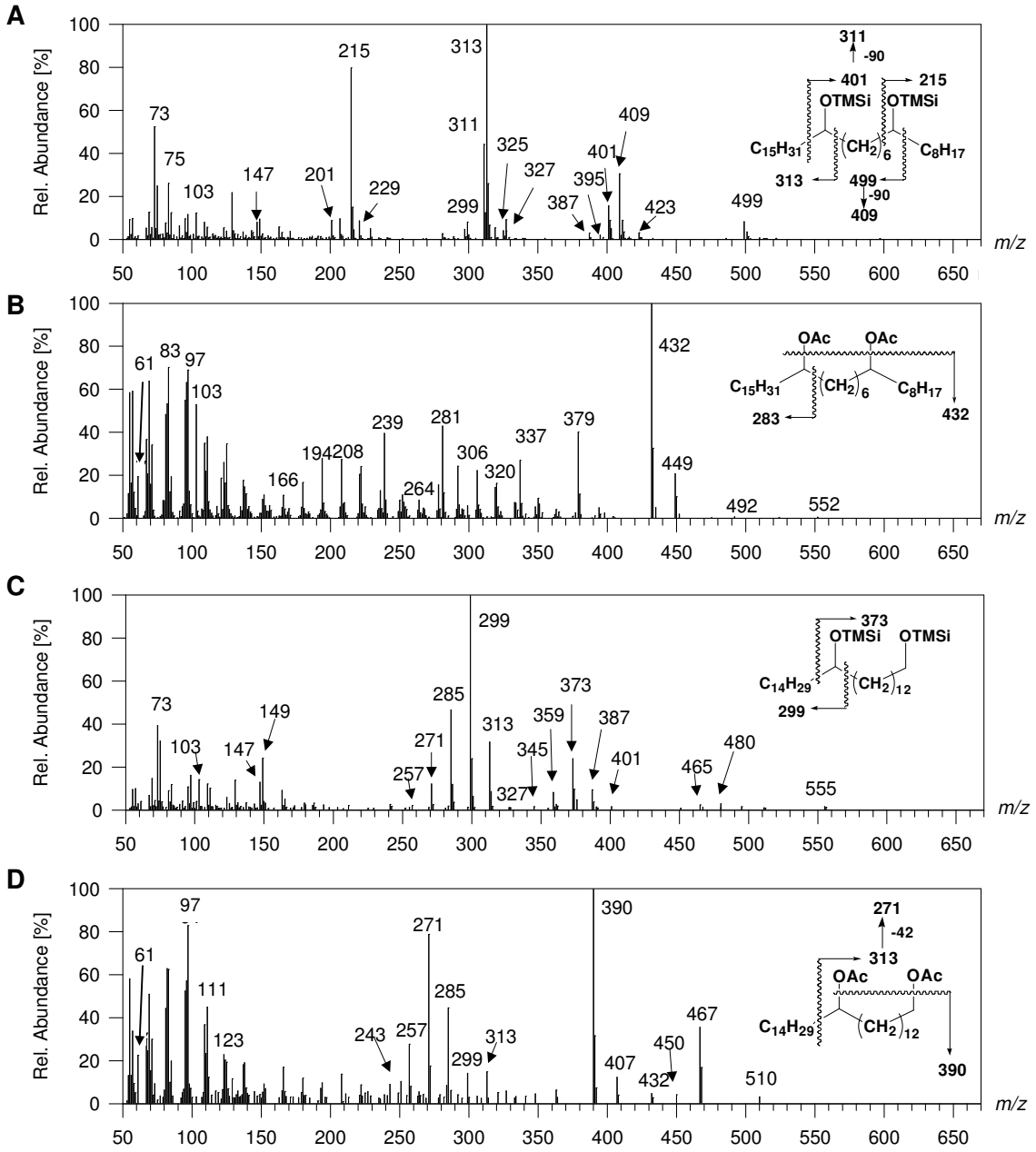

Figure 4.1: Mass spectra of the representative derivatives of the alkanediols in the leaf wax of pea. (A) The bis TMSi ethers of the secondary/secondary hentriacontanediol isomer mixture, (B) the bis acetates of the secondary/secondary hentriacontanediol isomer mixture, (C) the bis TMSi ethers of the primary/secondary octacosanediol isomer mixture, and (D) the bis acetates of the primary/secondary octacosanediol isomer mixture.

The secondary/secondary alkanediol structure of fraction **B1** was confirmed by transforming the hydroxyl groups into acetate esters. The reaction product was subjected to BSTFA

derivatization after acetylation, and the resulting mass spectrum indicated complete acetylation, as it lacked TMSi signals *m/z* 73 and 75 while showing a prominent ion *m/z* 61 ($[AcOH_2]^+$) (Fig. 4.1B). Interestingly, a prominent ion *m/z* 103 was detected in the acetate mass spectrum, even though it is known to be characteristic for OTMSi ethers. To verify that this fragment was due to acetate fragmentation, the mass spectra of acetates of three standard compounds were acquired. The bis acetates of nonacosane-5,10-diol and octacosane-1,9-diol both showed high abundance of *m/z* 103, while this was not observed for nonacosan-11-ol acetate (Fig. 4.2). Hence, this fragment can be considered an elimination product $[AcOHAc]^+$ characteristic for alkanediol bis acetates. In the high mass region of the acetate mass spectrum of **B1**, a series of ions *m/z* 552, 492, 449 and 432 was detected, and could be interpreted as M^+, $[M\text{-}AcOH]^+$, $[M\text{-}AcOH\text{-}Ac]^+$ and $[M\text{-}(AcOH)_2]^+$, respectively, of hentriacontanediol bis acetate. This experiment confirmed both the alkanediol structure and the C_{31} carbon backbone of **B1**. The presence of α-fragments *m/z* 269 ($[CH_3(CH_2)_{11}CHOAc]^+$), 283 ($[CH_3(CH_2)_{12}CHOAc]^+$) and 297 ($[CH_3(CH_2)_{13}CHOAc]^+$) further corroborated the presence of multiple isomers hentriacontane-9,16-diol, -8,15-diol and -10,17-diol. All three hentriacontanediol isomers described here had not been reported for plant cuticular waxes before.

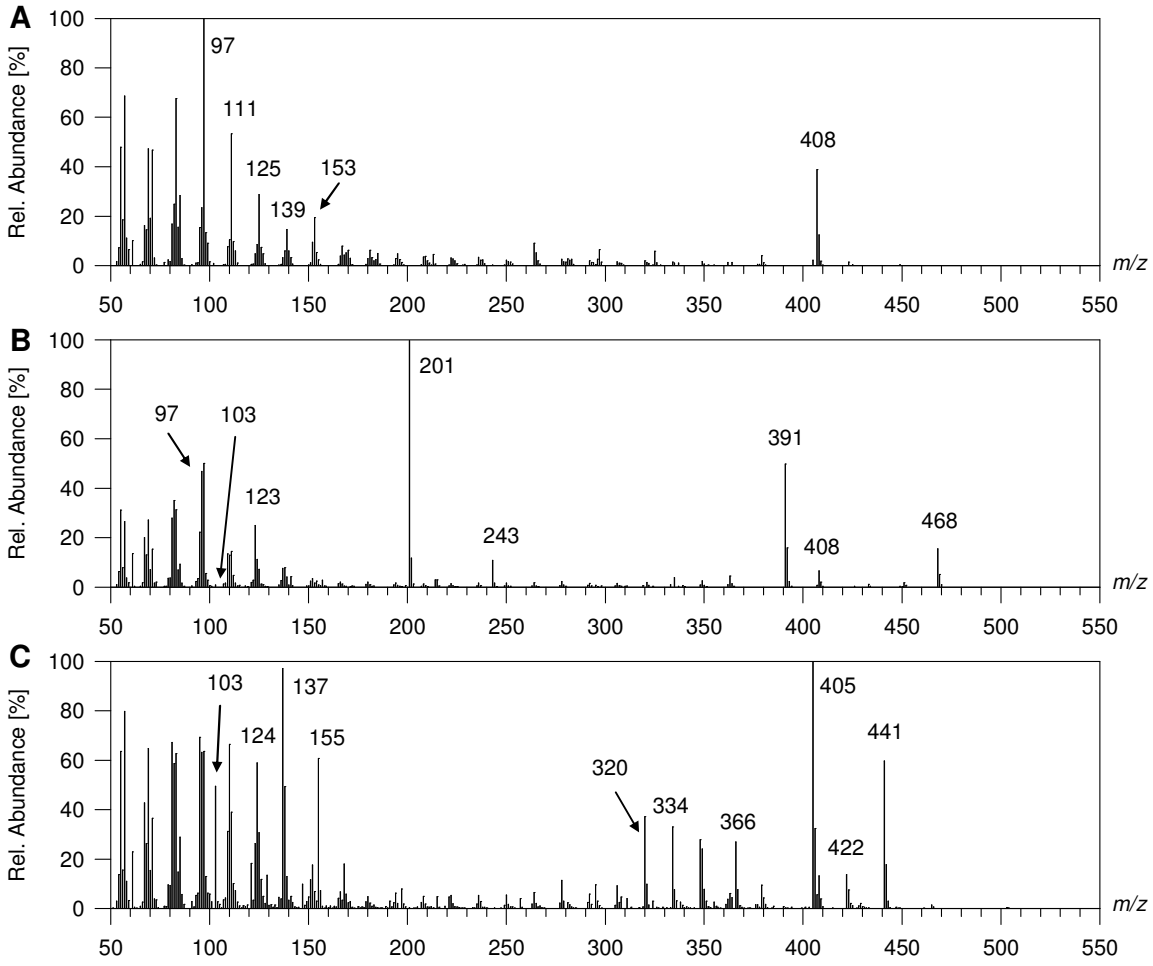

Figure 4.2: Mass spectra of the acetates of the reference compounds. (A) Nonacosan-11-ol, (B) octacosane-1,9-diol and (C) nonacosane-5,10-diol

4.2.1.3 Primary/secondary Alkanediols

Fraction **B2** contained two homologues, likely of compounds with two hydroxyl groups as they co-migrated with the hentriacontanediols **B1** on TLC. The TMSi derivatives of compound class **B2** (Fig. 4.1C) accordingly showed mass spectral fragments *m/z* 73, 75, 103 and 147 characteristic for alkanediols. Moreover, the prominent signal *m/z* 149 indicated a diol geometry with one primary and one secondary functional group.[128] The primary/secondary alkanediol structure was further supported by the presence of (only) two α-fragments $[C_nH_{2n}OTMSi]^+$ and $[C_mH_{2m-1}(OTMSi)_2]^+$.[128] To test for the presence of carbonyl groups, the constituents of fraction **B2** were treated with lithium aluminum hydride,

followed by BSTFA derivatization. The resulting mass spectral data were identical to the TMSi ethers without lithium aluminum hydride treatment, showing that no functional groups other than hydroxyl groups were present. In conclusion, molecular ions and corresponding fragments $[M\text{-}CH_3]^+$ could be assigned, and both homologues in **B2** were identified as primary/secondary hexacosanediol and octacosanediol (C_{26} and C_{28} alkanediols), respectively.

The TMSi mass spectral data showed several α-fragments within each of the two groups $[C_nH_{2n}OTMSi]^+$ and $[C_mH_{2m-1}(OTMSi)_2]^+$ differing by 14 mass units, indicating the presence of several isomers. The two types of α-ions represented opposite ends of the alkanediol molecules, as they originated from cleavage of the two C-C bonds adjacent to the secondary functional group. Therefore, pairs of α-ions from both types belonged to the same isomer and could be recognized based on their identical relative abundance. Matching pairs confirmed the molecular weight of the alkanediol homologues, and accounted for all the α-fragments detected. Thus, the α-ions of the TMSi ethers provided independent confirmation for the alkanediol structures of **B2**. Overall, isomeric primary/secondary hexacosanediols with secondary hydroxyl groups between C-12 and C-15 were detected, whereas C_{28} isomers ranging from octacosane-1,12-diol to octacosane-1,17-diol were identified.

To further corroborate the alkanediol structure, compounds in **B2** were treated with acetic anhydride. The resulting products had a prominent mass spectral fragment at *m/z* 61, interpreted as $[AcOH_2]^+$ and therefore diagnostic for acetates. Furthermore, the fragments *m/z* 467 ($[M\text{-}Ac]^+$), *m/z* 450 ($[M\text{-}AcOH]^+$), *m/z* 407 ($[M\text{-}Ac\text{-}AcOH]^+$) and *m/z* 390 ($[M\text{-}(AcOH)_2]^+$), involving the loss of one and two acetyl moieties, were characteristic for bis acetates of alkanediols. Based on these series of fragments the ions at *m/z* 482 and *m/z* 510 in the two homologues of **B2** could be interpreted as the molecular ions of bis acetates of hexacosanediol and octacosanediol, respectively, confirming the presence of exactly two hydroxyl functions (Fig. 4.1D). Different from the fragmentation pattern of secondary/secondary diol acetates, the mass spectral data showed prominent daughter fragments Δ*m/z* -42 below the α-ions. The acetate of an octacosane-1,9-diol standard showed a very similar fragmentation pattern (*m/z* 201), whereas no corresponding fragments were observed for the acetate of a nonacosane-5,10-diol standard (Fig. 4.2). Hence, the daughter

fragments Δ*m/z* -42 are diagnostic for α-ions containing a terminal OAc group, probably due to loss of CH_2=C=O.

Finally, octacosane-1,14-diol acetate was synthesized to verify the structure assignment. After derivatization with acetic anhydride, the synthetic octacosane-1,14-diol bis acetate was analyzed on GC-MS. The GC peak of the putative octacosane-1,14-diol acetate co-eluted with the synthetic standard (Fig. 4.3A,B). The mass spectral fragments described for putative octacosane-1,14-diol bis acetate also matched the mass spectral data of the synthetic standard. (Fig. 4.3C,D).

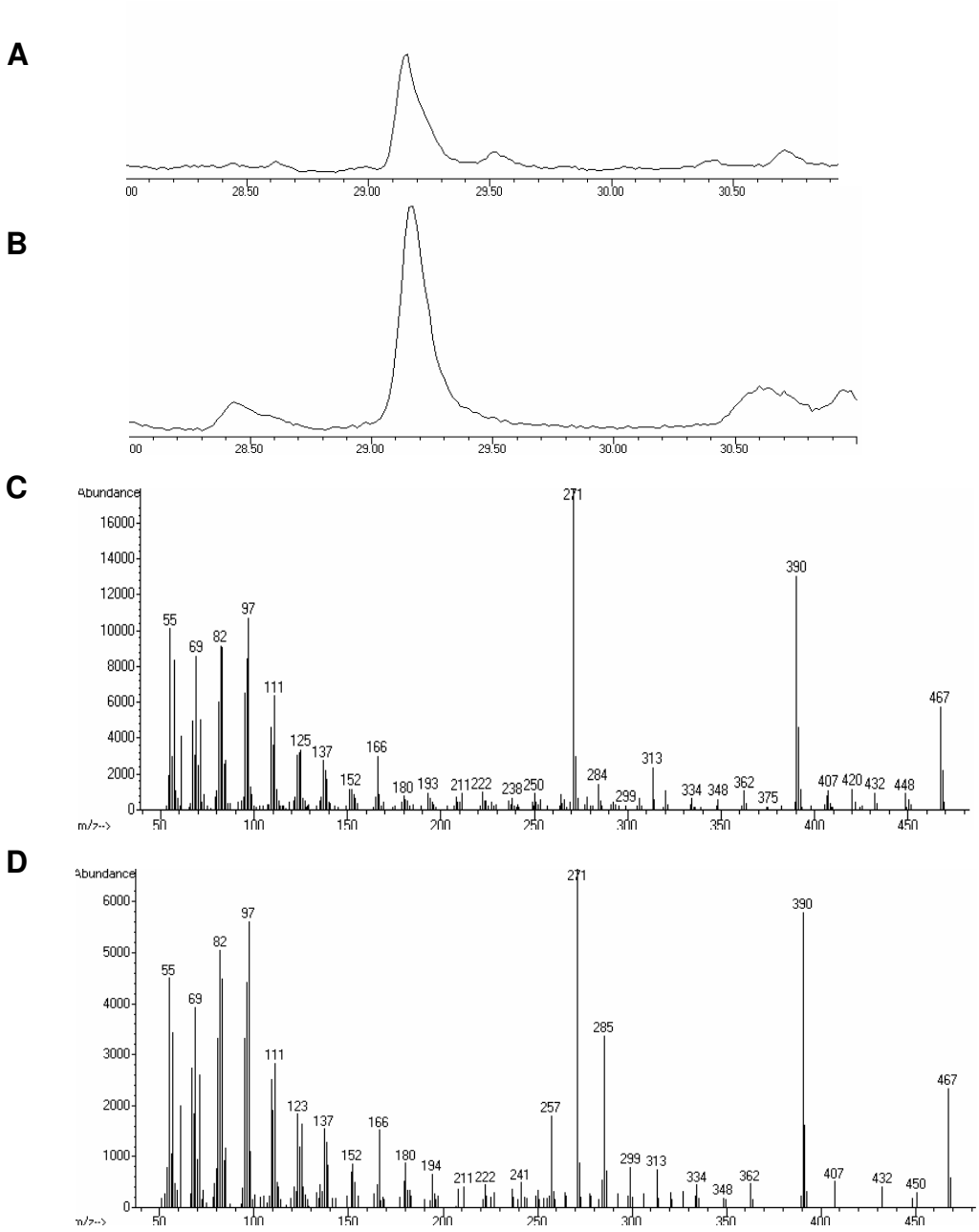

Figure 4.3: Comparison of GC-MS data of the synthetic standards and candidate structures. (A) GC trace of the synthetic bis acetates of octacosane-1,14-diol, (B) GC trace of the acetates of compound class **B2,** (C) mass spectrum of synthetic bis acetate of octacosane-1,14-diol and (D) mass spectrum of the acetates of compound class **B2**

4.2.2 Quantification of Secondary Alcohols and Alkanediols

GC-FID quantification showed that the C_{31} homologue dominated (94%), while secondary alcohols with other chain lengths contributed only minor amounts (1.4 - 2.2%) (Table 4.1). This result is in agreement with previous reports on the chain length distribution of secondary alcohols in pea wax.[39,114] Due to the relatively small differences in molecular geometry, the various isomers within each secondary alcohol homologue could not be separated by GC. Therefore, the relative amounts of isomers had to be quantified by the intensity of α-ions in the mass spectra (Table 4.2). Within the different homologues, the C_{30} and C_{32} secondary alcohols contained mainly one isomer, triacontan-15-ol (88%) and dotriacontan-16-ol (82%), respectively. In contrast, the homologues with odd-numbered chain lengths had more even distributions of various isomers. Among the C_{31} alcohols, hentriacontan-16-ol dominated (62%), while the C_{33} alcohols contained tritriacontan-15-ol, -16-ol and 17-ol in a ratio of approximately 1:2:1, and the C_{29} alcohols contained nearly equal amounts of nonacosan-14-ol and -15-ol. The secondary alcohol fraction accounted for 4.7% of the total leaf wax of pea (24.3 ± 2.9 µg/cm²). Adaxial and abaxial waxes, amounting to 16.9 µg/cm² and 25.3 µg/cm²,[39] were found to contain 0.3% and 7.3% of secondary alcohols, respectively. Wax extracts from both surfaces of the leaves had very similar secondary alcohol compositions (data not shown).

Table 4.1: Relative composition (%) of the secondary alcohols, secondary/secondary alkanediols, primary/secondary alkanediols, primary alcohols and alkanes in the total wax of *Pisum sativum* leaves.[a]

Homologue chain length	Homologue composition	Isomer composition within homologues						Homologue composition[b]
		C-12	C-13	C-14	C-15	C-16	C-17	
Secondary Alcohols								**Alkanes**
C_{29}	1.9 ± 0.6		2.7 ± 0.3	48.1 ± 0.8	49.2 ± 0.9			1.4 ± 0.3
C_{30}	2.2 ± 0.8		1.0 ± 0.2	10.6 ± 0.3	88.5 ± 0.2			1.2 ± 0.04
C_{31}	93.9 ± 2.3	0.2 ± 0.01	0.2 ± 0.02	2.0 ± 0.1	35.6 ± 0.2	62.0 ± 0.3		94.7 ± 0.4
C_{32}	1.4 ± 0.7			4.0 ± 0.3	13.8 ± 1.0	82.2 ± 0.9		1.0 ± 0.1
C_{33}	1.4 ± 0.6		1.7 ± 0.7	13.3 ± 1.3	23.9 ± 0.8	41.0 ± 1.5	20.0 ± 0.7	1.6 ± 0.05
Secondary/ secondary diols					**C-8**[c]	**C-10**[c, d]	**C-9**[c]	
C_{31}	100 ± 0				8.4 ± 0.4	7.0 ± 0.3	84.6 ± 0.5	
Primary/ secondary diols								**primary Alcohols**
C_{26}	tr[e]	tr	tr	tr	tr			56.6 ± 3.3
C_{28}	100 ± 0	0.8 ± 0.1	15.8 ± 0.6	53.3 ± 0.7	24.6 ± 0.2	4.8 ± 0.2	0.7 ± 0.1	34.2 ± 2.7

[a] Mean values (of five independent samples) and SE are given for the percentage (%) of isomers within individual homologues and of homologues within individual compound classes. The isomer compositions were calculated based on relative abundance of α-ions resulting from OTMSi derivatives

[b] Calculated from coverages (μg/cm^2) reported by Gniwotta et al.[39]

[c] Position of one of the hydroxyl group in the alkanediols. The position of the other hydroxyl group is indicated as in the corresponding secondary alcohols.

[d] Hentriacontane-10,17-diol is shown under C-15 as it is identical with "hentriacontane-15,22-diol".

[e] Trace, i.e. less than 0.1% of the fraction detectable

Table 4.2: Mass spectral data of TMSi ethers of secondary alcohols

compounds	Common fragments (relative intensity)			Characteristic fragments (relative intensity)	
Nonacosan-13-ol	73 (25.6)	75 (16.1)	103 (6.8)	271 (2.3)	327 (2.2)
Nonacosan-14-ol	481 (4.7)			285 (50.7)	313 (51.9)
Nonacosan-15-ol				299 (100)	
Triacontan-13-ol	73 (19.5)	75 (12.1)	103 (6.8)	271 (1.1)	341 (1.3)
Triacontan-14-ol	495 (5.1)	510 (0.2)		285 (10.4)	327 (10.8)
Triacontan-15-ol				299 (100)	313 (97.3)
Dotriacontan-14-ol	73 (15.7)	75 (13.1)	103 (3.1)	285 (5.7)	355 (5.8)
Dotriacontan-15-ol	523 (3.8)			299 (12.0)	341 (15.8)
Dotriacontan-16-ol				313 (100)	327 (94.6)
Tritriacontan-13-ol	73 (6.4)	75 (14.2)	103 (7.4)	257 (0.2)	383 (4.5)
Tritriacontan-14-ol	537 (6.0)			285 (18.2)	369 (14.4)
Tritriacontan-15-ol				299 (25.2)	355 (39.7)
Tritriacontan-16-ol				313 (36.9)	341 (50.8)
Tritriacontan-17-ol				327 (100)	

Due to the poor separation of the alkanediol isomers, they could not be quantified by GC-FID. Hence, similar to the quantification of secondary alcohol isomers, the percentage of the hentriacontanediol isomers in the total leaf wax was calculated by normalizing the relative intensity of α-fragments. Hentriacontane-9,16-diol accounted for 85% of the three isomers (Table 4.2), while hentriacontane-8,15-diol and -10,17-diol accounted for 8% and 7%, respectively. The secondary/secondary diol fraction accounted for 0.5% of the total pea leaf wax. Adaxial and abaxial waxes contained 0.2% and 0.7% of secondary/secondary alcohols, respectively and had very similar secondary/secondary diol compositions (data not shown).

The total leaf wax contained 0.3% primary/secondary alkanediols, corresponding to a coverage of 0.7 μg/cm².[39] Based on the relative abundance of α-fragments in the MS of TMSi ethers of both homologues, the percentages of the alkanediol isomers was quantified (Table 4.2). Within the C_{28} homologue, octacosane-1,14-diol was the most prominent isomer (53%), while octacosane-1,13-diol and -1,15-diol contributed another 16% and 25%, respectively. Due to the very low amount of hexacosanediols, their isomers could not be quantified. To my knowledge, hexacosane-1,12-diol, -1,15-diol and octacosane-1,16-diol have not been reported previously. Primary/secondary alcohols amounted to 0.6% of the

adaxial wax mixture, while they could not be detected in extracts from the abaxial side of the leaf.

4.3 Discussion

Many questions came with the discovery of the hydroxylase MAH1 in Arabidopsis. How wide-spread is this enzyme function in symmetric secondary alcohol biosynthesis of other species? Which substrates do these hydroxylases use? How similar is the regiospecificity of these MAH1-like hydroxylases? Chemical analyses of waxes from various plant species will provide first answers to these questions and may guide future molecular genetics studies. In this chapter, previously unknown secondary alcohol isomers and alkanediols in pea leaf wax were identified. The isomer compositions of secondary alcohols will give insights into the properties of the enzyme introducing the hydroxyl groups (section 4.3.1). The biosynthesis of alkanediols will be discussed in sections 4.3.2 and 4.3.3 based on the quantification results for those compound classes.

4.3.1 MAH1-like Enzymes in Pea Leaves

It is believed that in *Brassica oleracea, B. napus* and Arabidopsis the secondary alcohols (for example nonacosan-15-ol) are biosynthesized by direct hydroxylation of the corresponding alkanes. Analogously, the secondary alcohols in pea (*Pisum sativum*) leaf wax are very likely biosynthesized from corresponding alkanes, as the chain length distributions of alkanes[39] and secondary alcohols were found to be very similar (Table 4.2). Both compound classes showed complete homologous series C_{29}-C_{33} with a dominant chain length of C_{31}. Further evidence supporting a biosynthetic relationship between these two compound classes comes from the finding that both alkanes and secondary alcohols accumulated to relatively high concentrations in the abaxial wax, but not in the adaxial wax of pea leaves. Since the secondary alcohols in pea are synthesized from alkanes, the question arises whether this occurs through hydroxylation catalyzed by an enzyme similar to the Arabidopsis MAH1.

In vitro assays using *Brassica oleracea* leaf discs showed that alkane hydroxylation in this system occurs with only limited regiospecificity, as substantial amounts of both isomeric secondary alcohols nonacosan-14-ol and nonacosan-15-ol were formed.[113] In Chapter 3, the

isomeric composition of secondary alcohols in Arabidopsis also indicated a limited regiospecificity of MAH1 with a preference for hydroxylating the central carbon. Compared with these Brassicaceae, the secondary alcohol homologues in pea leaf wax had a broader isomer distribution. Nonetheless, the relative isomer abundance suggested that the hydroxylase(s) in pea is (are) able to selectively hydroxylate alkane substrates at certain carbon positions. Two factors may be proposed to contribute to the specificity of the hydroxylase(s) in pea: (1) the hydroxylase(s) show(s) a high preference for the central carbon in odd-numbered homologues, e.g. for hentriacontan-16-ol (62%), or the carbon next to the centre of even-numbered chains, e.g. for triacontan-15-ol (88%) and dotriacotan-16-ol (82%); (2) hydroxylation occurs preferentially on C-16, e.g. for nonacosan-14-ol (alias "nonacosan-16-ol") and tritriacontan-16-ol. These two factors are very similar to the ones contributing to the Arabidopsis MAH1 regiospecificity.

Combining all the above information, it appears very likely that a MAH1-like enzyme is involved in wax secondary alcohol formation in pea leaves. Thus, it may now be hypothesized that MAH1-like enzymes are involved in biosynthesis of symmetric secondary alcohols occurring in the waxes of plant species outside the Brassicaceae. Such enzymes similar to the enzyme(s) discussed for wax secondary alcohol biosynthesis in *Brassica* species [113] and identified in Arabidopsis [112] maybe fairly widespread in diverse plant lineages, and could be targeted for further studies where plant wax analyses reveal the presence of symmetric secondary alcohols.

4.3.2. Biosynthesis of Secondary/secondary Alkanediols in Pea Leaves

The three secondary/secondary hentriacontanediols identified in pea wax had striking similarity to the co-occurring secondary alcohols, sharing the predominant C_{31} chain length and one hydroxyl function on either the central carbon (C-16) or the carbon next to it. Furthermore, these diols and the secondary alcohols were found at relatively high concentrations only in the wax on the abaxial side of the leaves. It therefore appears very plausible that both compound classes are biosynthetically related, the alcohols serving as precursors for direct hydroxylation to the corresponding diols (Fig. 4.4). Accordingly, hentriacontan-15-ol likely is the precursor for the formation of hentriacontane-8,15-diol and -

10,17-diol, while hentriacontan-16-ol is the intermediate en route to hentriacontane-9,16-diol. This hypothesis implies that both hydroxyl functions of the secondary/secondary diols are introduced directly into a pre-existing alkyl chain, and not during elongation in a polyketide-like fashion. The first hydroxylation likely takes place on C-15/C-16 before a second hydroxylation occurs in a distance of eight methylene units away from it. The alternative sequence of hydroxylation steps seems unlikely as no hentriacontan-8-ol, -9-ol or -10-ol isomers were found. The wax chemical data suggest that the second hydroxylation step occurs with substrate- and regiospecificity. Hentriacontan-16-ol and hentriacontan-15-ol occurred in the wax at a ratio of 2:1, while the isomer ratio of the corresponding diol products was 5:1, indicating a preference for hentriacontan-16-ol as a substrate. The constant distance between both OH functions in the diols further suggests that the hydroxylating enzyme is able to selectively introduce the second function depending on the position of the first hydroxyl group. This characteristic distinguishes this hydroxylase from the MAH1-like enzymes discussed so far (Chapter 3 and above), making it likely that the pea leaf possesses two enzymes, one very similar to MAH1 (section 4.3.1) and the other one less related.

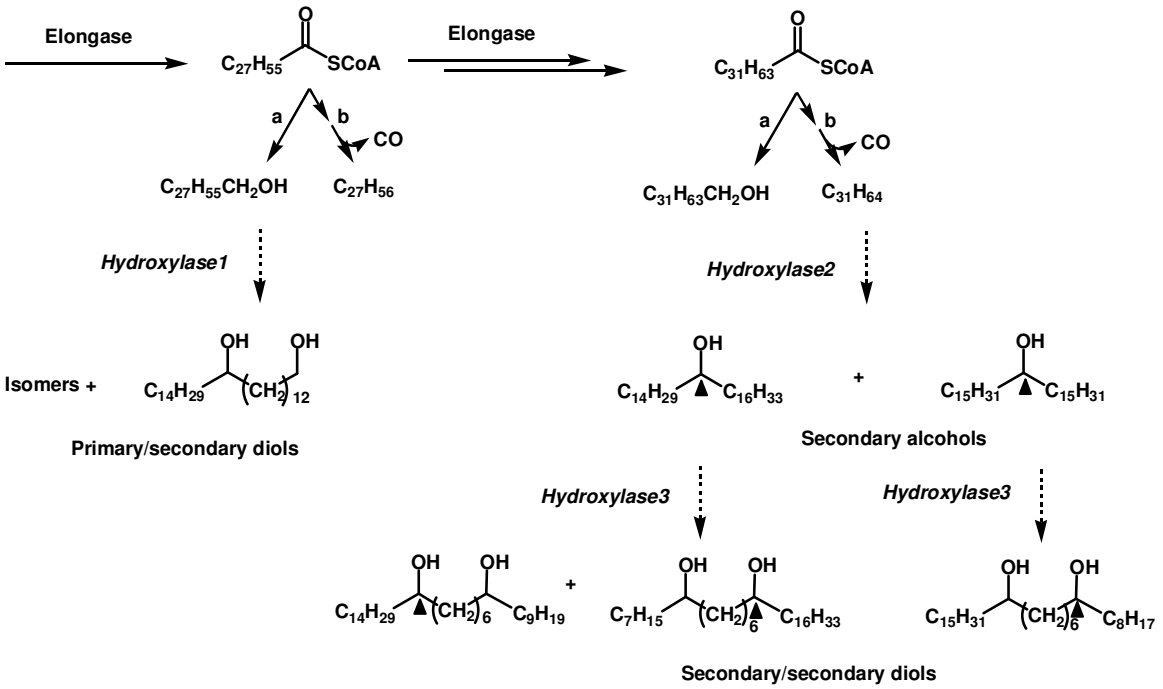

Figure 4.4: Proposed biosynthetic pathways leading to symmetric secondary alcohol, primary/secondary and secondary/secondary alkanediol isomers in the leaf wax of pea. Only octacosanediols and hentriacontanediols are depicted as examples. After the acyl-CoAs are elongated to certain chain lengths, primary alcohols and alkanes are produced through the (a) acyl reduction and (b) decarbonylation pathways (arrows) (sections 1.3.2.2 and 1.3.2.3), respectively. Primary/secondary alkanediol isomers and secondary alcohol isomers are proposed to result from hydroxylation of primary alcohols and alkanes by hydroxylase1 and hydroxylase2, respectively (dashed arrows). The resulting secondary alcohols may then be further functionalized by hydroxylase3 to secondary/secondary alkanediols. The carbons with hydroxyl groups originating from secondary alcohols are highlighted by black triangles. Based on the present results, it cannot be decided whether the three hydroxylase activities shown here are due to identical or distinct but similar enzymes.

4.3.3. Biosynthesis of Primary/secondary Alkanediols in Pea Leaves

The primary/secondary alkanediols in pea had exclusively even-numbered chain lengths matching the homologue pattern of the primary alcohols that mainly co-occurred on the adaxial side of the leaf.[39] These results suggest that the primary alcohols serve as the substrates for further hydroxylation towards those diols (Fig. 4.4). The primary function originates from the acyl group generated by elongation, while the secondary function is only later introduced by oxidation of a methylene unit. This hydroxylation step has a preference for carbons near the centre of the substrate chain, and might thus be catalyzed by a MAH1-like hydroxylase similar or identical to the enzyme involved in pea secondary alcohol

synthesis. The alternative order of steps, invoking secondary alcohols as precursors for chain-end hydroxylation, is very unlikely as both secondary alcohols with chain lengths C_{26} or C_{28} and primary/secondary alkanediols corresponding to the C_{29}-C_{33} secondary alcohols were absent.

In summary, three compound classes containing secondary hydroxyl groups were detected in pea cuticular wax. It seems likely that all the secondary hydroxyl groups are introduced by hydroxylases rather than during elongation. These hydroxylases show different substrate usages and regiospecificities. The hydroxylase involved in secondary alcohol biosynthesis is similar to MAH1 in terms of substrate preference (alkanes as substrates) and regiospecificity. The hydroxylase involved in primary/secondary alkanediol biosynthesis also prefers to hydroxylate central carbons while uses primary alcohols as substrates, and is therefore also similar to MAH1. The hydroxylase introducing the second hydroxyl group in the secondary/secondary alkanediols hydroxylates pre-existing symmetric secondary alcohols with strict regiospecificity different from MAH1. Therefore, pea shows a more diversified hydroxylase family than Arabidopsis.

Chapter 5 Novel Very Long Chain 5-hydroxyaldehydes in the Needle Cuticular Wax of Yew (*Taxus baccata*)

5.1 Introduction

Wax constituents containing secondary functional groups can be biosynthesized by hydroxylating alkanes, primary alcohols and secondary alcohols, e.g., nonacosan-14-ol and -15-ol in Arabidopsis, *Brassica napus* and *B. oleracea*; octacosane-1,14-diol and hentriacotane-9,16-diol in pea (*Pisum sativum*). The studies in the last two chapters focused on investigating the hydroxylases introducing the hydroxyl groups in those plant systems. It was found that the hydroxylases show a limited regiospecificity when there are no pre-existing secondary functional groups in the substrates, thus resulting in isomeric products with functional groups on adjacent carbon positions.

Alternatively, secondary functional groups can be introduced during elongation. Biochemical evidence had shown that the two carbonyl groups in β-diketones are introduced during chain elongation in barley.[154] Because the carbon chains are elongated by adding a C_2 unit (Fig. 1.4 and Fig. 1.7), functional groups can only be introduced onto carbon atoms having odd numbers of methylene units in between, giving 1,3-, 1,5- and 1,7-substitution patterns. In recent years, diverse wax components with such 1,x-substitution patterns have been identified in many plant species.[128,131] Their characteristic functional group substitution patterns suggested that these functional groups are introduced during elongation (section 1.3.3.4). To further substantiate elongation hypothetical pathways (the third objective of the thesis), the potential intermediates and corresponding products have to be identified.

The reported wax constituents with 1,x-substitution patterns were detected together with asymmetric secondary alcohols and/or ketones, e.g., hexacosane-1,7-diol, octacosane-1,9-diol and triacontane-1,11-diol were detected together with nonacosan-10-ol in the leaf waxes of various poppy species; 1-hydroxyhentriacontan-7-one, -9-one, -11-one and 13-one were detected together with nonacosan-10-one in frond cuticular wax of royal fern (*Osmunda regalis*).[128,131] It is known that many gymnosperms contain nonacosan-10-ol as (one of) the

major wax component(s), therefore, yew (*Taxus baccata*) was selected here to search for new structures containing secondary functional groups.

The experiments were conducted in two steps. In the first step, yew needle total wax was extracted, and then the previously known compounds were identified and quantified by GC-MS and GC-FID. In the second step, the wax mixture was separated on TLC. The fractions containing unknown compounds that were suspected to contain secondary functional groups were transformed into various derivatives and analyzed by GC-MS.

5.2 Results

5.2.1 Chemical Analysis of Total Wax

The yew needle wax contained fatty acids (21%), alkanediols (19%), phenyl esters (15%), and secondary alcohols (9%) together with smaller amounts of aldehydes, primary alcohols, alkanes, alkyl esters and tocopherols (Table 5.1). The single most prominent constituents were nonacosan-10-ol, nonacosane-4,10-diol and nonacosane-5,10-diol, each amounting to approximately 10% of the total wax. In addition, trace amounts of other isomeric alkanediols were detected (nonacosane-3,10-diol, nonacosane-6,10-diol, nonacosane-7,10-diol and nonacosane-10,13-diol). Complete homologous series of fatty acids (C_{20}-C_{32}), primary alcohols (C_{21}-C_{32}) and aldehydes (C_{26}-C_{32}) were present. They were all dominated by even-numbered chain lengths, whereas the series of *n*-alkanes (C_{25}-C_{29}) was dominated by odd numbered chain lengths. The chain length distribution of alkyl esters (C_{42}-C_{46}) showed a maximum at C_{44}. The phenyl esters consisted of 4-(3',4'-dihydroxyphenyl)-2-butyl esters of C_{20}-C_{26} fatty acids, 3-(4'-hydroxyphenyl)-propyl esters of C_{22}-C_{28} fatty acids, and 3-(3',4'-dihydroxyphenyl)-propyl esters of C_{22}-C_{26} fatty acids. The only other cyclic compounds identified were α-, β-, δ- and γ-tocopherol. Overall, 96 compounds were identified and accounted for 85% of the total wax (34.1 $\pm$ 1.3 μg/cm^2), while another 15% of the wax mixture remained unknown. Therefore, the yew needle wax was found to have a composition relatively similar to that of other gymnosperm species.[155,156]

Table 5.1: Compositions of the total cuticular wax mixture extracted from yew needles. Mean values (of five independent samples) ± standard errors (SE) are given for the coverage (µg/cm^2) of individual homologues of the major compound classes.

Chain length	Aldehydes	Alkanes	Fatty acids	Alkyl esters	Primary Alcohols	Dihydroxy-phenyl-butanoids[b]	Hydroxy-phenyl-propanoids[b]	Dihydroxy-phenyl-propanoids[b]	Tocopherols	Secondary Alcohols	Secondary/ secondary Diols	Unidentified
C_{20}	-	-	0.1 ± 0.01	-	-	0.6 ± 0.2	-	-	-	-	-	-
C_{21}	-	-	tr[a]	-	tr	0.2 ± 0.1	-	-	-	-	-	-
C_{22}	-	-	0.5 ± 0.02	-	0.3 ± 0.04	0.8 ± 0.1	0.3 ± 0.04	-	-	-	-	-
C_{23}	-	-	0.1 ± 0.01	-	tr	tr	0.2 ± 0.04	0.1 ± 0.04	-	-	-	-
C_{24}	-	-	1.3 ± 0.1	-	0.2 ± 0.04	0.5 ± 0.1	0.8 ± 0.1	tr	-	-	-	-
C_{25}	-	0.1 ± 0.04	0.2 ± 0.02	-	tr	-	0.1 ± 0.04	0.7 ± 0.1	-	-	-	-
C_{26}	0.1 ± 0.04	0.1 ± 0.01	0.7 ± 0.1	-	0.1 ± 0.04	tr	0.4 ± 0.04	0.1 ± 0.04	-	-	-	-
C_{27}	0.2 ± 0.01	0.3 ± 0.04	0.4 ± 0.04	-	0.1 ± 0.02	-	tr	0.3 ± 0.1	-	-	-	-
C_{28}	0.9 ± 0.04	tr	2.1 ± 0.2	-	0.2 ± 0.04	-	tr	-	-	-	-	-
C_{29}	0.1 ± 0.04	0.2± 0.02	0.4 ± 0.04	-	-	-	-	-	-	3.0 ± 0.4	6.4 ± 0.2	-
C_{30}	0.3 ± 0.1	-	1.0 ± 0.1	-	0.1 ± 0.04	-	-	-	-	-	-	-
C_{31}	-	-	tr	-	tr	-	-	-	-	-	-	-
C_{32}	0.3 ± 0.02	-	0.3 ± 0.2	-	tr	-	-	-	-	-	-	-
Total	1.9 ± 0.1	0.7 ± 0.1	7.2 ± 0.8	2.4 ± 0.4	1.2 ± 0.3	2.2 ± 0.1	0.9 ± 0.1	1.3 ± 0.2	0.9 ± 0.1	3.0 ± 0.4	6.4 ± 0.2	5.0 ± 0.5

[a] tr, traces; i. e. less than 0.05 µg/cm^2
[b] Chain lengths refer to the carbon number of fatty acid fragment of the phenyl esters

5.2.2 Identification of 1,5-Bifunctional Components

All the unidentified compounds were minor components. To eliminate the interference from major constituents, the wax mixture was separated on TLC. Fourteen fractions were isolated. Twelve of them contained mainly identified wax constituents. The other two fractions were found to contain unidentified compounds, designated as compound classes **A** and **B**.

5.2.2.1 1,5-Alkanediols

Compound class **A** (R_f 0.05), migrating between secondary/secondary alkanediols (R_f 0.08) and fatty acids (R_f 0.03), likely contained either a primary and a secondary hydroxyl group, or else three or more secondary hydroxyl and carbonyl groups. The TMSi derivative of the most prominent compound in compound class **A** showed alcohol characteristic fragments *m/z* 73, 75, 103 and a diol signal *m/z* 147 (Fig. 5.1). In addition, a fragment *m/z* 149 that is characteristic for primary/secondary alkanediols was detected. The fragment *m/z* 85 had been interpreted as $[C_5H_9O]^+$ and found to be characteristic for 1,5-alkanediols.[130] The 1,5-alkanediol nature was confirmed by an α-fragment *m/z* 247 ($[C_5H_9(OTMSi)_2]^+$) together with its daughter ion *m/z* 157 ($[C_5H_8OTMSi]^+$). This α-ion together with the second α-fragment *m/z* 481 ($[C_{24}H_{48}OTMSi]^+$) was used to propose a candidate structure, dotriacontane-1,5-diol, which was confirmed by a fragment *m/z* 611 ($[M\text{-}CH_3]^+$) and molecular ion *m/z* 626. The GC profile of fraction **A** showed ten more peaks, all with matching mass spectral characteristics of TMSi ethers of primary/secondary diols (Table 5.2). Based on the chain length specific α-fragments and molecular ions, the compounds were identified as a homologous series of 1,5-alkanediols ranging from C_{28} to C_{38}.

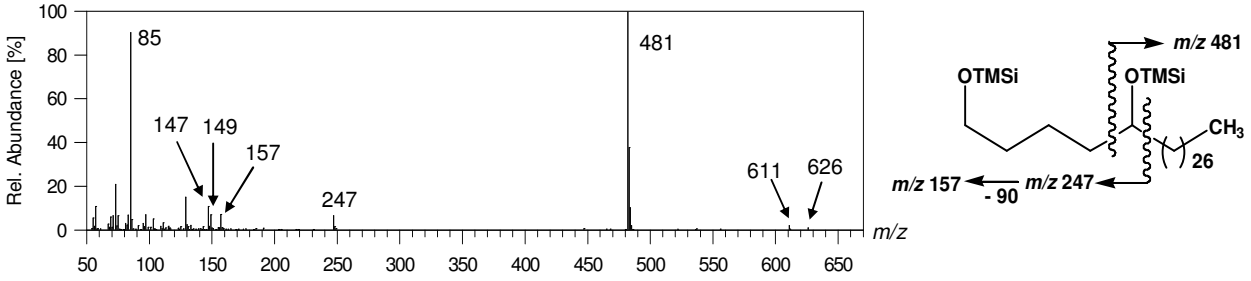

Figure 5.1: Mass spectrum and fragmentation diagram of bis TMSi ether of dotriacontane-1,5-diol.

Table 5.2: Mass spectral data of 1,5-alkanediol TMSi ethers, 5-hydroxyaldehyde TMSi derivatives and underivatized 5-hydroxyaldehydes.

Compounds	Fragments characteristic for the compound class[a] Relative Intensity%							Fragments characteristic for the homologue Relative Intensity%					
TMSi ethers of 1,5-alkanediols	**73**	**85**	**103**	**147**	**149**	**157**	**247**	**M**		**M-15**		**$C_nH_{2n}OTMSi$**	
Octacosane-1,5-diol	40	83	25	23	10	9	5	**570**	-	**555**	2	**425**	100
Nonacosane-1,5-diol	-	-	-	-	-	3	2	**584**	-	**569**	2	**439**	100
Triacontane-1,5-diol	45	90	30	25	10	10	7	**598**	0.5	**583**	2	**453**	100
Hentriacontane-1,5-diol	32	87	27	20	9	9	8	**612**	-	**597**	1	**467**	100
Dotriacontane-1,5-diol	32	86	7	13	8	8	7	**626**	0.2	**611**	0.4	**481**	100
Tritriacontane-1,5-diol	36	93	9	15	8	8	7	**640**	-	**625**	0.6	**495**	100
Tetratriacontane-1,5-diol	25	95	6	12	8	7	7	**654**	-	**639**	0.5	**509**	100
Pentatriacontane-1,5-diol	26	100	6	12	9	8	7	**668**	-	**653**	0.5	**523**	95
Hexatriacontane-1,5-diol	22	100	3	10	9	9	8	**682**	-	**667**	0.6	**537**	94
Heptatriacontane-1,5-diol	24	100	6	12	8	9	7	**696**	-	**681**	0.6	**551**	96
Octatriacontane-1,5-diol	25	100	4	14	9	8	7	**710**	-	**695**	0.7	**565**	95
TMSi ethers of 5-hydroxyaldehydes	**73**	**103**	**119**	**173**				**M**		**M-15**		**$C_nH_{2n}OTMSi$**	
5-Hydroxytetracosanal	8	27	100	29				**440**	2	**425**	22	**369**	19
5-Hydroxyhexacosanal	9	25	100	25				**468**	2	**453**	23	**397**	12
5-Hydroxyheptacosanal	10	27	100	24				**482**	1	**467**	20	**411**	13
5-Hydroxyoctacosanal	11	22	100	16				**496**	1	**481**	13	**425**	9
5-Hydroxynonacosanal	12	21	100	17				**510**	1	**495**	13	**439**	9
5-Hydroxytriacontanal	12	21	100	17				**524**	1	**509**	13	**453**	10
5-Hydroxylhentriacontanal	11	22	100	16				**538**	1	**523**	12	**467**	9
5-Hydroxydotriacontanal	11	19	100	18				**552**	1	**537**	12	**481**	10
5-Hydroxytritriacontanal	13	23	100	18				**566**	2	**551**	14	**495**	10
5-Hydroxytetratriacontanal	14	19	100	17				**580**	1	**565**	11	**509**	10
5-Hydroxypentatriacontanal	12	20	100	16				**594**	1	**579**	12	**523**	9
5-Hydroxyhexatriacontanal	13	20	100	19				**608**	1	**593**	13	**537**	9
Acetates of 1,5-alkanediols	**61**	**85**						**M-60-43**		**M-120**			
Tetracosane-1,5-diol	8	100						**365**	19	**348**	30		
Hexaconsane-1,5-diol	8	100						**393**	17	**376**	28		
Heptacosane-1,5-diol	9	100						**407**	19	**390**	30		
Octacosane-1,5-diol	8	100						**421**	18	**404**	29		
Nonacosane-1,5-diol	9	100						**435**	15	**418**	30		
Triacontane-1,5-diol	9	100						**449**	14	**432**	28		
Hentriacontane-1,5-diol	10	100						**463**	16	**446**	29		
Dotriacontane-1,5-diol	9	100						**477**	14	**460**	32		
Tritriacontane-1,5-diol	9	100						**491**	14	**474**	29		
Tetratriacontane-1,5-diol	10	100						**505**	13	**488**	35		
Pentatriacontane-1,5-diol	9	100						**519**	15	**502**	32		
Hexatriacontane-1,5-diol	8	100						**533**	14	**516**	29		

Continued on the next page

Compounds	Fragments characteristic for the compound class[a] Relative Intensity%		Fragments characteristic for the homologue Relative Intensity%	
5-hydroxyaldehydes	**98**	**111**	**M-18**	
5-Hydroxytetracosanal	100	36	**350**	7
5-Hydroxyhexacosanal	100	30	**378**	7
5-Hydroxyheptacosanal	100	29	**392**	4
5-Hydroxyoctacosanal	100	28	**406**	5
5-Hydroxynonacosanal	100	29	**420**	6
5-Hydroxytriacontanal	100	27	**434**	5
5-Hydroxylhentriacontanal	100	27	**448**	5
5-Hydroxydotriacontanal	100	26	**462**	5
5-Hydroxytritriacontanal	100	27	**476**	5
5-Hydroxytetratriacontanal	100	28	**490**	6
5-Hydroxypentatriacontanal	100	28	**504**	5
5-Hydroxyhexatriacontanal	100	27	**518**	4

[a] In addition to the characteristic fragments common to all the compounds, fragments *m/z* 55, 57, 71 were also found in all the mass spectra.

5.2.2.2 5-Hydroxyaldehydes

Compound class **B** (R_f 0.14) migrated between primary alcohols (R_f 0.17) and secondary/secondary alkanediols (R_f 0.08) on TLC, and therefore likely contained compounds with a (secondary) hydroxyl group and one (or more) carbonyl group(s). Further GC separation resulted in twelve distinct peaks with similar mass spectral characteristics, indicating that compound class **B** is a homologous series. Combining all the mass spectral data from different derivatives of all twelve compounds, it was eventually concluded that compound class **B** represented a homologous series of 5-hydroxyaldehydes comprising chain lengths C_{24} and C_{26} to C_{36}. This was corroborated by further GC-MS comparisons with a synthetic standard 5-hydroxyoctacosanal. Since this is also the most abundant homologue in the compound class, the structure elucidation will be described using it as an example.

After derivatization with bis-(*N*,*O*-trimethylsilyl)-trifluoroacetamide (BSTFA), the mass spectra of the most abundant compound in **B** showed fragments *m/z* 73, 75 and 103 characteristic for an OTMSi group (Fig. 5.2A). While this indicated the presence of one hydroxyl group, the lack of a diol signal *m/z* 147 made it unlikely that a second hydroxyl group was present. Instead, the characteristic base peak *m/z* 119, which had previously been reported as a characteristic fragment for non-vicinal ketols,[137,157] indicated the presence of one or more carbonyl groups in the molecule. The fragment *m/z* 173 could be interpreted as an α-ion $[C_5H_8O_2TMSi]^+$ and thus pointed to the 1,5-geometry between a carbonyl and a

hydroxyl group. The compound was further characterized by another α-ion *m/z* 425 ($[C_{24}H_{48}OTMSi]^+$), a fragment *m/z* 481 ($[M\text{-}CH_3]^+$) and the molecular ion *m/z* 496. In the spectra of all the other compounds in **B** only the latter three signals differed by 14 mass units (Table 5.2), indicating that they were homologous compounds. It can be concluded that these homologues differed in the number of CH_2 groups in a hydrocarbon chain attached on one side of the 1,5-bifunctionality, rather than between both functional groups.

The number and position of carbonyl groups in the compounds was assessed by reduction of the homologous mixture with lithium aluminum hydride, followed by BSTFA derivatization (Fig. 5.2B). The fragments *m/z* 147 and 149 showed that the reduced derivatives were diols, and that they each contained one primary and one secondary hydroxyl group.[128] All the characteristic signals for 1,5-alkanediols (section 5.2.2.1),[137] were detected in the mass spectra of all twelve homologues, including the fragments *m/z* 85, *m/z* 247 ($[C_5H_9(OTMSi)_2]^+$) and its daughter ion *m/z* 157 ($[C_5H_8OTMSi]^+$). The major compound in the mixture of reduction products showed fragments *m/z* 425 and 555 ($[M\text{-}CH_3]^+$), thus confirming its structure as octacosane-1,5-diol, and the structure of the other compounds as homologous 1,5-alkanediols (Table 5.2). Taken together, this experiment confirmed the 1,5-ketol geometry of compounds in **B** and excluded the presence of any further functional groups.

To further corroborate the 5-hydroxyaldehyde structure, compounds in **B** were reduced with lithium aluminum hydride and then further derivatized with acetic anhydride. The resulting products (Fig. 5.2C) had a prominent mass spectral fragment *m/z* 61, interpreted as $[AcOH_2]^+$ diagnostic for acetates. Furthermore, the fragments *m/z* 450 ($[M\text{-}AcOH]^+$), *m/z* 407 ($[M\text{-}Ac\text{-}AcOH]^+$) and *m/z* 390 ($[M\text{-}(AcOH)_2]^+$), involving the loss of one and two acetyl moieties, were characteristic for bis acetates of alkanediols (Chapter 4). The molecular ion *m/z* 510 of octacosanediol bis acetate confirmed the presence of exactly two hydroxyl functions. Since the base peak *m/z* 85 was found for both the bis acetates and for the corresponding bis TMSi ethers, it is clearly diagnostic for 5-hydroxyalkanediols irrespective of the hydroxyl derivatives.

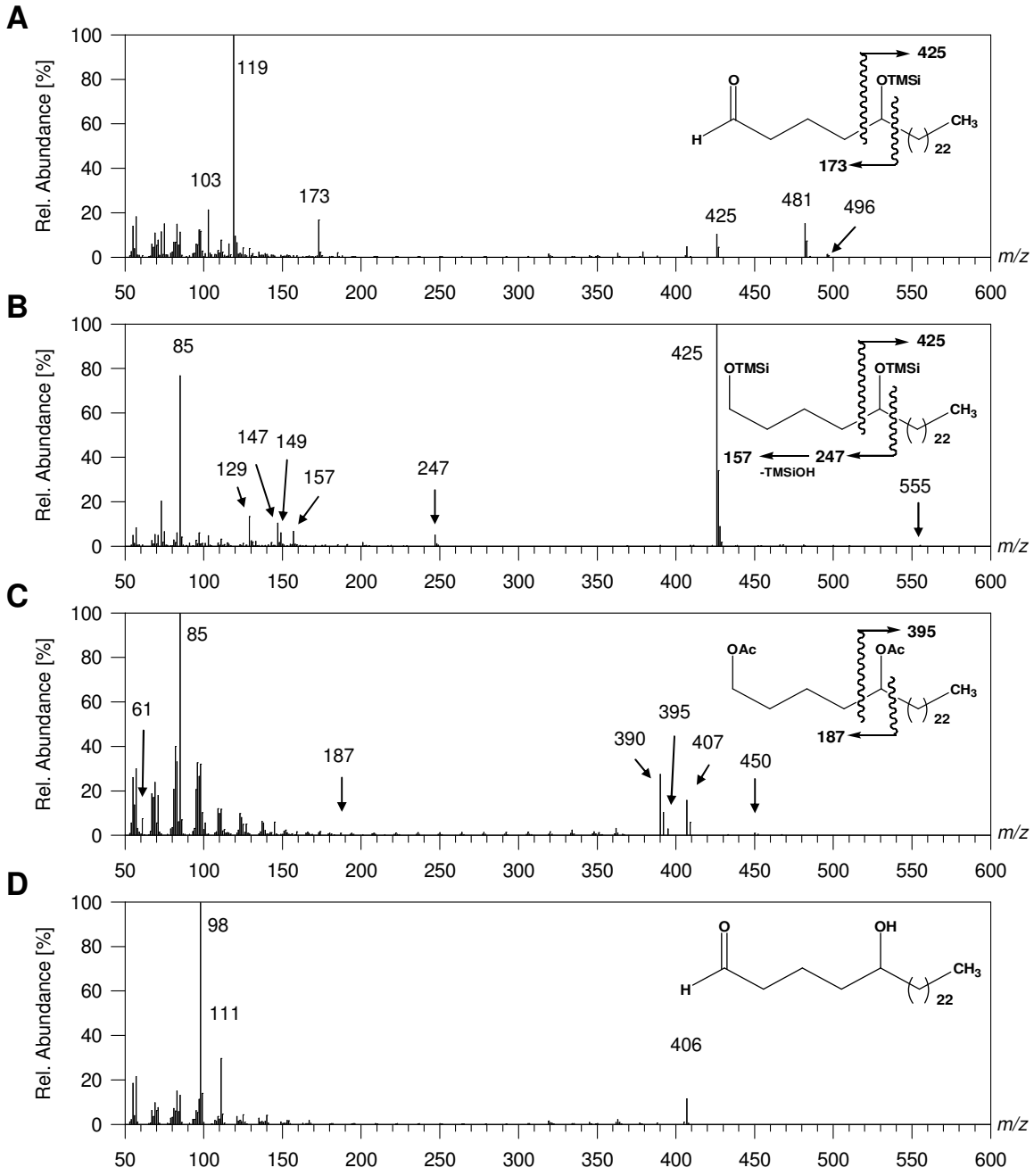

Figure 5.2: Mass spectra of representative derivatives of 5-hydroxyaldehydes in the needle wax of yew. (A) TMSi ether of 5-hydroxyoctacosanal, (B) bis TMSi ether of octacosane-1,5-diol, (C) bis acetate of octacosane-1,5-diol and (D) underivatized 5-hydroxyoctacosanal.

The mass spectra of underivatized 5-hydroxyoctacosanal (Fig. 5.2D) showed prominent fragments *m/z* 98 and *m/z* 111 that can be interpreted as $[C_6H_{10}O]^+$ resulting from water elimination from the molecular ion followed by McLaffety rearrangement, and $[C_7H_{11}O]^+$ resulting from water elimination followed by β-fragmentation, respectively. Due to the presence of a hydroxyl group, water can be easily eliminated from the molecular ion, resulting in the fragment *m/z* 406 $[M\text{-}H_2O]^+$ with relatively high abundance. For the other homologues, this fragment differed by 14 mass units, whereas the other fragments *m/z* 98 and *m/z* 111 stayed constant (Table 5.2).

In summary, the spectral information indicated the presence of one hydroxyl and one carbonyl group with primary/secondary 1,5-geometry, narrowing the candidate structures of the prevalent homologue to the isomers 5-hydroxyoctacosanal and 1-hydroxyoctacosan-5-one. The latter structure seemed highly unlikely because: (1) the presence of a primary hydroxyl group and a carbonyl group would give rise to a polarity higher than that observed in our TLC experiments; (2) the α-fragment of the mid-chain functional group (*m/z* 425 for the TMSi derivatives) was not affected by LAH treatment, showing that this functionality cannot be reduced and therefore likely is a hydroxyl group; (3) the mass spectrum of the TMSi ether of 5-ketooctacosanol would very likely give an α-fragment *m/z* 351 (instead of *m/z* 425), which could not be detected.

Since the spectral interpretation strongly favoured a 5-hydroxyaldehyde structure for compounds in **B**, one representative of the homologous series, 5-hydroxyoctacosanal, was synthesized for final proof of structure (Fig. 5.3).[143] The key step was the cross metathesis catalyzed by Grubbs catalyst between a terminal olefin and a vinylboronate ester. The resulting long chain vinylboronate ester was purified on preparative TLC, and then the terminal double bond of the vinylboronate ester was oxidized to an aldehyde by trimethylamine *N*-oxide (Me_3NO). It was found that the GC retention time and mass spectral fragmentation pattern of the synthetic 5-hydroxyoctacosanal were identical to those of the most abundant homologue of compound class **B** (Fig. 5.4). The compounds in compound class **B** were thus identified as a series of 5-hydroxyaldehydes comprising chain lengths C_{24} and C_{26} to C_{36}.

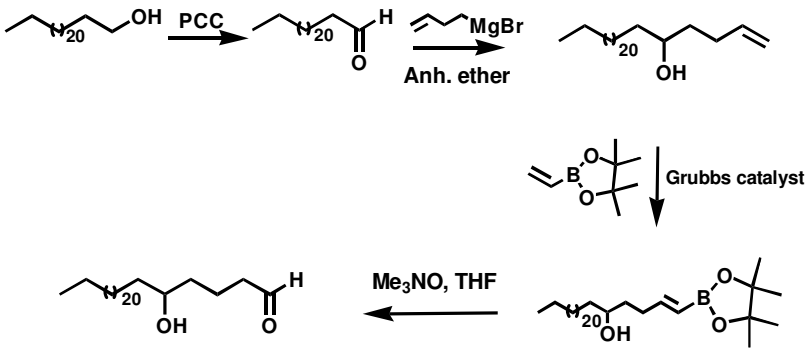

Figure 5.3: Synthesis of 5-hydroxyloctacosanal

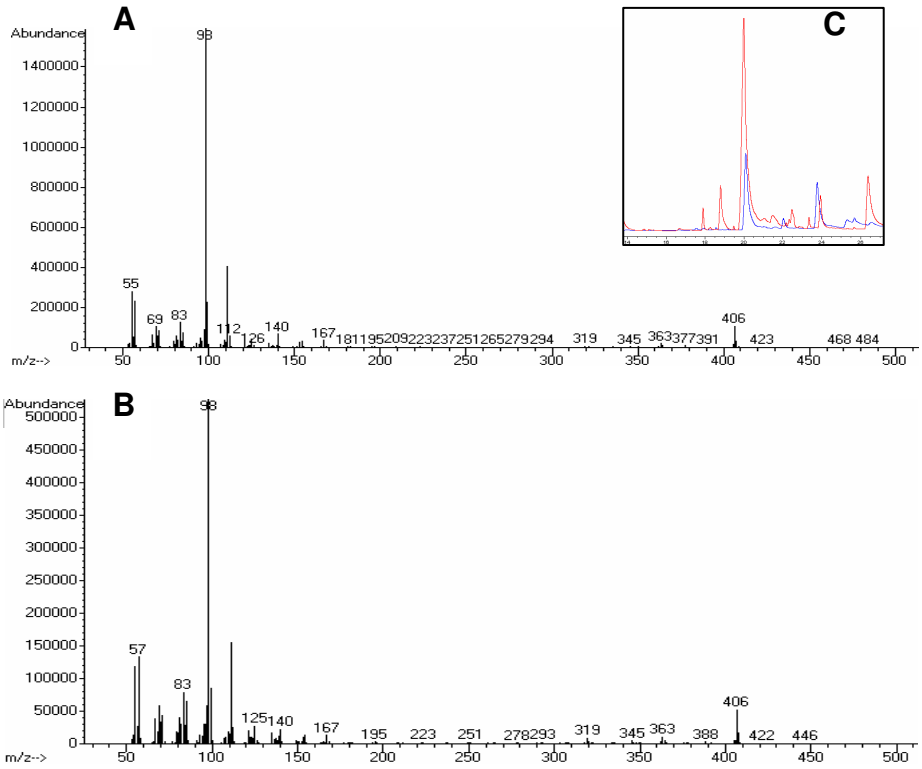

Figure 5.4: Comparison of the GC-MS data of the synthetic standard and one of the unknown compounds. (A) Mass spectrum of synthetic 5-hydroxyoctacosanal, (B) mass spectrum of one of the underivatized compounds of compound class **B**, and (C) GC traces of synthetic 5-hydroxyoctacosanal (red line) and one of the GC peaks of compound class **B** (black line)

5-Hydroxyaldehydes and 1,5-diols were dominated by even-numbered chain lengths. Within 5-hydroxyaldehydes, 5-hydroxyoctacosanal (42%), 5-hydroxytriacontanal (22%) and 5-hydroxydotriacontanal (19%) were the most abundant homologues (Fig. 5.5A). 1,5-

Alkanediols were more evenly distributed. Interestingly, this homologous series had similar change length range to 5-hydroxyaldehydes (Fig. 5.5B).

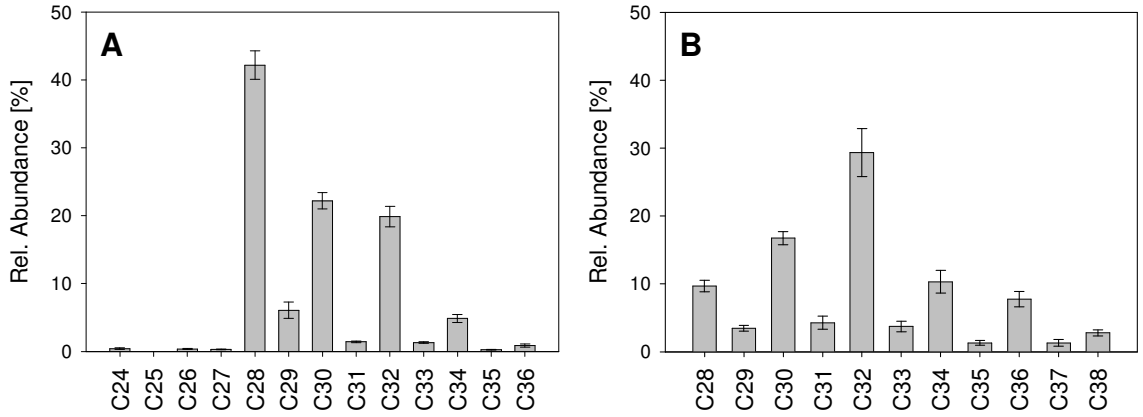

Figure 5.5: Chain length distribution (%) of (A) 5-hydroxyaldehydes (n=5, ± SE) and (B) 1,5-alkanediols (n=3, ± SE) in yew needle wax.

5.3 Discussion-Biosynthesis of 1,5-Bifunctional Wax Components

The similar chain length distributions of 5-hydroxyaldehydes and 1,5-alkanediols suggested a biosynthetic relationship between both compound classes. Furthermore, as for other primary/secondary bifunctional components, the predominance of even-numbered homologues in both series made it very likely that both compound classes are formed, in analogy to other common wax components, on pathways involving acyl reduction rather than decarbonylation (sections 1.3.2.2 and 1.3.2.3). The constant 1,5-geometry of all alkanediols and hydroxyaldehydes detected here suggested that the secondary functional group is introduced during elongation. In analogy to β-diketone biosynthesis (section 1.3.3.3), one round of elongation may start with β-hydroxyacyl-CoA intermediates instead of the corresponding acyl-CoAs (Fig. 5.6). The resulting 5-hydroxyacyl-CoAs could be modified into 5-hydroxyacids, 5-hydroxyaldehydes, or 1,5-alkanediols. 5-Hydroxy-fatty acids were not detected in yew needle wax, but their δ-lactone derivatives have been identified in the leaf cuticular wax of *Cerinthe minor*.[130] Alternatively, one round of elongation may start with a β-ketoacyl-CoA intermediate instead of a β-hydroxyacyl-CoA intermediate (not shown in Fig 5.6). The keto group could be retained during the elongation steps and reduced to a hydroxyl group in later biosynthetic steps.

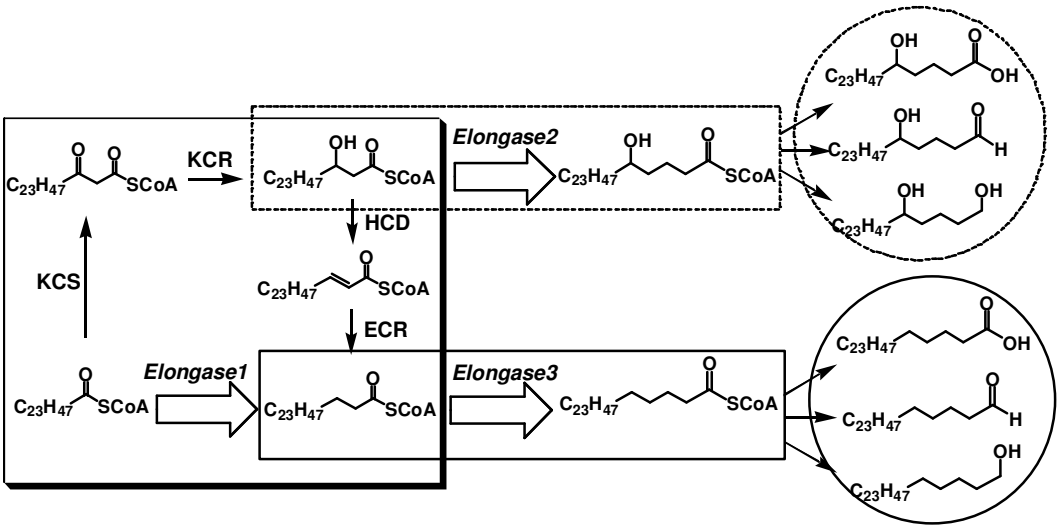

Figure 5.6 Proposed biosynthetic pathway leading to 5-hydroxyaldehydes and 1,5-alkanediols in the needle wax of yew. Only the C_{28} homologues are depicted as an example. In normal wax biosynthesis (shown in boxes with black line), acyl-CoA chains are elongated by elongase complex(es) containing β-ketoacyl-CoA synthase (KCS), β-ketoacyl-CoA reductase (KCR), dehydratase (HCD) and enoyl-CoA reductase (ECR) (shown in box with shade). Multiple rounds of elongation lead to C_{28} acyl-CoA, which is further modified into the corresponding free fatty acid, aldehyde and alcohol (circled with black line). A polyketide-like pathway is proposed for biosynthesis of 5-hydroxyaldehydes and 1,5-alkanediols (shown in box with dashed lines). A hydroxacyl-CoA intermediate is elongated directly and the resulting 5-hydroxyacyl-CoA is further modified (shown in dashed cycle). Two or more of the elongase complexes shown may be identical.

Chapter 6 Nonacosan-10-ol Biosynthesis in California Poppy (*Eschscholzia californica*) Leaves: Biochemical Assays

6.1 Introduction

Polyketides are structurally a very diverse family of natural products. This structural diversity notwithstanding, the functional groups in polyketide natural products are always arranged so that they have an odd number of carbons on the hydrocarbon chain between them, resulting in 1,3-, 1,5- or 1,7-relative positions between the functional groups. These structural characteristics are due to the fact that these functional groups are always introduced during chain elongation by addition of C_2 units. Conversely, the functional groups cannot be introduced onto the other carbons in between, and two polyketide functional groups cannot have 1,2-, 1,4- or 1,6-positions relative to each other. In plant cuticular waxes, diverse components with polyketide structural characteristics have been detected, e.g., β-diketones and primary/secondary alkanediols with 1,3-, 1,5- and 1,7-substitution patterns (sections 1.3.3.3 and 1.3.3.4).[115,116] Furthermore, biochemical evidence indicates that the two carbonyl groups in β-diketones found in the wax of barley are introduced during chain elongation on polyketide-like pathways.[124,125]

Nonacosan-10-ol is a major wax constituent in many plant species.[135,155,158] In contrast to the more even isomer distribution of the C_{29} symmetric secondary alcohols in Arabidopsis and *Brassica* species (section 1.3.3.1 and Chapter 3), nonacosan-10-ol has been found to either occur without other isomers, or at least strongly dominate the C_{29} secondary alcohol homologue where it occurs (>95%).[149] Therefore, it had been suspected that the hydroxyl group in nonacosan-10-ol is introduced during elongation rather than by hydroxylation.[132,137] Similar to the introduction of the carbonyl groups in the β-diketone hentriacontane-14,16-dione (Fig. 1.7), for nonacosan-10-ol biosynthesis a hydroxyl group could be introduced during the cycle of elongating C_{20} acyl-CoA to C_{22} acyl-CoA (Fig. 6.1). C_{20} β-hydroxyacyl-CoA could be generated by omitting HCD and ECR functions during this elongation cycle, and the β-hydroxy-intermediate could then be further elongated and finally modified to nonacosan-10-ol. Alternatively, the functional group could be introduced as a carbonyl group

by omitting KCR, HCD and ECR functions and, thus, C_{20} β-ketoacyl-CoA instead of β-hydroxyacyl-CoA would serve as an intermediate for further elongation and modification to nonacosan-10-ol. Either way to introduce the hydroxyl group is fundamentally different from hydroxylation.

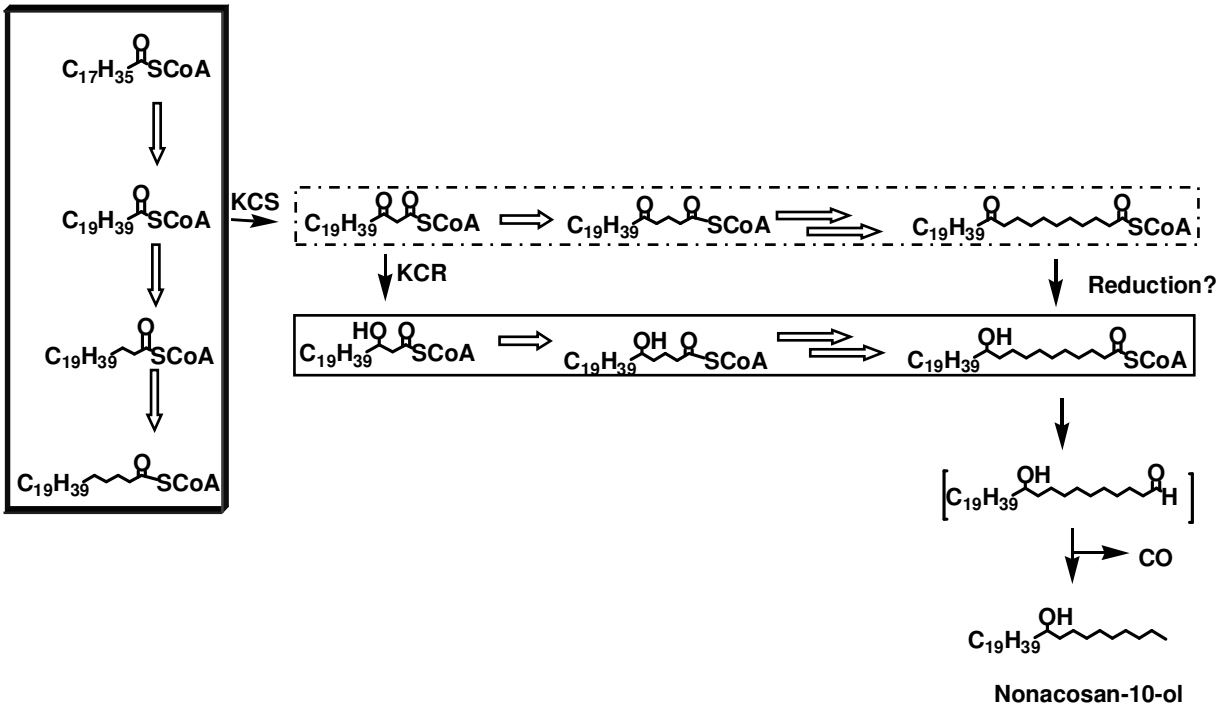

Figure 6.1: Hypothetical pathways leading to nonacosan-10-ol in California poppy. The hydroxyl group could be introduced by omitting ECR and HCD functions from an elongase complex extending C_{20} acyl-CoA to C_{22} acyl-CoA, resulting in C_{22} β-hydroxyacyl-CoA (shown in the box with black line). Alternatively, a carbonyl group could be introduced by an isolated KCS, effectively omitting KCR, ECR and HCD functions from the complex. This would result in C_{22} β-ketoacyl-CoA (shown in the box with dashed line), and then the carbonyl group could be reduced later along the pathway. Reduction of this carbonyl group could occur at a later stage than where it is indicated. Normal carbon chain elongation is shown in the box with shade. Hollow arrows indicate enzyme complex activities, and black arrows indicate a single enzyme activity.

In plant species containing both nonacosan-10-ol and wax components with primary functional groups, two elongation systems must exist: a normal elongation system generating VLCFAs for modification into alkanes and primary alcohols, and a special elongation system to introduce the secondary functional group leading to nonacosan-10-ol. Acyl-CoA substrates with various chain lengths should all be indiscriminately elongated by the normal elongation system. In contrast, the special elongation system involved in nonacosan-10-ol biosynthesis

should have preference for certain acyl CoA chain lengths, thus leading to the characteristic structure of this secondary alcohol. Because the functional group must be introduced during the cycle of elongating C_{20} acyl-CoA to C_{22} acyl-CoA, acyl-CoAs with chain lengths of C_{20} or shorter should serve as substrates for the special elongation system, while acyl-CoA substrates with 22 or more carbons should not be elongated by it.

Direct evidence supporting this elongation hypothesis for the biosynthesis of asymmetric secondary alcohols is missing to date. Therefore, the general goal of the current work is to test the hypothesis (third objective of the thesis). Specifically, two questions will be answered in this study: (1) Does a special elongation system exist that can introduce a secondary functional group en route to nonacosan-10-ol? (2) If such a special elongation system exists, does it introduce a hydroxyl group or a carbonyl group?

As described above, the existence of the special elongation system can be evaluated by comparing elongation products formed from C_{18}/C_{20} acyl-CoA substrates with those from C_{22} or longer chain acyl-CoA substrates. The approach taken here was to test elongating activities towards C_{18}, C_{20} and C_{22} acyl-CoA using assays for condensing enzymes by incubation with [2-^{14}C]malonyl-CoA. Because condensation is the first step of the four reactions in one elongation cycle, both normal and special (truncated) elongation cycles should yield labeled products in these assays that can easily be detected.

The nature of the secondary functional groups introduced during elongation, a hydroxyl *vs*. carbonyl group, can be inferred by identifying the elongation products. If the predicted special elongation system exists, then β-ketoacyl-CoA or β-hydroxyacyl-CoA intermediates should accumulate. Under most work-up conditions they would be (partially) converted to methyl ketones or methyl alcohols, respectively, and could be detected as such. In contrast, normal elongation is expected to yield elongated acyl-CoA products that should be converted into free fatty acids during work-up.

Many gymnosperms contain nonacosan-10-ol as the major constituent in their cuticular waxes. However, it is difficult to handle gymnosperm tissues for biochemical assays.

Therefore, the following biochemical experiments could not be carried out with yew needles, even though previous wax analyses had shown them to contain candidate polyketide structures (Chapter 5). California poppy (*Eschscholzia californica*) leaves are known to also contain large amount of nonacosan-10-ol in their cuticular wax,[132] and the poppy leaves offer technical advantages over gymnosperm needles. Therefore, California poppy leaf microsomes were used for the assays.

6.2 Results

To test the elongation systems involved in nonacosan-10-ol biosynthesis, three experiments were conducted. The first was a control experiment in which yeast and Arabidopsis stem microsomes were used to ensure that acyl-CoA substrates can be elongated under the experimental conditions. California poppy microsomes were used in the second experiment to test the hypothetical pathway. In the third experiment, NADPH concentrations of the assays were varied to confirm the production of methyl ketones detected in the second experiment.

6.2.1 Elongation Assays with Arabidopsis and Yeast Microsomes

C_{18}, C_{20} or C_{22} acyl-CoA were incubated with [2-^{14}C]malonyl-CoA in the presence of Arabidopsis or yeast microsomes. The reactions were stopped by adding sodium hydroxide and heating. The hydrolyzed products were extracted with $CHCl_3$ and separated on normal phase TLC. As shown in figure 6.2A, in the Arabidopsis microsome assay each of the three substrates produced a product band co-migrating with a fatty acid standard. TLC analysis of the incubation products of the yeast microsome assays showed that each substrate produced three product bands (Fig 6.2B). One of these product bands co-migrated with a fatty acid standard (region **a**), one band was located at the solvent front (region **c**) and one migrated slightly further than a ketone standard (region **b**). The product bands in region **b** seemed to migrate differently in the three lanes for different acyl-CoA substrates. This was likely due to uneven TLC development since the standards on either side of the plate also migrated differently. Thus, each lane showed the same product pattern.

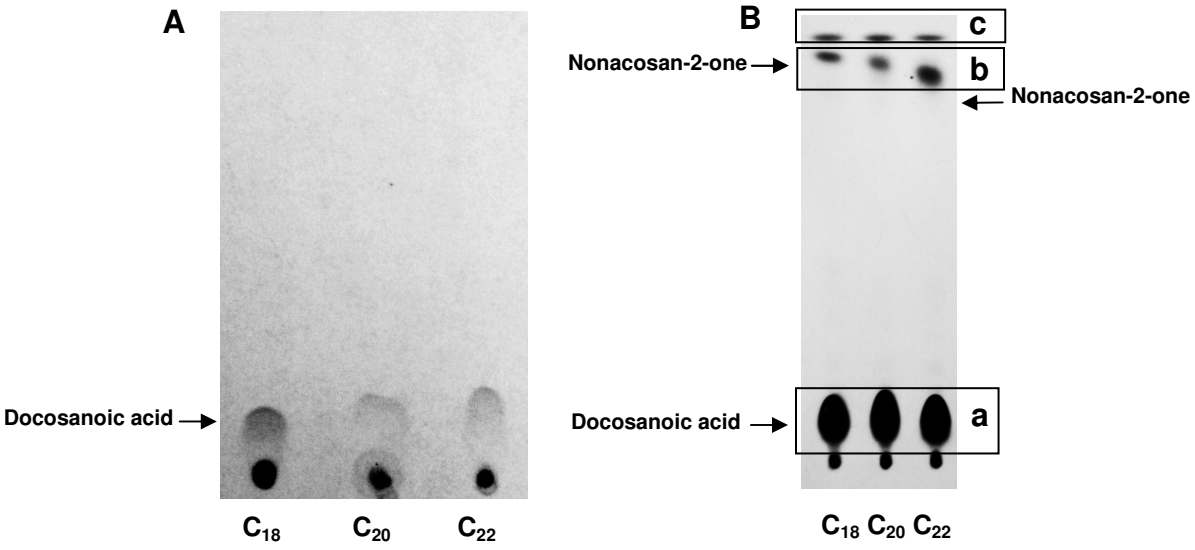

Figure 6.2: Autoradiogram of normal phase TLC analyses of the elongation assay products generated by incubating [2-^{14}C]malonyl-CoA and acyl-CoAs in the presence of (A) Arabidopsis microsomes and (B) yeast microsomes. NADPH was used as reducing agent. Arrows indicate the center of the standards run alongside. Squares in B indicate the three product regions (see text).

6.2.2 Elongation Assays with California Poppy Microsomes

C_{18}, C_{20} or C_{22} acyl-CoA were incubated with [2-^{14}C]malonyl-CoA in the presence of California poppy microsomes. TLC analysis showed that, when C_{18} acyl-CoA was used as the substrate, one product band co-migrated with fatty acids (standard not shown in the figure) and another band co-migrated with octadecan-2-one (Fig. 6.3). The same product pattern was observed for C_{20} acyl-CoA as the substrate. In contrast, incubation with C_{22} acyl-CoA produced only one band co-migrating with fatty acids, while a less polar product band co-migrating with octadecan-2-one was not detected. The difference between lane 2 and lane 3 was observed in repeated experiments, and was also observed when the assay was conducted with 3 mM NADPH (data not shown).

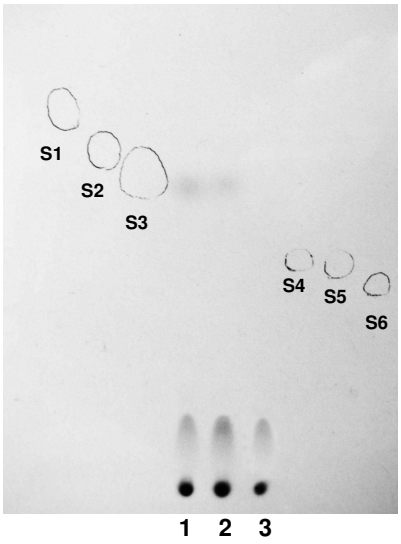

Figure 6.3: Autoradiogram of normal phase TLC analyses of products of the California poppy microsome elongation assay with [2-^{14}C]malonyl-CoA and acyl-CoAs with different chain lengths at 0.5 mM NADPH. The TLC plate was developed with a mixture of hexane and ethyl acetate (12:1). Lane 1, C_{18} acyl-CoA; lane 2, C_{20} acyl-CoA; lane 3, C_{22} acyl-CoA. S1, nonacosan-2-one; S2, tricosan-2-one; S3, octadecan-2-one; S4, nonacosan-10-ol; S5, hexacosan-10-ol; S6, tricosan-7-ol. All the standards have no radioactivity and therefore were visualized under UV after primuline staining and marked with pencil. The spots shown at the origin are likely acetic acid.

The product band co-migrating with octadecan-2-one was clearly separated from secondary alcohol standards. Therefore, the products in this band were not likely secondary alcohols. When chloroform was used to develop the TLC, this band still co-migrated with octadecan-2-one (data not shown), indicating that this product band contained methyl ketones.

Depending on the number of elongation cycles that the substrates went through, the methyl ketone products could have different chain lengths. Thus, standards with different chain lengths were used in an attempt to determine the product chain length. As shown in figure 6.3, methyl ketones with longer chains migrated further. Nonacosan-2-one (C_{29}, **S1**) was clearly separated from tricosan-2-one (C_{23}, **S3**) while tricosan-2-one was slightly separated from octadecan-2-one (C_{18}, **S3**). In a series of secondary alcohol standards tested alongside, nonacosan-10-ol (C_{29}, **S4**) was found to be hardly distinguishable from hexacosan-10-ol (C_{26},

S5). Thus it seemed unlikely that TLC can separate methyl ketones having a chain length difference less than three carbons. Accordingly, the exact chain lengths of the methyl ketones formed in the elongation assay remained unknown.

6.2.3 NADPH Requirement for California Poppy Microsome Elongation Activity

Previous studies had shown that, in the absence of NADPH, β-ketoacyl-CoAs accumulate since they cannot be reduced to β-hydroxyacyl-CoAs and produce acyl CoA end products of elongation cycles, giving rise to methyl ketones as products after work-up under strong basic conditions.[159] The major effect observed in the above experiment was the detection of methyl ketones for C_{20} (and C_{18}) acyl-CoA as the substrate(s) and the absence of methyl ketones for C_{22} acyl-CoA as the substrate. The formation of methyl ketones, at least from some of the substrates, could be due to deficient NADPH levels in the assays. In this case, methyl ketone formation should be abolished by increasing amounts of NADPH. To test whether the composition of the elongation products depended on the NADPH concentration, C_{20} acyl-CoA was incubated with varying NADPH concentrations in the presence of California poppy microsomes. When NADPH was omitted, only methyl ketones were detected while the fatty acid band was missing (Fig. 6.4A). In contrast to this result, when the concentration of NADPH was varied between 0.5 mM and 20 mM, methyl ketones and fatty acids were both detected for each assay under different NADPH concentrations (Fig. 6.4B).

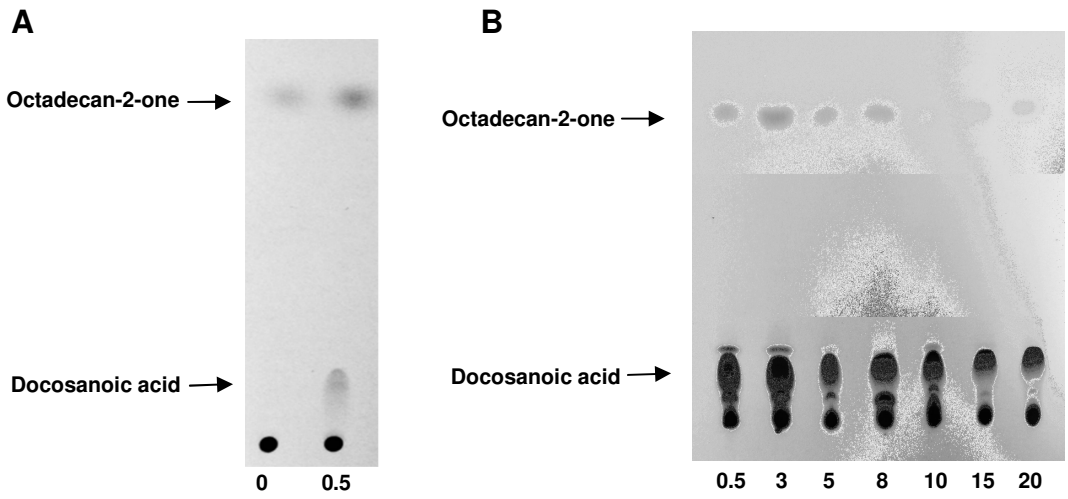

Figure 6.4: Autiradiogram of normal phase TLC analyses of elongation products using California poppy microsomes with [2-^{14}C]malonyl-CoA and C_{20} acyl-CoA under different NADPH concentrations. TLC plates were developed with hexane and ethyl acetate (12:1). (A) Elongation assays without NADPH and with 0.5 mM NADPH and (B) elongation assays performed with different NADPH concentrations. The NADPH concentrations (mM) used in each assay are indicated beneath each lane. The two sets of assays were conducted with different batches of California poppy microsomes.

6.3 Discussion

In the current study, C_{18}, C_{20} and C_{22} acyl-CoAs were incubated with California poppy microsomes to test whether the functional group in nonacosan-10-ol is introduced during elongation. The different product patterns between the substrates in the poppy microsome assay indicated the presence of a special elongation system capable of forming products with secondary functional groups, which will be discussed in section 6.3.1. Furthermore, the detection of methyl ketones in the poppy microsome assay provided first evidence for the nature of the functional group introduced by the special elongation system, as discussed in section 6.3.2. In the last section of this chapter, two possible routes to introduce the functional groups will be proposed.

6.3.1 California Poppy Has a Special Elongation System Capable of Forming Products with Secondary Functional Groups

In the current study, assays were conducted with microsomes from three organisms, Arabidopsis, yeast and California poppy. In all the assays and for each of the substrates, a polar band was detected that co-migrated with fatty acids and, thus, likely contained fatty acids. An attempt to determine the chain lengths of these fatty acid products has failed because normal phase TLC cannot distinguish between fatty acid homologues (data not shown). Consequently, the number of elongation cycles that each acyl-CoA substrate went through remained unknown. However, as described in the introduction, because these fatty acids were radioactively labeled, it was certain that the acyl-CoA substrates had been elongated by completing all four reactions in at least one elongation cycle, thus indicating that the elongation assay conditions were appropriate.

For Arabidopsis, only fatty acids were detected for all three substrate chain lengths, demonstrating that all the acyl-CoA substrates were indiscriminately elongated by (a) normal elongation system(s). For yeast, three product bands were detected for each substrate. The products in band **a** are fatty acids as they co-migrated with a fatty acid standard. The products in band **b** are likely ethyl esters based on polarity. The products in band **c** remain unknown. Three product bands were detected with the same pattern for all three substrates. Therefore, the elongation systems in yeast were found not to discriminate between acyl-CoA substrate chain lengths either. The differences of products between yeast and Arabidopsis remain unknown.

For California poppy, in addition to fatty acids, methyl ketones were detected for C_{18} and C_{20} acyl-CoA as the substrates, but not for C_{22} acyl-CoA as the substrate. Such chain length discrimination has not been seen in the Arabidopsis and yeast microsome assays conducted in this study and had not been reported in previous elongation assays.[79] It is unlikely that the effect was caused by the assay condition because, as discussed above, similar amounts of fatty acids were detected as products for each substrate, indicating that normal elongation occurred and was not disturbed. Therefore, the difference in the product patterns between C_{20}

acyl-CoA and C_{22} acyl-CoA must be caused by the presence of a special elongation system in California poppy.

Insufficient amounts of NADPH as an explanation for the production of methyl ketones in the special poppy elongation system can be excluded because methyl ketones were still detectable when 20 mM NADPH was used. As shown in the VLCFA elongation cycle (section 1.3.1), one complete elongation cycle contains one condensation reaction and two reduction reactions. Accordingly, one elongation cycle requires one molecule of malonyl-CoA and two molecules of NADPH. Under normal assay conditions, the NADPH concentration (0.5 mM) was nearly thirty-fold higher than that of malonyl-CoA (0.018 mM). Therefore, methyl ketone formation cannot be due to deprivation of reducing agent, but must instead be due to the presence of a special elongation system lacking reducing enzymes in California poppy.

6.3.2 A Carbonyl Group is Introduced during Elongation Leading to Nonaocosan-10-ol

The second question to be answered in this study was whether a hydroxyl group or a carbonyl group is introduced during elongation. As discussed above, the results of the current study showed that C_{18} and C_{20} acyl-CoA were elongated into elongated β-ketoacyl-CoA products by the special poppy elongation system. It can be excluded that β-hydroxyacyl-CoA products were formed instead, as they would have given methyl alcohols upon work-up, and these would have been separated from methyl ketones and detected alongside secondary alcohol standards under the TLC conditions used. Thus, all the evidence indicated that the functional group introduced during elongation by the poppy system is a carbonyl group. A similar elongation system has been detected for β-diketone biosynthesis in which two carbonyl groups are introduced consecutively during chain elongation.[125,126]

The results of the current biochemical assays provided the first evidence to support the polyketide-like pathway for nonacosan-10-ol biosynthesis. Although more experiments are needed to confirm the current result and to further characterize the pathway (Chapter 8), a breakthrough has been achieved for the understanding of the polyketide-like pathway for cuticular wax secondary alcohol biosynthesis.

6.3.3 Two Routes to Introduce the Carbonyl Group for Nonacosan-10-ol Biosynthesis

Four milestone levels can be distinguished towards a complete understanding of nonacosan-10-ol biosynthesis. On the first level, it is necessary to distinguish between hydroxyl group introduction via hydroxylation or elongation. On the second level, it has to be determined which functional group is originally introduced, a hydroxyl group or a carbonyl group. On the third level, it must be investigated on which specific route this functional group is introduced. Finally, the fourth level is related to the third level, and is aimed at understanding the enzyme(s) that is(are) responsible for introducing the functional group. The current work has covered the first two levels. In this section, I will start discussing the third and the fourth levels and continue the discussion in the following two chapters.

In the introduction to this chapter, only one possible route for introducing the carbonyl group was mentioned in analogy to polyketide biosynthesis (Fig. 6.5, *Pathway1*). On this route, a special elongation complex contains only condensing enzyme activity while the other three enzyme activities are omitted and, thus, C_{22} β-ketoacyl-CoA could be produced. Alternatively, the carbonyl group could also be introduced by a special, fully functional elongation complex containing all four enzyme activities (*Pathway2*). However, different from normal elongase complexes, this elongase complex could intercept the C_{22} β-ketoacyl-CoA intermediate from the normal elongation pathway and elongate this intermediate. Although the final result would be the same for both routes and similar individual enzymes are involved, the exact combinations of enzymes are different for both pathways. These two pathways are not likely to function together. However, neither of them can be ruled out based on the current evidence. After the carbonyl group is introduced by a special elongase complex, the ketoacyl-CoA intermediate would be further elongated on either of the pathways. Because of the presence of a keto group, it is likely that the enzymes, especially KCS, in these elongases are different from those in normal elongation complexes. KCS elongating keto-acyl-CoA has not been described, however, LfKCS3 from *Lesquerrela fendleri* is known to be able to elongate hydroxyacyl-CoAs.[65]

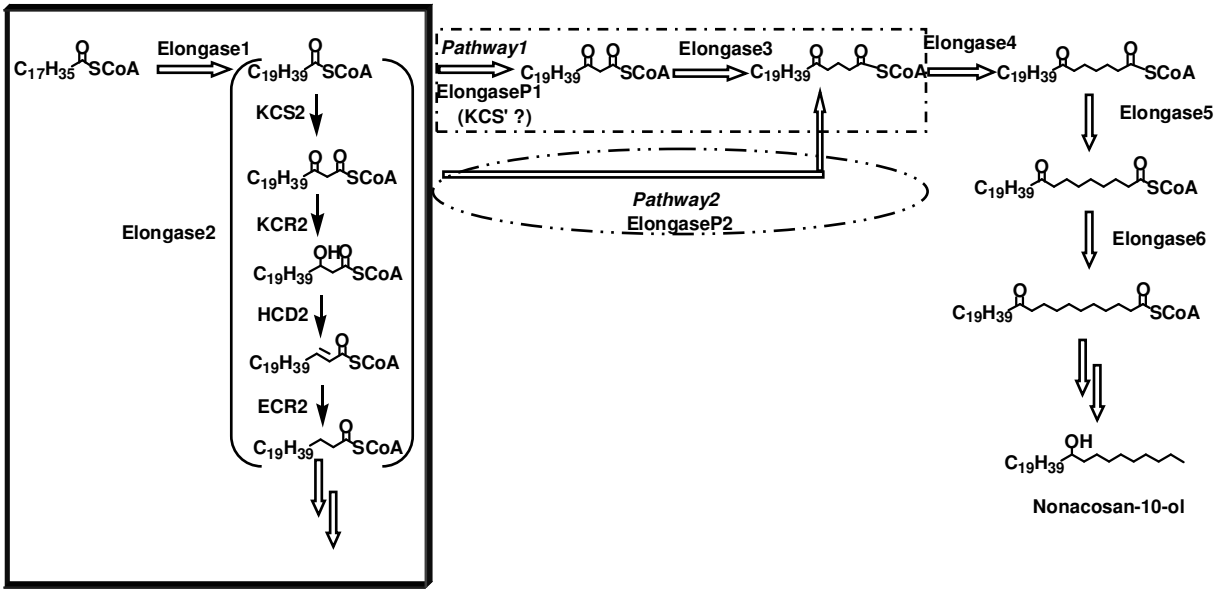

Figure 6.5: The modified hypothetical pathways leading to nonacosan-10-ol in California poppy. The normal elongation pathway is indicated in the box with shade. The carbonyl group could be introduced through two pathways. On *Pathway1* the elongaseP1 would contain only condensation activity, possibly a KCS' (shown in box with dashed line). On *Pathway2* a special elongaseP2 could intercept the C_{20} β-ketoacyl-CoA intermediate (shown in oval with dashed line). Elongases1-6 contain four enzymes: KCS, KCR, HCD and ECR. Elongase1 and elongase2 are likely different from elongases3-4 because elongase1 and elongase2 use acyl-CoAs as substrates while elongases3-4 use ketoacyl-CoAs as substrates. Elongases 5-6 could be the same as elongases 1-2 because When the distance between the in-chain and end-chain keto group increases, the in-chain keto group would have smaller effect on elongases.

Chapter 7 Cloning and Characterization of *KCS* cDNAs from California Poppy (*Eschscholzia californica*) Leaves

7.1 Introduction

The results of the biochemical assays described in the last chapter indicated that the hydroxyl group of nonacosan-10-ol in California poppy (*Eschscholzia californica*) leaf wax is introduced during elongation. The detection of methyl ketones as products formed from C_{18} and C_{20} acyl-CoA substrates indicated that, instead of a hydroxyl group, a carbonyl group is introduced during the round of elongating C_{20} acyl-CoA to C_{22} acyl-CoA. In the last chapter, it has been discussed that the carbonyl group can be introduced on one of two possible routes involving different combinations of enzyme activities. This raises the question which of these enzymes is responsible for introducing the carbonyl group during elongation en route to nonacosan-10-ol in California poppy. On *Pathway1*, the carbonyl group could be introduced by a single condensing enzyme that could be either a KCS functioning alone, without the other three enzyme activities associated with it in a normal elongase complex, or a polyketide synthase (PKS). On *Pathway2* the functional group could be introduced by a special elongase complex by intercepting C_{22} β-ketoacyl-CoA generated in the normal elongation cycle from C_{20} acyl-CoA to C_{22} acyl-CoA. Because KCSs catalyze the first step of elongation cycles (section 1.3.1), it was expected that a KCS in the special elongase complex, but not the other three enzymes associated with it, would intercept C_{22} β-ketoacyl-CoA on *Pathway2*. Thus, a condensing enzyme was predicted to be the key enzyme to introduce the carbonyl group on both routes. As predicted on the two hypothetical routes (Fig 6.5), the condensing enzyme on *Pathway1* would have a substrate preference for C_{20} acyl-CoA, or the condensing enzyme on *Pathway2* would have a preference for C_{22} β-ketoacyl-CoA. Thus, a deeper understanding of the hypothesized elongation pathway for asymmetric secondary alcohol biosynthesis will depend on further investigations into the condensing enzymes involved.

To further support the hypothetical pathway and provide molecular tools for future studies of the polyketide-like pathway (the fourth objective of the thesis), the work in this chapter focused on studying condensing enzymes that may be involved in introducing the carbonyl

group leading to nonacosan-10-ol in California poppy. It has been mentioned above that a polyketide synthase catalyzing a single condensation reaction could be responsible for the introduction of the carbonyl group on *Pathway1*. However, because the known plant polyketide synthases catalyze iterative condensations followed by cyclizations, e.g., chalcone synthase and stilbene synthase,[140,141] and because polyketide synthases that catalyze a single condensation reaction have not been identified in plants, the attention was focused on KCSs first. The goal set for the current work was to provide molecular tools needed for future studies of the elongation pathway leading to nonacosan-10-ol. Experiments were conducted in two stages, first by cloning full length cDNAs encoding putative KCS enzymes from California poppy leaves and then by partial functional characterization of the predicted KCS enzymes by heterologous expression. Based on the heterologous expression data, the biochemical function of the characterized KCS will be discussed. Finally, the effectiveness of the heterologous expression systems used in this study will also be discussed.

7.2 Results

7.2.1 Cloning of Putative *KCS* cDNAs from California Poppy

The first step towards the goal of the current study was to clone the full length cDNAs encoding putative KCSs. To this end, a homology-based approach was first adopted to clone a full length cDNA, *PKCSI*. Later, as a California poppy floral bud expressed sequence tag (EST) database became available,[160] another two cDNAs, *Eca2* and *Eca9*, were cloned.

7.2.1.1 Homology-based Approach

Sequence alignment of the known *KCS*s from Arabidopsis and other plant species revealed that the sequences of the *KCS* gene family were not well conserved, making it difficult to find consensus sequences for primer design. Thus, sequences from distantly related plant species sharing high levels of identity were selected for sequence alignment to find consensus sequences. As a result, alignments of *KCS*s from Arabidopsis (*FDH*, *FAE1*), Indian cress (*Tropaeolum majus*), cotton (*Gossypium hirsutum*), rice (*Oryza sativa*) and a liverwort (*Marchantia polymorpha*) revealed two highly conserved regions around nucleotides 751 bp and 1432 bp (numbering for Arabidopsis *FIDDLEHEAD*) (Fig. 7.1). Two degenerate primers, MconF3 and MconR3, were designed according to the two consensus

sequences. RNA was isolated from actively growing California poppy leaves, because these leaves were expected to have peak activity of nonacosan-10-ol biosynthesis based on previous studies on wax accumulation in other plant species.[84] The isolated RNA was reverse transcribed and the resulting cDNA mixture was used as template for PCR with the MconF3 and MconR3 primers. The PCR yielded three fragments with sizes of approximately 1200 bp, 800 bp and 700 bp that were cloned and sequenced. Alignment of the predicted peptide corresponding to the 700 bp fragment with the corresponding fragment (amino acid 216 to 428) of Arabidopsis FAE1 synthase revealed that they shared 85% amino acid identity. The predicted peptides corresponding to the other two fragments showed no similarity to any known KCSs. Therefore, specific primers were designed based on the sequence of the 700 bp fragment to obtain the full-length cDNA sequence using RACE technique. The resulting full length open reading frame, designated as *PKCSI*, was found to consist of 1608 nucleotides encoding a 536 amino acid protein.

A

Indian Cress	AAC	CTG	GGA	GGG	ATG	GGG	TGT	AGT	GCG	GGG	ATC	ATC	GGA	GTG	GAT	TTG	GCA
	N	L	G	G	M	G	C	S	A	G	I	I	G	V	D	L	A
Cotton	AAC	CTT	GGT	GGC	ATG	GGG	TGC	AGT	GCT	GGG	ATT	ATA	GCC	GTG	GAC	TTG	GCT
	N	L	G	G	M	G	C	S	A	G	I	I	A	V	D	L	A
Rice	AAC	CTC	GGC	GGC	ATG	GGG	TGC	AGC	GCC	GGC	GTC	ATC	GCG	GTG	GAC	CTC	GCC
	N	L	G	G	M	G	C	S	A	G	V	I	A	V	D	L	A
At FDH	AAC	CTT	GGA	GGG	ATG	GGA	TGT	TCG	GCT	GGA	ATC	ATA	GCT	ATT	GAT	CTT	GCT
	N	L	G	G	M	G	C	S	A	G	I	I	A	I	D	L	A
At FAE1	AAT	CTA	GGA	GGA	ATG	GGT	TGT	AGT	GCT	GGT	GTT	ATT	GCC	ATT	GAT	TTG	GCT
	N	L	G	G	M	G	C	S	A	G	V	I	A	I	D	L	A
Liverwort	AAC	CTT	GGC	GGG	ATG	GGA	TGC	AGT	GCT	GGT	GTG	ATA	TCT	ATC	GAT	CTT	GCC
	N	L	G	G	M	G	C	S	A	G	V	I	S	I	D	L	A

B

Indian Cress	GGA	AAC	ACT	TCT	AGC	AGC	AGC	ATA	TGG	TAT	GAG	CTG	GCA	TAC	ATG
	G	N	T	S	S	S	S	I	W	Y	E	L	A	Y	M
Cotton	GGT	AAC	ACT	TCA	AGC	AGC	AGT	ATA	TGG	TAC	GAG	TTA	GCT	TAC	ATA
	G	N	T	S	S	S	S	I	W	Y	E	L	A	Y	M
Rice	GGC	AAC	ACG	TCG	AGC	AGC	AGC	ATC	TGG	TAC	GAG	CTG	GCT	TAC	ATA
	G	N	T	S	S	S	S	I	W	Y	E	L	A	Y	M
At FDH	GGA	AAC	ACT	TCT	AGC	AGT	GGA	ATC	TGG	TAT	GAG	TTG	GCT	TAC	ATG
	G	N	T	S	S	S	G	I	W	Y	E	L	A	Y	M
At FAE1	GGG	AAT	ACT	TCA	TCT	AGC	TCA	ATT	TGG	TAT	GAA	TTA	GCA	TAC	ATA
	G	N	T	S	S	S	S	I	W	Y	E	L	A	Y	M
Liverwort	GGT	AAT	ACT	TCG	TCC	TCA	TCC	ATC	TGG	TAC	GAA	CTG	GCA	TAC	ATA
	G	N	T	S	S	S	S	I	W	Y	E	L	A	Y	M

Figure 7.1: Highly conserved regions of KCSs from Arabidopsis (*FDH*, *FAE1*), Indian cress (*Tropaeolum majus*), cotton (*Gossypium hirsutum*), rice (*Oryza sativa*) and a liverwort (*Marchantia polymorpha*). Consensus of oligonucleotide and corresponding amino acid sequences are given for the regions between (A) *AtFDH* nucleotides 751 bp -801 bp and (B) *AtFDH* nucleotides 1432 bp -1479 bp. The nucleotide positions used for primer design are highlighted in grey.

7.2.1.2 EST-based Approach

An EST database of California poppy floral buds was published in 2006.[160] A search in this EST database with the query sequences of *FAE1*, *FDH* and *CER6* cDNAs taken from the Arabidopsis genome database revealed that 18 out of 6,000 sequences had similarities to the query sequences (Table 7.1). The 18 sequences were arbitrarily given names starting with Eca followed by a number, e.g., eca01-5ms1-e11 was designated as Eca1. The lengths of the sequences ranged from 134 bp to 674 bp, while the currently known full length *KCS* cDNAs are 1500 bp to 2000 bp long. Thus, the Eca sequences matched only small regions of the known full length *KCS* cDNAs, and these regions were only partially overlapping. Only in three cases did these overlapping regions reveal that pairs of sequences belonged to the same

full length cDNA (4th column in table 7.1). It cannot be decided whether some of the other fragments belong to different regions of the same full length cDNA, or whether they all represent unique reading frames. Consequently, 15 of the 18 sequences in the database must be treated as independent candidates for unique *KCS* cDNAs at this point.

Table 7.1: Summary of putative KCS cDNAs in the California poppy floral bud EST database

Name	ID in the database	Lengths (bp)	Approximate distance to 5'-end of the full length cDNA sequences	Note
Eca1	eca01-5ms1-e11	603	1100	
Eca2	eca01-35ms3-g12	621	128	Identical to *Eca4*
Eca3	eca01-13ms1-f07	502	304	
Eca4	eca01-46ms3-a09	426	36	Identical to *Eca2*
Eca5	eca01-7cs3-b08	296	N/A	
Eca6	eca01-3cs4-g09	602	640	
Eca7	eca01-12cs1-e07	472	519	85% similarity to *Eca6*
Eca8	eca01-53ms1-g11	472	53	Identical to Eca13
Eca9	eca01-12cs4-e03	512	0	85% similarity to *Eca8* Identical to *Eca12*
Eca10	eca01-38ms1-c03	134	200	
Eca11	eca01-12cs1-h12	472	53	97% identical to *Eca8*
Eca12	eca01-38ms2-d05	458	30	Identical to *Eca9*
Eca13	eca01-46ms4-b04	275	105	Identical to *Eca8*
Eca14	eca01-35ms4-e04	487	460	
Eca15	eca01-38ms1-h07	674	571	
Eca16	eca01-7cs1-f02	427	673	98% similarity to *Eca15*
Eca17	eca01-26ms1-c09	292	661	
Eca18	eca01-25ms1-f07	558	N/A	

Since I was not able to clone the full length sequences of all 15 cDNAs, criteria were set to select candidates to be cloned. The first criterion was based on gene expression patterns. The gene encoding the KCS that could introduce the carbonyl group was expected to be highly expressed in young leaves because nonacosan-10-ol is actively biosynthesized in them. Therefore, the transcript levels of the cDNA fragments in young leaves were to be assessed by RT-PCR. For the following reasons, not all 15 sequences were assessed (individually). The database indicated that the sequences of *Eca10* (eca01-38ms1-c03) and *Eca17* (eca01-7cs1-f02) were not accurate enough for primer design. High sequence similarities between the fragments *Eca8* (eca01-53ms1-g11) and *Eca11* (eca01-12cs1-h12) would not allow the design of specific primers to distinguish these two sequences. Therefore, their transcript levels could not be assessed separately. Neither could *Eca15* (eca01-7cs1-f02) and *Eca16*

(eca01-38ms1-h07) be assessed separately. As a consequence, the expression levels of only 13 sequences were semi-quantitatively assessed by RT-PCR, and nine of them were assessed individually. To obtain PCR products in comparable lengths, the two primers for each sequence were designed to be 150 bp to 200 bp apart. Gel electrophoresis showed that *Eca14* and *Eca18* were not transcribed in young leaves. The transcript level of *Eca1* was relatively low. *Eca2*, *Eca6*, *Eca7* and *Eca9* were highly transcribed. The remaining six sequences had moderate transcript levels (Fig 7.2).

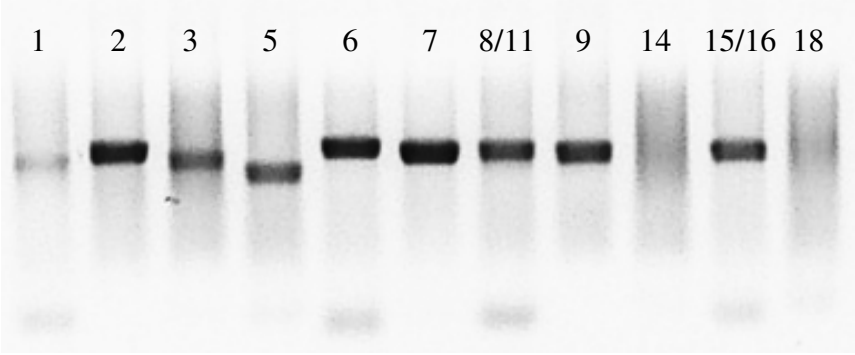

Figure 7.2: RT-PCR analysis of the cDNAs encoding putative KCSs in young California poppy leaves. The number above each lane corresponds to the Eca numbers, e.g., 1 corresponds to Eca1.

The second criterion to select the candidates for further cloning was based on technical requirements to clone full length sequences. Among the sequences with the highest expression levels in leaves, *Eca2* (same as *Eca4*) and *Eca9* were targeted first. The fragment of *Eca2* was very close to the 5'-end of the expected full length sequence, making it relatively easy to obtain the 5'-end full length sequence. For *Eca9*, only 3'-RACE was required. The resulting full length sequences of *Eca2* and *Eca9* consist of 1482 and 1596 nucleotides, encoding 494 and 532 amino acid proteins, respectively.

7.2.2 Sequence Analysis of Putative *KCS* cDNAs from California Poppy

The putative KCS enzymes, PKCSI, Eca2 and Eca9, deduced from the corresponding cDNA sequences shared 60% to 76% identity with the known plant β-ketoacyl-CoA synthases (Fig 7.3). Sequence alignments showed that all three deduced proteins had the conserved cysteine

residue that is essential for condensation activity.[161] Phylogenetic analysis showed that the predicted protein Eca2 was closely related to CER6, while Eca9 clustered with FIDDLEHEAD, and PKCSI with both At2g26640 and At5g43760 (Fig 7.4).

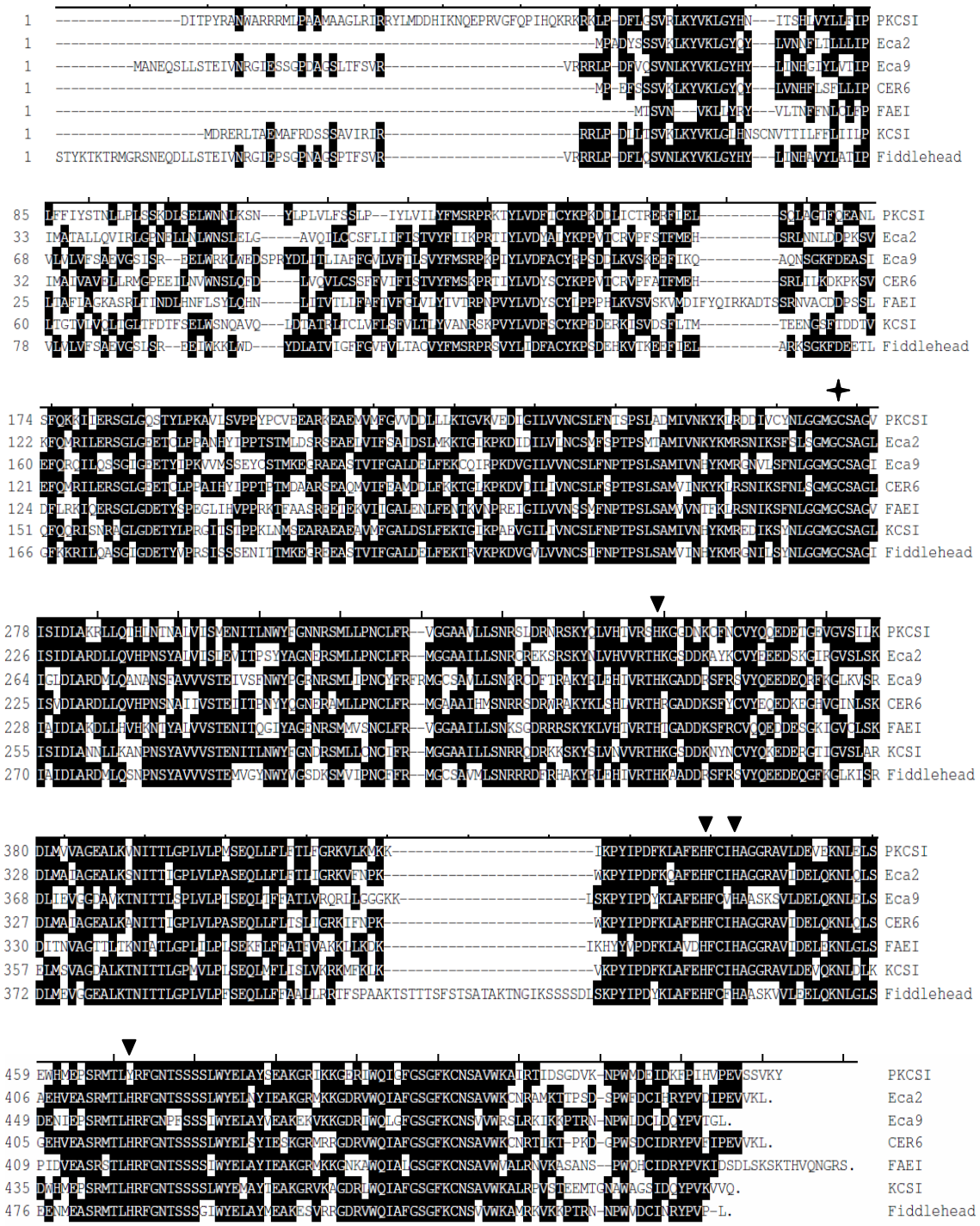

Figure 7.3: Alignment of deduced amino acid sequences of the three putative β-ketoacyl-CoA synthases PKCSI, Eca2 and Eca9 from California poppy with KCS enzymes from Arabidopsis. The identical amino acids are shaded. Active cysteine and histidine residues are labeled with stars and triangles, respectively. His420 in FAE1 is not conserved in PKCSI. Sequence alignments were assembled by the ClustalW algorithm (DNAStar)

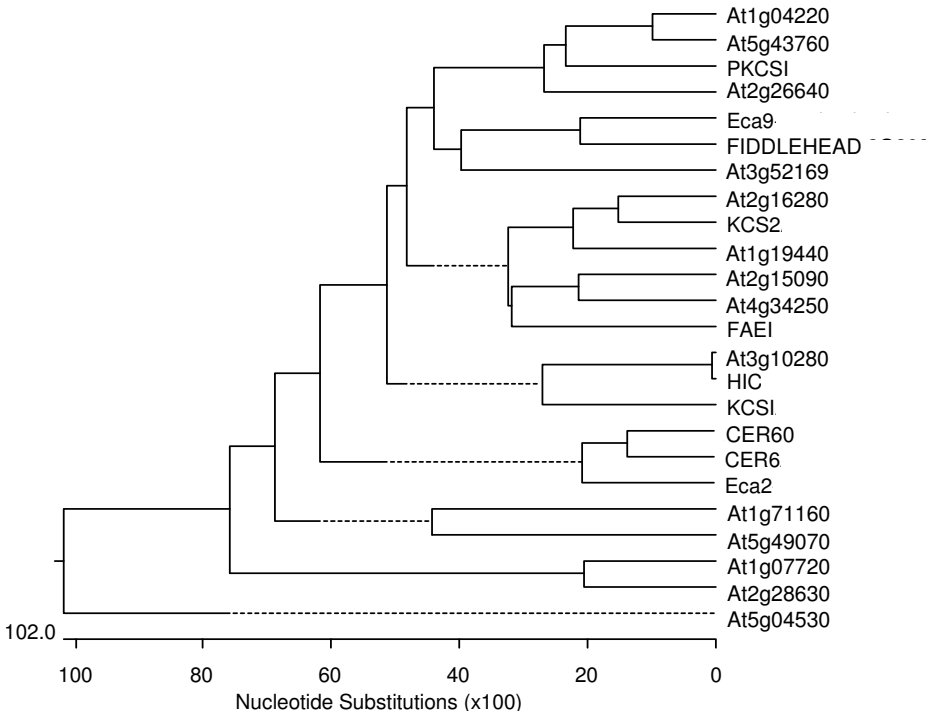

Figure 7.4: Phylogenetic analysis comparing the predicted poppy proteins, PKCSI, Eca2, Eca9 with the known and the putative KCSs from the Arabidopsis genome database. Sequence alignments were assembled by the ClustalW algorithm (DNAStar)

KCS proteins closely resembling in biochemical functions are known to cluster together in phylogenetic trees and, hence, phylogenetic analyses have been used to predict biochemical functions of KCS proteins.[75,162] The KCS introducing the carbonyl group should have substrate preference for C_{20} or C_{22} acyl chains and, therefore, the predicted proteins that might elongate C_{20} and C_{22} substrates were targeted first for characterization. Because the condensing enzymes At1g04220, At5g43760 and At2g26640 had shown activities for C_{18}, C_{20} and C_{22} acyl-CoA substrates,[79,81] the members of the same clade are likely to be able to elongate one or all of the acyl-CoAs with C_{18}-C_{22}. Consequently, PKCSI was characterized first because it was in this clade. Eca2 was excluded for characterization in this study because it had highest similarity with CER6, an enzyme known to elongate substrates with C_{24} or more carbons.[52] Because the biochemical function of FIDDLEHEAD remains unknown, the

substrate preference of the putative KCS Eca9 clustering with it could not be predicted, and it was therefore also excluded from this study. Hence, only PKCSI was selected for further functional characterization while the other predicted proteins were left for future studies.

7.2.3 Functional Characterization of Putative *KCS* cDNAs

The short life cycle of yeast (*Saccharomyces cerevisiae*) makes it a convenient tool to quickly characterize gene functions. Also, functions of putative KCSs had been successfully characterized by over-expression of the corresponding cDNAs in wild type yeast.[50,71] Therefore, functional characterization of PKCSI was first attempted by over-expression in yeast. However, Arabidopsis is expected to be a more suitable over-expression system for functional characterization of the product of genes/cDNAs that have been cloned from higher plants. Thus, the function of PKCSI was further characterized in Arabidopsis.

7.2.3.1 Over-expression in Yeast

PKCSI cDNA was linked to the galactose-inducible GAL1 promoter in a yeast expression vector, pYES2. The pYES2-*PKCSI* plasmid was transformed into wild type yeast cells. The transgenic yeast cells were grown for four days after induction with galactose, then treated with methanolic HCl to transform acyl chains (free fatty acids, acyl-CoAs and glycerides) to fatty acid methyl esters (FAMEs), and extracted with chloroform. To analyze the fatty acid profile, the extracts were analyzed by GC. The results showed that the extracts from the yeast cells harbouring the pYES2-*PKCSI* plasmid were composed of the same fatty acid derivatives as the extracts from wild type yeast cells, including long chain fatty acids (C_{16} and C_{18}), very-long-chain fatty acids (C_{20}-C_{26}, even numbered chains only) and C_{26} α-hydroxy-fatty acid. C_{16} and C_{18} fatty acids together with C_{26} α-hydroxy-fatty acid accounted for over 95% of the total fatty acid derivatives. These three compounds did not show apparent differences between the wild type cells and pYES2-*PKCSI* transformed cells. Within the very long chain fatty acids (C_{20}-C_{26}, the relative amount of C_{22} fatty acid increased from 2% (wild type cells) to 6% (transformed cells). Similarly, the relative amount of C_{24} fatty acids in the transformed cells showed a three-fold increase compared to that in the wild type cells (Fig. 7.5). C_{20} fatty acid could not be quantified due to its low amount.

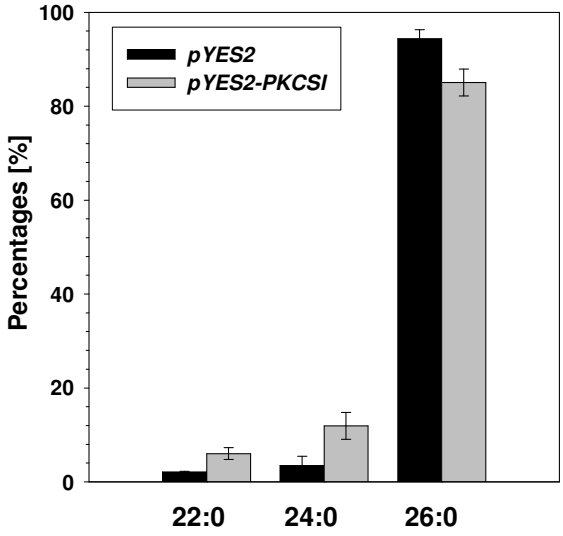

Figure 7.5: Quantification of VLCFAs in yeast cells. The relative abundance of each chain length was calculated within very-long-chain fatty acids. Data are given as mean (of five clones from five transformation events) ± standard error.

7.2.3.2 Over-expression in Arabidopsis

To test if PKCSI could produce compounds with carbonyl groups in the Arabidopsis stem wax, or have an effect on Arabidopsis stem wax composition, *PKCSI* was over-expressed in wild type Arabidopsis (ecotype Columbia-0) under the control of the cauliflower mosaic virus CaM35S promoter. Seedlings with *PKCSI* insertion were selected by germinating seeds on medium containing antibiotics. Fifty-two antibiotic-resistant T_1 plants (first generation of plants after transformation) were recovered and their stem waxes were extracted individually with chloroform. The coverages of the stem waxes of most of the transformants were the same as those of the Arabidopsis wild type, but some lines showed higher wax coverages, e.g., the lines of T1-17, T1-27 and T1-36 (Fig. 7.6A). The seeds were collected from six lines with high wax coverages and from eight lines showing normal wax coverages, germinated on medium with antibiotics and transferred to soil. Within each T_2 line, stem waxes from three plants were analyzed individually. The wax coverages of T_2 plants showed no evident difference from those of the wild type Arabidopsis (Fig 7.6B). Detailed analyses of stem waxes of the transgenic lines (T_1 and T_2 plants) did not show novel compounds or changes in the chain length distributions (data not shown). The transcription levels of *PKCSI* in six T_2 lines were assessed by RT-PCR (Fig 7.6C). The RNA was extracted from stems of several

plants within an individual transgenic line. Among the six examined lines, only the line T2-36 did not show *PKCSI* transcripts.

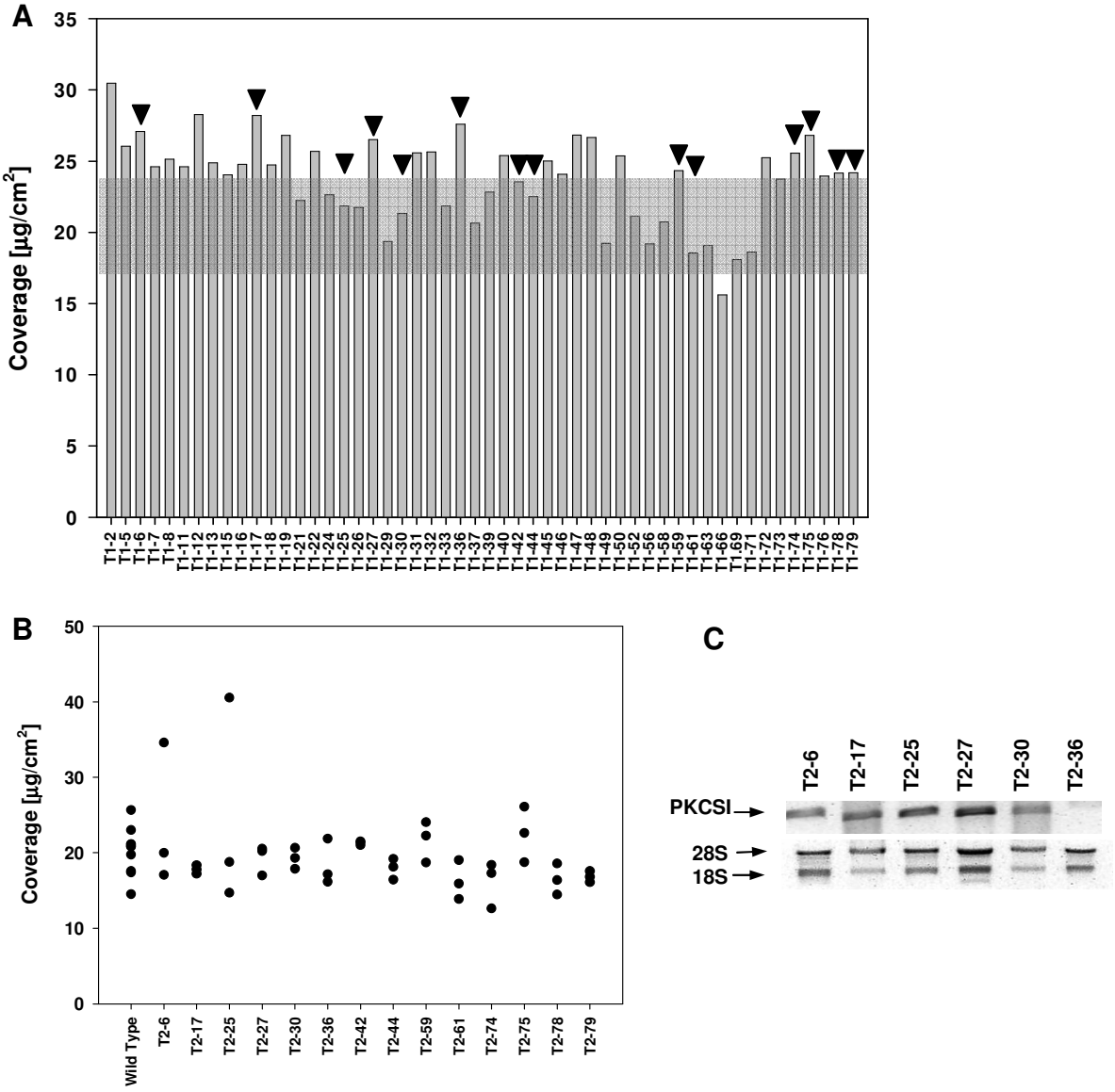

Figure 7.6: Stem wax coverages of *PKCSI* transgenic Arabidopsis and RT-PCR analysis of *PKCSI* transcript levels in the transgenic Arabidopsis stems. (A) Stem cuticular wax coverages of 52 independent T_1 transgenic lines. Each bar represents the wax coverage of a single transgenic line. The range of stem wax coverages of Arabidopsis wild type is shaded across the graph (n=5). The lines selected for further testing in the T_2 generation are highlighted with triangles. (B) Stem cuticular waxes of 14 independent T_2 transgenic lines. For each independent line three replicates are depicted in the same column. Each spot represents the wax coverage obtained from a single plant. (C) RT-PCR analysis of *PKCSI* transcript levels in the stems of six T_2 transgenic lines.

Arabidopsis seeds contain mainly unsaturated fatty acids together with small quantities of saturated very-long-chain fatty acids (C_{20} and C_{22}), providing a low background for characterizing the function of PKCSI. Therefore, *PKCSI* cDNA was over-expressed under the control of the seed specific *FAE1*-promoter in Arabidopsis. T_2 seeds were collected from each of the 42 T_1 transformants to determine their fatty acid compositions by converting seed oil to FAMEs. The overall saturated and unsaturated fatty acid chain length distribution patterns of the transgenic seeds were very similar to that of wild type seeds (Table 7.2). However, the average ratio of C_{18} to C_{20} fatty acid decreased from 2.9 in wild type seeds to 2.0 in pFAE1-*PKCSI* transformed seeds, suggesting an increase in the C_{20} fatty acid content. Eighteen independent T_2 lines were found to have a significant decrease in the C_{18} to C_{20} fatty acid ratios (1.3 to 1.6) of their seed oil (Fig. 7.7A). Eight lines of these T_2 seeds were planted and re-selected on medium with antibiotics. Within each T_3 line, seeds of at least seven plants were collected and analyzed separately. All the T_3 seeds showed lower C_{18} to C_{20} fatty acid ratios than those of the wild type seeds (Fig. 7.7B).

Table 7.2: Fatty acid compositions(%) of the seed oil of Arabidopsis wild type and pFAE1-*PKCSI* transgenic plants.

Fatty acids	**Wild Type Seeds (n=5)**	**T_2 Seeds (average of all the 42 lines)**
16:0	7.9 ± 0.3	7.6 ± 0.1
18:0	4.7 ± 0.4	4.3 ± 0.2
18:1	13.5 ± 0.2	13.6 ± 0.1
18:2	30.7 ± 0.3	30.6 ± 0.5
18:3	20.5 ± 0.2	20.7 ± 0.2
20:0	1.6 ± 0.1	2.2 ± 0.1
20:1	20.5 ± 0.4	20.3 ± 0.2
22:1	0.6 ± 0.1	0.7 ± 0.02

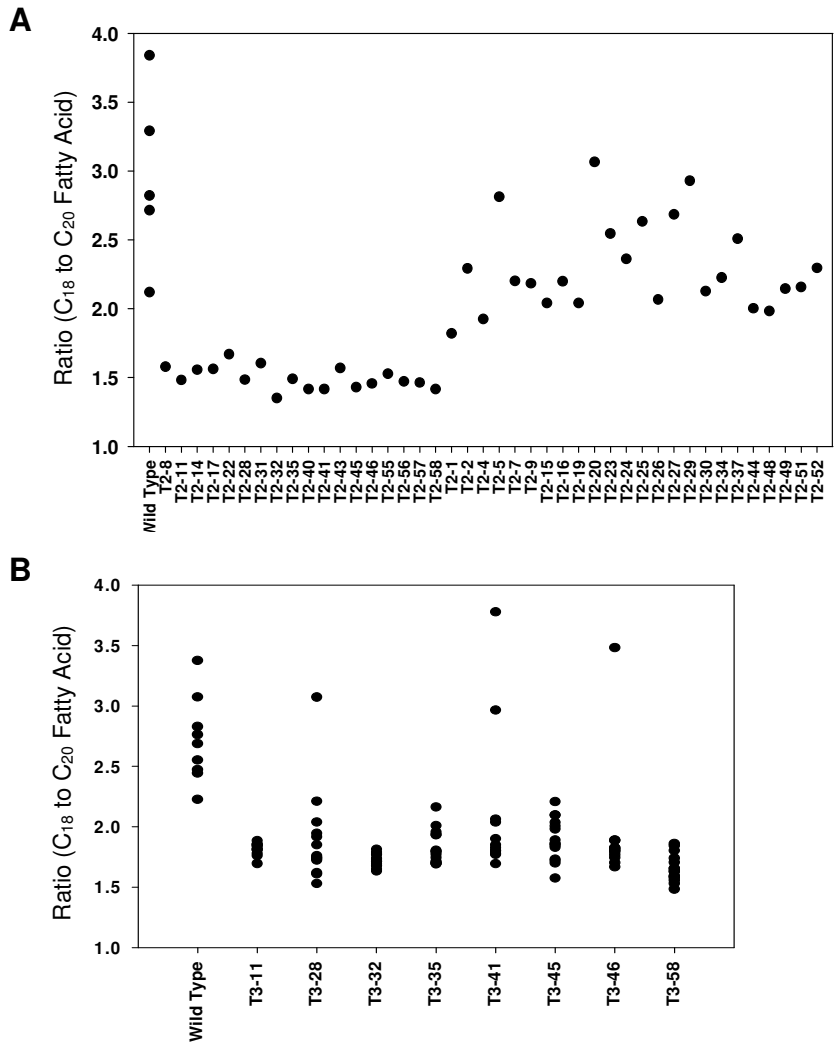

Figure 7.7: The ratio of C_{18} to C_{20} fatty acid content in seeds of Arabidopsis wild type and pFAE1-*PKCSI* transgenic plants. Each spot represents the ratio obtained from pooled seeds of a single plant. (A) Forty-two independent T_2 lines. The lines with low C_{18} to C_{20} fatty acid ratios are intentionally depicted together. (B) Eight independent T_3 lines. The numbering of the T_3 lines corresponds to that of the T_2 lines.

The transcript levels of *PKCSI* in T_2 seeds were examined by RT-PCR using the actin sequence as an amplification and loading standard (Fig 7.8). Variations of the transcript levels were observed among the lines that were examined. *PKCSI* transcripts were not detected in lines 2, 4 and 5. The transcript levels of lines 15 and 48 were relatively low while the remaining lines showed relatively high transcript levels.

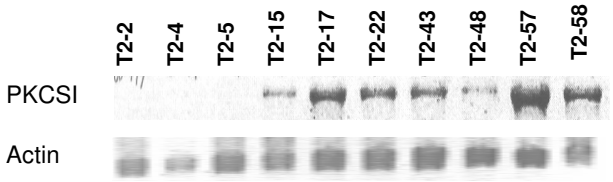

Figure 7.8: RT-PCR analysis of *PKCSI* transcript levels in transgenic Arabidopsis seeds. RNA was extracted from green seliques of T_2 seeds of pFAE1-*PKCSI* transformed Arabidopsis. The line numbers are indicated above each lane.

7.3 Discussion

The goal of the current work was to provide molecular tools to study the elongation pathway leading to nonacosan-10-ol. The first step toward this goal was to clone cDNA sequences that might encode the KCS that could introduce the functional group en route to nonacosan-10-ol. Three full length cDNAs encoding putative KCSs were cloned from California poppy leaves. Based on the biochemical functions predicted by the phylogenetic analysis, one of the putative KCSs, PKCSI, was selected for further characterization to confirm its function. Thus, the biochemical function of PKCSI will be discussed based on the heterologous expression data in section 7.3.1. The effectiveness of wild type Arabidopsis and yeast as tools to characterize the functions of *KCS* cDNAs will then be discussed in section 7.3.2.

7.3.1 Biochemical Functions of PKCSI

The results of yeast and Arabidopsis over-expression experiments suggested that PKCSI elongates C_{18}, C_{20} and C_{22} acyl-CoA in the heterologous expression systems. In the transformed yeast, the increased amounts of C_{22} and C_{24} fatty acids suggested that PKCSI elongates C_{20} and C_{22} acyl chains. In the seeds of pFAE1-*PKCSI* transformed Arabidopsis, the C_{18} to C_{20} fatty acid ratio decreased compared with that of the seeds of wild type Arabidopsis, suggesting that PKCSI elongates C_{18} acyl-CoA. The change of the C_{18} to C_{20} fatty acid ratio was found correlated with the *PKCSI* transcript levels, confirming that the change of the C_{18} to C_{20} fatty acid ratio was caused by the expression of *PKCSI*. Thus, the over-expression experiments gave matching overall results, pointing to a preference of

PKCSI for acyl-CoA substrates with C_{18} to C_{22} chain lengths and the formation of products with C_{20}-C_{24} chain lengths. In contrast to this, PKCSI did not show C_{20} and C_{22} elongation activity in the Arabidopsis seed over-expression experiment. However, this maybe explained by the insufficient amounts of C_{20} acyl-CoA for further elongation.

In both the Arabidopsis and yeast over-expression experiments, PKCSI did not show a substrate preference for C_{20} acyl-CoA over C_{22} acyl-CoA, as predicted for the condensing enzyme that would be crucial for *Pathway1*. Neither did PKCSI show preferential activity towards C_{22} ketoacyl-CoA as a substrate, as predicted for *Pathway2*. However, the lack of these predicted functions in the heterologous expression system does not necessarily mean that PKCSI is not the KCS introducing the carbonyl group during elongation leading to nonacosan-10-ol. The expected biochemical function of the KCS that could introduce the carbonyl group en route to nonacosan-10-ol, either the one on *Pathway1* or the one on *Pathway2*, is quite different from the functions of the known KCSs. Thus, the interactions between this KCS and the other three enzymes in the special elongase complex could be different from those between enzymes in the normal elongation complexes. The special KCS might require appropriate partner enzymes, either in its own elongase complex or in others where it intercepts intermediates. Consequently, the heterologous expression of this special *KCS* may result in a false function due to the lack of appropriate partner enzymes.

7.3.2 Heterologous Expression Systems for Biochemical Characterization of KCSs

The fatty acid profile changes in the transformed yeast and Arabidopsis were not substantial. In the yeast cells harbouring *PKCSI* cDNA, C_{22} and C_{24} fatty acids were less than 5% of the total fatty acids. In the seeds of pFAE1-*PKCSI* transformed Arabidopsis, although the C_{20} saturated fatty acid content increased, it was still less than 5% of the total seed oil. Such small changes suggested a low PKCSI enzyme activity that could be attributed to several reasons. One of them could be because of low enzyme concentration in a heterologous environment. Heterologous protein expression is known to cause many unsolved problems on the levels of transcription, translation and protein folding.[163] In this study, RT-PCR of transgenic Arabidopsis suggested that *PKCSI* was transcribed. However, the transcript may not be properly translated, thus resulting in a low protein concentration. Another possible

reason could come from PKCSI itself. Some condensing enzymes had been found to have low condensation activities, e.g., At2g26640 and At4g34510.[81] The third possible reason could be that the native KCSs in the wild type Arabidopsis and yeast have masked the function of PKCSI.

Although heterologous expression may cause problems for characterizing biochemical functions of unknown proteins, this approach is still one of the major ways to characterize gene functions. For some of the problems, e.g., false results and low protein concentrations, there is no easy way to solve them. The other problems can be minimized by wisely chosen expression systems. For example, mutants lacking proper KCS functions will decrease the problem caused by native KCS enzymes masking heterologous KCS functions. Thus, yeast *Δelo2Δelo3* double mutant and Arabidopsis *fae1* mutant would be better systems for heterologous expression.

Chapter 8 Summary and Future Studies

8.1 Summary

The research in this thesis addressed the question how secondary hydroxyl groups are introduced into the secondary alcohols, alkanediols and ketols found in plant cuticular waxes. This general question led to four specific objectives that will be summarized in section 8.1.1. To achieve these objectives, chemical analyses of cuticular waxes, biochemical assays and cloning experiments were conducted. The results will be summarized in section 8.1.2 corresponding to Chapters 3-7. These results led us to a deeper understanding of the biosynthetic pathways on which the secondary hydroxyl groups are introduced, as will be discussed in section 8.1.3.

8.1.1 Objectives

The general goal of my PhD research was to study how the secondary functional groups in secondary alcohols, alkanediols and ketols in plant cuticular waxes are introduced. Two fundamentally different pathways are known to be involved in introducing the secondary functions in some plant wax compounds. One of these pathways relies on hydroxylation of elongated substrates. Evidence obtained by biochemical and molecular genetics experiments indicates that symmetric secondary alcohols, alkanediols and ketols in the waxes of *Brassica* species and Arabidopsis are biosynthesized through hydroxylation. On the second pathway, hydroxyl functions are introduced during elongation of carbon chains in a way similar to polyketide biosynthesis. Biochemical evidence indicates that the carbonyl groups of β-diketones in barley are introduced during elongation. Functional groups introduced in this way can only be located on specific carbon positions. The absolute dominance of nonacosan-10-ol in many plant cuticular waxes leads to the hypothesis that the hydroxyl group on C-10 is introduced during chain elongation.

The evidence supporting these two pathways is on different levels. For the hydroxylation pathway, a substrate-product relationship had been established between alkanes and symmetric secondary alcohols. The Arabidopsis *MAH1* gene, encoding the hydroxylase that catalyzes this step had been cloned and characterized. Therefore, two specific objectives

were formed to further the understanding of this pathway, which were (1.1) to test the substrate-product relationship between secondary alcohols and alkanediols/ketols, and (1.2) to study the substrate preference and regiospecificity of MAH1 and MAH1-like hydroxylases. For the elongation hypothesis, all the supporting evidence relied on chemical data and molecular genetics or biochemical information was lacking. Therefore, two specific objectives related to this hypothetical pathway were (2.1) to test the hypothesis and (2.2) to provide molecular tools for further characterizing the pathway. To this end, I analyzed cuticular waxes of various species in detail, conducted biochemical assays and cloned candidate genes.

8.1.2 Results

In the stem wax from wild type Arabidopsis, not only new secondary alcohol isomers were identified, but also the new compound classes of alkanediols and ketols (Chapter 3). The functional groups in these compounds are all located around the central carbon of the hydrocarbon chain, suggesting that the functional groups are introduced by MAH1 or MAH1-like enzymes.[39] In Chapter 4, pea leaf wax was investigated. Two novel compound classes were identified for the first time in plant cuticular wax: novel secondary/secondary alkanediols were found to consist of hentriacontane-8,15-diol, -10,17-diol and -9,16-diol that are characterized by constant numbers of methylene units between the two hydroxyl groups. These diols are likely biosynthetically related to hentriacontan-15-ol and -16-ol, the major wax constituents in pea leaf wax. As a second novel compound class, primary/secondary alcohols were found with secondary hydroxyl groups located around the center of the carbon chain. Thus, their structural characteristics matched those of the co-occurring symmetric secondary alcohols, suggesting that the secondary hydroxyl groups are introduced by hydroxylases similar to MAH1.

Detailed analyses of yew (*Taxus baccata*) needle wax showed that the major constituents were nonacosan-10-ol, nonacosane-4,10-diol and nonaocosane-5,10-diol. In addition, alkanediols and hydroxyaldehydes with 1,5-geometries of functional groups were identified (Chapter 5). The characteristic substitution pattern of the functional groups in these two

compound classes suggested that they are biosynthetically related to each other, and that the functional groups are introduced during elongation.

Finally, the hypothesis that secondary hydroxyl groups in asymmetric secondary alcohols like nonoacosan-10-ol are introduced during elongation was tested by incubation of ^{14}C-labeled substrates with poppy leaf microsomes (Chapter 6). A difference of the product pattern was observed between C_{20} (and C_{18}) acyl-CoA and C_{22} acyl-CoA substrates. This result was in agreement with the predictions based on the hypothetical pathway, providing the first biochemical evidence that the hydroxyl group in nonacosan-10-ol is introduced during carbon chain elongation. The detection of methyl ketones for C_{18} and C_{20} acyl-CoA substrates indicated that a carbonyl group rather than a hydroxyl group is introduced during elongation. To provide molecular tools for future studies of the hypothetical pathway, three cDNAs encoding putative KCSs were cloned and one of them, *PKCSI*, was functionally characterized by over-expression in wild type Arabidopsis and yeast (Chapter 7). The results showed that *PKCSI* elongated C_{18}, C_{20} and C_{22} acyl CoAs in the heterologous expression systems. The heterologous expression data suggested that wild type Arabidopsis and yeast may not be suitable for functional characterization of the condensing enzymes introducing the functional groups en route to nonacosan-10-ol.

8.1.3 Discussion

8.1.3.1 Substrate Diversity of Hydroxylases Involved in Wax Biosynthesis

Early biochemical evidence indicated that the MAH1-like hydroxylases use alkanes as substrates. The diverse structures identified in the current studies indicated that alkanes are not the only substrates of the MAH1-like hydroxylases. The ketols identified in Arabidopsis stem wax suggested that symmetric secondary alcohols can also serve as substrates for hydroxylation, leading to alkanediols and ketones, and on to the final ketol products. Between one and three hydroxylations occur, all with preference for the carbons at or near the center of the hydrocarbon chain. In pea leaves, co-localization of primary alcohols and symmetric primary/secondary alcohols indicated that primary alcohols can be substrates for further hydroxylations by MAH1-like enzymes as well. As discussed in section 1.3.3.6, the hydroxyl groups on C-3 to C-12 in the asymmetric secondary/secondary alkanediols, e.g., the

nonacosane-x,10-diols found in yew needle wax, are likely also introduced by hydroxylating pre-existing secondary alcohols. It seems that this hydroxylase is different from MAH1-like enzymes because the hydroxyl groups introduced by it all located closer to one end of the carbon chain. In summary, hydroxylases involved in wax biosynthesis are characterized by a relatively high flexibility as they can accept very diverse substrates to carry out hydroxylation reactions.

8.1.3.2 Regiospecificity and Substrate Chain Length Specificity of Hydroxylases Involved in Wax Biosynthesis

As discussed in the above section, the hydroxylases use various VLCFA derivatives (chain length longer than 20 carbons) as substrates to synthesize wax components with secondary functional groups. These potential substrates frequently occur in broad homologous series, giving the enzymes a wide choice of methylene groups for hydroxylation. Compared with this broad substrate range, MAH1-like enzymes show a relatively narrow product specificity. It is surprising that the hydroxylases are found to have regiospecificity and/or substrate chain length specificity, even though characteristic functionalities that could serve as markers orienting the enzyme are frequently missing or can be located in distant locations within the substrate (for example at the chain end in primary alcohols serving as substrates for mid-chain specific hydroxylation). Based on the product isomer compositions (Chapters 3-5), the hydroxylases can be classified into three groups according to their regiospecificity.

The first group contains the strict mid-chain hydroxylases that are involved in the biosynthesis of symmetric secondary alcohols, secondary/secondary alkanediols, primary/secondary alkanediols and ketols in Arabidopsis, *Brassica napus* and pea. These hydroxylases showed a preference for hydroxylating carbons in the middle of a carbon chain. In addition to regiospecificity, these enzymes showed substrate chain length specificity as well. Quantification of secondary alcohols in the leaf wax of Arabidopsis MAH1 over-expressors indicated that MAH1 has a chain length preference for the C_{29} substrate. Such substrate preference was also observed for the MAH1-like enzyme in pea. The coverage of hexacosanol was higher than that of octacosanol on the adaxial leaf surface, but the primary/secondary alkanediols were formed with a preference for the C_{28} homologue.

Different from the above mid-chain hydroxylases, the second group of hydroxylases introduces hydroxyl groups on the carbons closer to one end of the carbon chain. They will be called "end chain hydroxylases" in the following. An example for these hydroxylases is the enzyme introducing the hydroxyl groups on C-3 to C-12 in the asymmetric secondary/secondary alkanediols (see definition in section 1.3.3.6). This type of hydroxylases also shows regiospecificity, but has a wider carbon range than the strict mid-chain hydroxylases. The dominant amounts of nonacosane-4,10-diol and nonacosane-5,10-diol in yew needle wax suggested that the enzyme involved in this system has a certain specificity for hydroxylating on C-4 and C-5. In barley spikes, homologous series of C_{27}, C_{29} and C_{31} secondary alcohols with hydroxyl groups on C-9 to C-13 were detected.[164] The isomer composition suggested that these hydroxyl groups are introduced by a hydroxylase with limited regiospecificity as well. The regioselectivity of these end chain hydroxylases is not as predictable as that of the mid-chain hydroxylases. For the above two examples, the corresponding end chain hydroxylases may hydroxylate on C-4 leading to nonacosane-4,10-diol or on C-11 when forming nonacosan-11-ol. Discovery of more of these structures will lead us to a better understanding of the regioselectivity and substrate-specificity of the end chain hydroxylases.

The third group of hydroxylases has strict regiospecificity. The only example discovered so far is provided by the secondary/secondary alkanediols in pea, hentriacontane-9,16-diol, -8,15-diol and -10,17-diol. As discussed in Chapter 4, one of the hydroxyl groups is introduced by hydroxylating the pre-existing symmetric secondary alcohols on the carbon that is separated by seven methylene units from the hydroxyl group in the substrates. The substrate chain length specificity of this group of hydroxylases remains unknown. Because the C_{31} homologue dominates the symmetric secondary alcohols serving as substrates in this case, it is not clear whether the exclusive formation of C_{31} alkanediols is a result of substrate specificity or of substrate availability.

All the above evidence taken together, it can be inferred that limited regiospecificity is a general property of the hydroxylases involved in wax biosynthesis. Most of the hydroxylases

do not have strict substrate and regiospecificity, but the range can be as narrow as 2-3 methylene units.

8.1.3.3 The Condensing Enzyme Introducing Carbonyl Groups during Elongation

The biochemical evidence obtained in the assays described in Chapter 6 indicated that a carbonyl group rather than a hydroxyl group is introduced during elongation. Nonacosan-10-one had been detected as a major wax constituent on royal fern fronds and in other plant species. The identical substitution position in nonacosan-10-one and nonacosan-10-ol indicates that the carbonyl group in nonacosan-10-one is also introduced during elongation. It is known that plant polyketide synthases introduce functional groups by iterative condensation without reduction, thus, resulting in multiple carbonyl groups in the elongated chain, e.g., chalcone synthase and stilbene synthases. The β-diketones detected in barley are also likely biosynthesized by introducing two carbonyl groups in consecutive condensation reactions. To introduce these carbonyl groups into different compounds, condensing enzymes are required. For chalcone and stilbene biosynthesis, the corresponding enzymes have been cloned and characterized in many plant species. For β-diketones, nonacosan-10-ol and nonacosan-10-one biosynthesis, these condensing enzymes remain unknown. It has been hypothesized that the condensing enzyme involved in nonacosan-10-ol biosynthesis could be a KCS, or a PKS catalyzing a single condensation reaction on one of the proposed routes (Chapter 6, Fig 6.5). Although the substrate for this hypothetical condensing enzyme is different from the substrates for the known polyketide synthases, and the elongation rounds are also different between these two types of condensing enzymes, the hypothetical enzyme and the known polyketide synthases both catalyze condensation reactions without further reduction. Therefore, the similarity of the biochemical functions suggests that the hypothetical condensing enzyme is evolutionarily related to the PKSs. This hypothesis is yet to be investigated when the hypothetical condensing enzyme becomes available.

8.1.3.4 The Elongase Complexes Involved in Biosynthesizing Other Asymmetric Compounds

It has been described in Chapter 1 (sections 1.3.3.4 and 1.3.3.5), the known asymmetric compounds could be classified into three categories based on their structural characteristics.

Category one is characterized by varying chain lengths but fixed positions of secondary functional groups. In addition to 10-ketones with chain lengths of C_{27} to C_{31} in royal fern, 5-hydroxyaldehydes and 1,5-alkanediols identified in Chapter 5 in yew needle wax belong to this category as well. Category two is characterized by varying chain lengths and shifting positions of secondary functional groups, e.g., homologous series of hexacosane-1,7-diol, octacosane1,9-diol and triacontane-1,11-diol in Iceland poppy and homologous series of heptacosan-10-ol, nonacosan-12-ol and hentriacontan-14-ol in royal fern frond. Category three is characterized by fixed chain length and varying positions of secondary functional groups, e.g., dotriacontane-1,9-diol, -1,11-diol and -1,13-diol in *Myricaria germanica* as well as heptacosan-8-ol, -10-ol and -12-ol in Iceland poppy. Besides the above three categories, nonacosan-10-ol could be classified into an independent category because, different from the structural characteristics of compounds in other categories, nonacosan-10-ol has fixed position of secondary functional group and fixed carbon chain length.

The results of Chapter 6 and 7 indicated that the structural characteristics of nonacosan-10-ol are due to chain length specificity and elongation cycle specificity (the number of elongation cycles in which an elongase is involved) of elongases biosynthesizing nonacosan-10-ol. The constant carbon numbers before and after the introduction of the carbonyl group leading to nonacosan-10-ol indicate that the elongases involved (elongases1-6 in Fig. 6.5) have strict chain length specificity and elongation cycle specificity. In contrast, for 5-hydroxyaldehydes and 1,5-alkanediol, the elongases introducing secondary functional groups are expected to lack substrate chain length specificity, thus, resulting in alkyl chains with various chain lengths. However, the elongases (elongase2 in Fig 5.6) extending carbon chains after introduction of secondary functional groups likely have strict elongation cycle specificity, and therefore resulting in fixed positions of secondary functional groups.

Based on the knowledge mentioned above, the specificities of elongases involved in biosynthesizing other categories of asymmetric compounds can now be discussed. The elongases introducing secondary functional groups in category two asymmetric compounds must have strict substrate chain length specificity. For the homologous series of hexacosane-1,7-diol, octacosane1,9-diol and triacontane-1,11-diol in Iceland poppy, the functional groups

are introduced during the cycle of elongating C_{20} to C_{22} acyl-CoA (Fig. 1.8). However, due to the lack of elongation cycle specificity of the elongases extending chain length after introduction of secondary functional groups, the carbon chain lengths of final products vary. For compounds in category three, the elongases introducing secondary functional groups show the lack of substrate chain length specificity and the elongases extending chain length after introduction of secondary functional groups are expected to lack elongation cycle specificity. However, due to unknown reasons, all the products have the same chain length. In summary, the combination of substrate specificity and elongation cycle specificity results in a variety of asymmetric compounds. As discussed in section 1.3.1.1, both specificities are very likely controlled by KCS in an elongase complex, or more generally by condensing enzymes. Therefore, it will be of special importance to study the catalytic mechanisms of relevant condensing enzymes in plant systems containing asymmetric compounds in the cuticular wax mixtures.

8.2 Future Studies

8.2.1 Discovery of Diverse Hydroxylases

Diverse structures of wax components with secondary functional groups have been described in the current work. These diverse structures indicate a diversity of hydroxylases introducing those functional groups. One of these hydroxylases, MAH1 had been cloned and characterized, which is the first step towards understanding the function of the hydroxylase family. Cloning and characterization of the genes encoding other hydroxylases will further our knowledge of their catalytic properties and is of importance for evolutionary studies.

8.2.2 Further Elucidation of Nonacosan-10-ol Biosynthesis

The introduction of secondary hydroxyl groups by elongation is far less understood than the pathways involving hydroxylation. There are some experiments that can be done immediately based on the overall nonacosan-10-ol biosynthetic pathway and on the results of assays with ^{14}C-labeled precursors presented in this work.

(1) Examination of the chain length of methyl ketones produced in the poppy microsome assay. In the hypothetical pathway, the key intermediate is C_{22} β-ketoacyl-CoA. If this intermediate cannot be further elongated, methyl ketones will be produced under strong basic work-up conditions. Therefore, the methyl ketones detected in the assay are expected to have a chain length of 21 carbons for both C_{18} and C_{20} acyl-CoA as the substrates. This prediction needs to be confirmed.

(2) Search for other products with secondary functional group. It is not likely that nonacosan-10-ol will be produced in the *in vitro* assay because the entire pathway involves elongation, reduction, hydrolysis and decarbonylation enzyme activities. However, C_{22} β-ketoacyl-CoA could be further elongated to C_{24} 5-ketoacyl-CoA or longer chain ketoacyl-CoAs. After hydrolysis, they will be converted to keto-fatty acids. To better understand the elongation capacity under *in vitro* conditions and provide more evidence to support the hypothetical elongation pathway, these downstream keto-fatty acids products should be identified in appropriate systems.

On the long term, it is also important to know the exact sequence of steps on the pathway. As an entry point to this, the enzyme introducing the carbonyl group during elongation leading to nonacosan-10-ol should be studied. It has been mentioned in Chapter 6 that there are four levels towards a complete understanding of nonacosan-10-ol biosynthesis. Some questions on the first two levels have been answered by the results of the biochemical assays in this work. However, the two hypothetical routes to introduce the carbonyl group (third level) and the enzyme introducing the carbonyl group (fourth level) remain unknown (Fig. 6.5). As discussed in section 8.1.3.3, the condensing enzyme on *Pathway1* would provide information on evolutionary relationships among plant condensing enzymes. If the carbonyl group is introduced by a KCS in the special elongase complex on *Pathway2* (Chapter 7 introduction), discovery of this KCS would reveal a new sub-family of KCSs that can intercept substrates from a normal elongation pathway.

References

1. Walton, T. J. In *Methods of Plant Biochemistry*, Harwood, J. L., Boyer, J., Eds.; Academic Press: **1990;** pp 106-158.

2. Kim, K. S.; Park, S. H.; Jenks, M. A. *J. Plant Physiol.* **2007,** *164*, 1134-1143.

3. Jeffree, C. E. In *Insects and the Plant Surface*, Juniper, B., Southwood, R., Eds.; Edward Arnold: London, **1986;** pp 23-64.

4. Benitez, J.; Garcia-Segura, R.; Heredia, A. *Biochim. Biophys. Acta* **2004,** *1674*, 1-3.

5. Schae, J.; Stejskal, E. O. In *Topics in C-13 NMR spectroscopy*, Levy GC, Ed.; **1979;** pp 283-324.

6. Ray, A. K.; Chen, Z.-J.; Stark, R. E. *Phytochemistry* **1998,** *49*, 65-70.

7. Fang, X.; Qiu, F.; Yan, B.; Wang, H.; Mort, A. J.; Stark, R. E. *Phytochemistry* **2001,** *57*, 1035-1042.

8. Osman, S. F.; Irwin, P.; Fett, W. F.; O'Connor, J. V.; Parris, N. *J. Agric. Food Chem.* **1999,** *47*, 799-802.

9. Stark, R. E.; Yan, B.; Ratcliffe, O.; Chen, Z.; Fang, X.; Garbow, J. R. *Solid State Nucl. Magn. Reson.* **2000,** *16*, 37-45.

10. Gacea, J.; Schreiber, L.; Rodrigues, J.; Pereira, H. *Phytochemistry* **2002,** *61*, 205-215.

11. Ray, A. K.; Stark, R. E. *Phytochemistry* **1998,** *48*, 1313-1320.

12. Bianchi, G.; Murelli, C.; Vlahov, G. *Phytochemistry* **1992,** *31*, 3503-3506.

13. Markstadter, C.; Federle, W.; Jetter, R.; Riederer, M.; Holldobler, B. *Chemoecology* **2000,** *10*, 33-40.

14. Fernandes, A. M. S.; Baker, E. A.; Martin, J. T. *Annals of Applied Biology* **1964,** *53*, 43-58.

15. Ensikat, H. J.; Barthlott, W. *Int. J Plant Sci.* **2000,** *161* (1), 143-148.

16. Jetter, R.; Schaffer, S.; Riederer, M. *Plant Cell Environ.* **2000,** *23*, 619-628.

17. Riedel, M.; Eichner, A.; Jetter, R. *Planta* **2003,** *218*, 87-97.

18. Jetter, R.; Schaffer, S. *Plant Physiol.* **2001,** *126*, 1725-1737.

19. Haas, K.; Rentschler, I. *Plant Sci. Lett.* **1984,** *36*, 143-147.

20. Ensikat, H. J.; Boese, M.; Mader, W.; Barthlott, W.; Koch, K. *Chem. Phys. Lipids* **2006,** *144*, 45-59.

21. Jeffree, C. E. In *Biology of the Plant Cuticle*, Riederer, M., Muller, C., Eds.; **2006;** pp 11-125.

22. Jetter, R.; Riederer, M. *Bot. Acta* **1995,** *108*, 111-120.

23. Meusel, I.; Neinhuis, C.; Markstadter, C.; Barthlott, W. *Can. J. Bot.* **1999,** *77* (5), 706-720.

24. Schreiber, L.; Skrabs, M.; Hartmann, K. D.; Diamantopoulos, P.; Simanova, E.; Santrucek, J. *Planta* **2001,** *14*, 274-282.

25. Schöherr, J.; Lendzian, K. J. *Z. Pflanzenphysiol.* **1981,** *102,* 321-327.

26. Riederer, M.; Schreiber, L. *J. Exp. Bot.* **2001,** *52*, 2023-2032.

27. Hauke, V.; Schreiber, L. *Planta* **1998,** *207,* 67-75.

28. Vogg, G.; Fischer, S.; Leide, J.; Emmanuel, E.; Jetter, R.; Levy, A. A.; Riederer, M. *J. Exp. Bot.* **2004,** *55*, 1401-1410.

29. Mohammadian, M. A.; Watling, J. R.; Hill, R. S. *Acta oecologica* **2007,** *31,* 93-101.

30. Shepherd, T.; Griffiths, D. W. *New Phytol.* **2006,** *171,* 469-499.

31. Barthlott, W.; Neinhuis, C. *Planta* **1997,** *202,* 1-8.

32. Holmes, M. G.; Keiller, D. R. *Plant Cell Environ.* **2002,** *25,* 85-93.

33. Johnson, D. A.; Richards, R. A.; Turner, N. C. *Crop Sci.* **1983,** *24,* 318-325.

34. Long, L. M.; Patel, H. P.; Cory, W. C.; Stapleton, E. *Plant Biol.* **2003,** *30,* 75-81.

35. Cuadra, P.; Harborne, J. B.; Waterman, P. G. *Phytochemistry* **1997,** *45,* 1377-1283.

36. Jetter, R.; Klinger, A.; Schaffer, S. *Phytochemistry* **2002,** *61,* 579-587.

37. Hegde, Y.; Kolattukudy, P. E. *Physiol. Mol. Plant Pathol.* **1997,** *51,* 75-84.

38. Carver, T. L.; Thomas, B. J. *Plant Pathol.* **1990,** *39,* 367-395.

39. Gniwotta, F.; Vogg, G.; Gartmann, V.; Carver, T. L. W.; Riederer, M.; Jetter, R. *Plant Physiol.* **2005,** *139,* 519-530.

40. Gaume, L.; Perret, P.; Gorb, E.; Labat, J. J.; Rowe, N. *Arthropod Structure & Development* **2004,** *33,* 103-111.

41. Stoner, K. A. *Environ. Entomol.* **1990,** *19*, 730-739.

42. Bodnaryk, R. P. *Can. J. Plant Sci.* **1992,** *72*, 1295-1303.

43. Green, P. W. C.; Stevenson, P. C.; Simmonds, M. J.; Sharma, H. C. *J. Chem. Ecol.* **2003,** *29*, 811-821.

44. Bessoule, J. J.; Lessire, R.; Cassagne, C. *Arch. Biochem. Biophys* **1989,** *268,* 475-484.

45. Evenson, K. J.; Post-Beittenmiller, D. *Plant physiology* **1995,** *109,* 707-716.

46. Kohlwein, S. D.; Eder, S.; Oh, C. S.; Martin, C. E.; Gable, K.; Bacikova, D.; Dunn, T. M. *Mol. Cell. Biol.* **2001,** *21*, 109-125.

47. Han, G.; Gable, K.; Kohlwein, S. P.; Beaudoin, F.; Napier, J. A.; Dunn, T. M. *J. Biol. Chem.* **2002,** *277*, 35440-35449.

48. Denic, V.; Weissman, J. S. *Cell* **2007,** *130,* 663-677.

49. Kunst, L.; Taylor, D. C.; Underhill, E. W. *Plant Physiol. Biochem.* **1992,** *30* , 425-434.

50. Millar, A. A.; Kunst, L. *Plant J.* **1997,** *12*, 121-131.

51. Dunn, T. M.; Lynch, D. V.; Michaelson, L.V.; Napier, J.A. *Annals of Botany* **2004,** *92,* 483-497.

52. Millar, A. A.; Clemens, S.; Zachgo, S.; Giblin, E. M.; Taylor, D. C.; Kunst, L. *Plant Cell* **1999,** *11,* 825-838.

53. Fiebig, A.; Mayfield, J. A.; Miley, N. L.; Chau, S.; Fischer, R. L.; Preuss, D. *Plant Cell* **2000,** *12,* 2001-2008.

54. Hooker, T. S.; Millar, A. A.; Kunst, L. *Plant Physiol.* **2002,** *129,* 1568-1680.

55. Tod, J. d.; Post-Beittenmiller, D.; Jaworski, J. G. *Plant Physiol.* **2005,** *17* (2), 119-130.

56. Pruitt, R. E.; Vielle-Calzada, J. P.; Ploense, S. E.; Grossniklaus, U.; Lolle, S. J. . *Proc. Natl. Acad. Sci.* **2000,** *97* (3), 1311-1316.

57. Yephremov, A.; Wisman, E.; Huijser, P.; Wellesen, K.; Saedler, H. *Plant Cell* **1999,** *11,* 2187-2201.

58. Lolle, S. J.; Cheung, A. Y. *Dev. Biol.* **1993,** *155*, 250-258.

59. Gray, J. E.; Holroyd, G. H.; van der Lee, F. M.; Bahrami, A. R.; Sijmons, P. C.; Woodward, F. I.; Schuch, W.; Hetherington, A. M. *Nature* **2000,** *408,* 713-716.

60. Lassner, M. W.; Lardizabal, K.; Metz, J. G. *Plant Cell* **1996,** *8,* 281-292.

61. Moon, H.; Chowrira, G.; Rowland, O.; Blacklock, B.; Smith, M. A.; Kunst, L. *Plant Mol. Biol.* **2004,** *56,* 917-927.

62. Puyaubert, J.; Garbay, B.; Costagliolo, P.; Dieryck, W.; Roscoe, T. J.; Renard, M.; Cassagne, C.; Lessire, R. *Biochim. Biophys. Acta* **2001,** *1533,* 141-152.

63. Kanrar, S.; Venkateswari, J.; Dunreja, P.; Kirti, P. B. *Plant Cell Rep.* **2006,** *25,* 148-155.

64. Han, J.; Luhs, W.; Sonntag, K.; Zahringer, U.; Borchardt, D. S.; Wolter, F. P.; Heinz, E.; Frentzen, M. *Plant Mol. Biol.* **2001,** *46,* 229-239.

65. Moon, H.; Smith, M. A.; Kunst, L. *Plant Physiol.* **2001,** *127,* 1635-1643.

66. Mietkiewska, E.; Brost, J. M.; Giblin, E. M.; Barton, D. L.; Taylor, D. C. *Plant Sci.* **2007,** *173,* 198-205.

67. Qin, Y. M.; Pujol, F. M.; Hu, C. Y.; Feng, J. X.; Kastaniotis, A. J.; Hiltunen, J. K.; Zhu, Y. X. *J. Exp. Bot.* **2007,** *58*, 473-481.

68. Qin, Y. M.; Hu, C. Y.; Pang, Y.; Kastaniotis, A. J.; Hiltunen, J. K.; Zhu, Y. X. *Plant Cell* **2007,** *19,* 3692-3704.

69. Mietkiewska, E.; Giblin, E. M.; Wang, S.; Bartib, D. L.; Dirpail, J.; Brost, J. M.; Katavic, V.; Taylor, D. C. *Plant Physiol.* **2004,** *136,* 2665-2675.

70. Wang, X.; Kobiler, I.; Lichter, A.; Leikin-Frenkel, A.; Prusky, D. *Physiol. Mol. Plant Pathol.* **2004,** *65,* 171-180.

71. Zank, T. K.; Zahringer, U.; Lerchl, J.; Heinz, E. *Biochem. Soc. Trans.* **2000,** *28,* 654-658.

72. Zann, T.; Zahringer, U.; Beckmann, C.; Pohnert, G.; Boland, W.; Holtorf, H.; Peski, R.; Lerchl, J.; Heinz, E. *Plant J.* **2002,** *31*, 255-268.

73. Qi, B.; Beaudoin, F.; Fraser, T.; Stobart, A. K.; Napier, J. A.; Lazarus, C. M. *FEBS J.* **2002,** *510,* 159-165.

74. Tonon, T.; Harvey, D.; Larson, T. R.; Li, Y.; Grajam, I. *J. Appl. Phycol.* **2005,** *17,* 111-118.

75. Prasitchoke, P.; Kaneko, Y.; Bamba, T.; Fukusaki, E.; Kobayashi, A.; Harashima, S. *Gene* **2007,** *391,* 16-25.

76. Prasitchoke, P.; Kaneko, Y.; Sugiyama, M.; Bamba, T.; Fukusaki, E.; Kobayashi, A.; Harashima, S. *Appl. Microbiol. Biotech.* **2007,** *76,* 417-427.

77. Shimakata, T.; Stumpf, P. K. *Proc. Natl. Acad. Sci.* 1**982,** *79,* 5808-5812.

78. Clough, R. C.; Matthis, A. L.; Barnum, S.; Jaworski, J. G. J. *Biol. Chem.* **1992,** *287*, 20992-20998.

79. Paul, S.; Gable, K.; Beaudoin, F.; Cahoon, E.; Jaworski, J. G.; Napier, J. A.; Dunn, T. M. *J. Biol. Chem.* **2006,** *281*, 9018-9029.

80. Trenkamp, S.; Martin, W.; Tietjen, K. *Proc. Natl. Acad. Sci.* **2004,** *101*, 11903-11908.

81. Blacklock, B. J.; Jaworski, J. G. *Biochem. Biophys. Res. Commun.* **2006,** *346,* 583-590.

82. Blacklock, B.; Jaworski, J. G. *Eur. J. Biochem.* **2002,** *269,* 4789-4798.

83. Xu, X.; Dietrich, C. R.; Delledonne, M.; Xia, Y.; Wen, T.; Robertson, D. S.; Nikolau, B. J.; Schnable, P. S. *Plant Physiol.* **1997,** *115,* 501-510.

84. Suh, M. C.; Samuels, L.; Jetter, R.; Kunst, L.; Pollard, M.; Ohlrogge, J.; Beisson, F. *Plant Physiol.* **2005,** *139,* 1649-1665.

85. Beaudoin, F.; Gable, K.; Sayanova, O.; Dunn, T. M.; Napier, J. A. *J. Biol. Chem.* **2002,** *277*, 11481-11488.

86. Bernert, J. T.; Sprecher, H. *J. Biol. Chem.* **1979,** *254,* 11584-11590.

87. Lessire, R.; Bessoule, J. J.; Cook, L.; Cinti, D. L.; Cassagne, C. *Biochim. Biophys. Acta* **1993,** *1169,* 243-249.

88. Lessire, R.; Domergue, F.; Spinner, C.; Lucet-Levannier, K.; Lellouche, J.-P.; Mioskowski, C.; Cassagne, C. *Plant Physiol. Biochem.* **1998,** *36*, 205-211.

89. Lessire, R.; Chevalier, S.; Lucet-Levannier, K.; Lellouche, J.-P.; Mioskowski, C.; Cassagne, C. *Plant Physiol.* **1999,** *119,* 1009-1015.

90. Domergue, F.; Chevalier, S.; Creach, A.; Cassagne, C.; Lessire, R. *Lipids* **2000,** *35*, 487-494.

91. Bach, L.; Michaelson, L. V.; Haslam, R.; Bellec, Y.; Gissot, L.; Marion, J.; Costa, M. D.; Boutin, J.-P.; Miquel, M.; Tellier, F.; Domergue, F.; Markham, J. E.; Beaudoin, F.; Napier, J. A.; Faure, J.-D. *Proc. Natl. Acad. Sci.* **2008,** *105*, 14727-14731.

92. Gable, K.; Garton, S.; Napier, J.; Dunn, T. M. *J. Exp. Bot.* **2004,** *55*, 543-545.

93. Zheng, H.; Rowland, O.; Kunst, L. *Plant Cell* **2005,** *17,* 1467-1481.

94. Koornneef, M.; Hanhart, C. J.; Thiel, F. *J. Heredity* **1989,** *80,* 118-122.

95. Ji, X.; Jetter, R. *Phytochemistry* **2008,** *69,* 1197-1207.

96. Lai, C.; Kunst, L.; Jetter, R. *Plant J.* **2007,** *50,* 189-196.

97. Metz, J. G.; Pollar, M. R.; Anderson, L.; Hayes, T. R.; Lassner, M. W. *Plant Physiol.* **2000,** *122,* 635-644.

98. Jenks, M. A.; Tuttle, H. A.; Eigenbrode, S. D.; Feldmann, K. A. *Plant Physiol.* **1995,** *108,* 369-377.

99. Rowland, O.; Zheng, H.; Hepworth, S. R.; Lam, P.; Jetter, R.; Kunst, L. *Plant Physiol.* **2006,** *142,* 866-877.

100. Kolattukudy, P. E. *Arch. Biochem. Biophy.s* **1971,** *142* (2), 701-709.

101. Wang, X.; Kolattukudy, P. E. *FEBS Lett.* **1995,** *370,* 15-18.

102. Lardizabal, K.; Metz, J. G.; Sakamoto, T.; Hutton, W. C.; Pollard, M. R.; Lassner, M. W. *Plant Physiol.* **2000,** *122,* 645-655.

103. Kalscheuer, R.; Steinbuchel, A. *J. Biol. Chem.* **2003,** *278*, 8075-8082.

104. Cheng, J. B.; Russell, D.W. *J. Biol. Chem.* **2004,** *279*, 37798-37807.

105. Li, F.; Wu, X.; Lam, P.; Bird, D.; Zheng, H.; Samules, A. L.; Jetter, R.; Kunst, L. *Plant Physiol.* **2008,** *148,* 97-107.

106. Kolattukudy, P. E. *Plant Physiol.* **1968,** *43*, 1466-1470.

107. Kolattukudy, P. E.; Croteau, R.; Brown, L. *Plant Physiol.* **1974,** *54*, 670-677.

108. Kolattukudy, P. E.; Buckner, J. S.; Brown, L. *Biochem. Biophys. Res. Commun.* **1972,** *47*, 1306-1313.

109. Purdy, S. J.; Truter, E. V. *Proc. Roy. Soc. London Ser. B* **1963,** *158,* 553-556.

110. Holloway, P. J.; Brown, G. A.; Baker, E. A.; Macey, M. J. K. *Chem. Phys. Lipids* **1977,** *19,* 114-127.

111. Kolattukudy, P. E.; Liu, T.-Y. J. *Biochem. Biophys. Res. Commun.* **1970,** *41*, 1369-1374.

112. Greer, S.; Wen, M.; Bird, D.; Wu, X.; Samuels, L.; Kunst, L.; Jetter, R. *Plant Physiol.* **2007,** *145,* 653-667.

113. Kolattukudy, P. E.; Buckner, J. S.; Liu, T.-Y. J. *Arch. Biochem. Biophys.* **1973,** *156,* 613-620.

114. Holloway, P. J.; Brown, G. A. *Chem. Phys. L.* **1977,** *19*, 1-13.

115. Tulloch, A. P. *Can. J. Bot.* **1981,** *59,* 1213-1221.

116. Horn, D. H. S.; Kranz, Z. H.; Lamberton, J. A. *Aust. J. Chem.* **1964,** *17,* 464-476.

117. Jackson, L. L. *Phytochemistry* **1971,** *10,* 487-490.

118. von Wettstein-Knowles, P.; Netting, A. G. *Carlsberg Res. Commun.* **1976,** *41,* 225-235.

119. Bianchi, G. *Genetica Agraria* **1985,** *39* (4), 471-486.

120. Dierickx, P. *Phytochemistry* **1973,** *12,* 1498-1499.

121. Tulloch, A. P.; Weenink, R. O. *J. Chem. Soc. Chem. Commun.* **1966,** 225-226.

122. Dierickx, P.; Buffel, K. *Phytochemistry* **1972,** *11,* 2654-2655.

123. Tulloch, A. P. *Lipids* **1973,** *8,* 617-622.

124. Netting, A. G.; von Wettstein-Knowles, P. *Arch. Biochem. Biophys* **1976,** *174,* 613-621.

125. Mikkelsen, J. D. *Carlsberg Res. Commun.* **1979,** *44,* 133-147.

126. Mikkelsen, J. D.; von Wettstein-Knowles, P. *Arch. Biochem. Biophys* **1978,** *188*, 172-181.

127. Jetter, R. *Phytochemistry* **2000,** *55,* 169-176.

128. Jetter, R.; Riederer, M. *Phytochemistry* **1999,** *52,* 907-915.

129. Vermeer, C. P.; Nastold, P.; Jetter, R. *Phytochemistry* **2003,** *62*, 433-438.

130. Jetter, R.; Riederer, M. *Phytochemistry* **1999,** *50,* 1359-1364.

131. Jetter, R.; Riederer, M.; Seyer, A.; Mioskowski, C. *Phytochemistry* **1996,** *42*, 1617-1620.

132. Jetter, R.; Riederer, M. Ca*n. J. Bot. 19***96, 7**4*,* 419-430.

133. Osborne, R.; Stevenes, J. F. Ph*ytochemistry 19***96, 4**2 *(*5), 1335-1339.

134. Kim, K.; Whang, S. S.; Sun, B. J. *Plant Biol. 19***95, 3**8 *(*2), 181-193.

135. Koch, K.; Dommisse, A.; Barthlott, W. Cr*ystal Growth and Design 2*0**06, 6** *(*11), 2571-2578.

136. Prugel, B.; Lognay, G. *Phytochem. Anal. 1***996,** *7*, 29-36.

137. Jetter, R.; Riederer, M. J. *Chem. Ecol. 2***000,** *26 (*2), 399-411.

138. Berg, B.; Hannus, K.; Popoff, T.; Theander, O. In *Structure and Function of Northern Coniferous Forests - An Ecosystem Study, Ecol. Bull. vol. 32,* Persson, T., Ed.; Stockholm, **1980;** pp 391-400.

139. Beri, R. M.; Lemon, H. W. *Can. J. Chem.* ***1*****970,** *48,* 67-69.

140. Abe, I.; Utsumi, Y.; Oguro, S.; Noguchi, H. *FEBS Lett.* ***2*****004,** *562,* 171-176.

141. Abe, I.; Watanabe, T.; Noguchi, H. *Phytochemistry* ***2*****004,** *65,* 2447-2453.

142. Tantisewie, B.; Ruijgriok, H. W. L.; Hegnauer, R. *Pharm. Weekblad.* ***1*****969,** *104,* 1341-1355.

143. Njardarson, J. T.; Biswas, K.; Danishefsky, S. J. *Chem. Commun.* ***2*****002,** 2759-2761.

144. Taylor, D.C.; Weber, N.; Hogge, L.R.; Underhill, E.W. *Anal. Biochem* ***1*****990,** *184,* 311-316.

145. Pullman, M. E. *Anal. Biochem.* **1973,** *54,* 188-198.

146. Gietz, R. D.; Wood, R. A. In *Molecular Genetics of Yeast: Practical Approaches,* Johnston JA, Ed.; Oxford University Press: Oxford, **1994;** pp 121-134.

147. Teusink, R. S.; Bressan, R. A.; Jenks, M. A. *Int. J Plant Sci.* **2007,** *162*, 309-315.

148. Holloway, P. J.; Brown, G. A.; Baker, E. A.; Macey, M. J. K. *Chem. Phys. L.* **1977,** *19,* 114-127.

149. Holloway, P. J.; Jeffree, C. E.; Baker, E. A. *Phytochemistry* **1976,** *15,* 1768-1770.

150. Jenks, M. A.; Eigenbrode, S. D.; Lemieux, B. *In The Arabidopsis Book*. **2002**; pp 1-22.

151. Goodwin, S. M.; Rashotte, A. M.; Rahman, M.; Feldmann, K. A.; Jenks, M. A. *Phytochemistry* **2005,** *66,* 771-780.

152. Richter, W. J.; Burlingame, A. L. *Chem. Commun.* **1968,** *19,* 1158-1160.

153. Jetter, R.; Kunst, L.; Samules, A. L. In *Biology of the Plant Cuticle,* Riederer, M., Muller, C., Eds.; Blackwell: Sheffield, **2006;** pp 145-181.

154. von Wettstein-Knowles, P. In *Waxes: Chemistry, molecular biology and functions,* Hamilton, R. J., Ed.; The Oily Press: West Ferry, **1995;** pp 91-129.

155. Franich, R. A.; Wells, L. G.; Holland, P. T. *Phytochemistry* **1978,** *17,* 1617-1623.

156. Riederer, M. *Ecological Studies* **1989,** *77,* 157-192.

157. Shanker, K. S.; Kanjilal, S.; Rao, B. V. S. K.; Kishore, K. H.; Misra, S.; Prasad, R. B. N. *Phytochem. Anal.* **2007,** *18,* 7-12.

158. Dragota, S.; Riederer, M. *Annals of Botany* **2007,** *100,* 225-231.

159. Tanaka, T.; Hattori, T.; Kouchi, M.; Hirano, K.; Satouchi, T. *Biochim. Biophys. Acta* **1998,** *1393,* 299-306.

160. Carlson, J. E.; Leebens-Mack, J. H.; Wall, P. K.; Zahn, L. M.; Mueller, L. A.; Landherr, L. L.; Hu, Y.; Hut, D. C.; Arrington, J. M.; Choirean, S.; Becker , A.; Field, D.; Tanksley, S. D.; Ma, H.; dePamphilis, C. W. *Plant Mol. Biol.* **2006,** *62*, 351-369.

161. Ghanevati, M.; Jaworski, J. G. *Biochim. Biophys. Acta* **2001,** *1530,* 77-85.

162. Hanks; S.K.; Quinn, A. M.; Hunter, T. *Science* **1988,** *241*, 42-52.

163. Romanos, M. A.; Scorer, C. A.; Clare, J. J. *Yeast* **1992,** *8*, 423-488.

164. von Wettstein-Knowles, P.; Netting, A. G. *Carlsberg Res. Commun.* **1976,** *41*, 225-235.

Appendix I

List of Publications

Miao Wen, Reinhard Jetter (2008) Alkanediols and ketols in *A. thaliana* stem wax. *J. Exp. Bot.* submitted

Miao Wen, Reinhard Jetter (2007) Novel very-long-chain hydroxyaldehydes from the cuticular wax of *T. baccata* needles. *Phytochemistry*, 68, 2563-2569

Stephen Greers, **Miao Wen**, David Bird, Xuemin Wu, Lacey Samuels, Ljerka Kunst, Reinhard Jetter (2007) The cytochrome P450 enzyme CYP96A15 is the mid-chain alkane hydroxylase responsible for formation of secondary alcohols and ketones in stem cuticular wax of Arabidopsis. *Plant Physiology*, 145, 653-667

Miao Wen, Jason Au, Franka Gniwotta, Reinhard Jetter (2006) Very-long-chain secondary alcohols and alkanediols in cuticularwaxes of *Pisum sativum* leaves. *Phytochemistry*, 67, 2492-2502.

Miao Wen, Christopher Buschhaus, Reinhard Jetter (2006) Nanotubules on plant surfaces: Chemical composition of epicuticular wax crystals on needles of *Taxus baccata* L. *Phytochemistry*, 67, 1808-1817.